Nouveaux concepts dans la pharmacologie des récepteurs aux acides gras à chaîne courte FFA2 et FFA3

Elisabeth Lamodière Moussaud

THESE

pour l'obtention du diplôme de Docteur de l'Université de Bourgogne
Ecole doctorale Environnement, Santé, STIC
Spécialité : Sciences de la Vie

présentée et soutenue publiquement par

Elisabeth LAMODIÈRE

le 10 juin 2011

Nouveaux concepts dans la pharmacologie des récepteurs aux acides gras à chaîne courte FFA2 et FFA3

[New insights into the pharmacology of the short-chain free fatty acid receptors 2 and 3]

Directrice de thèse :

Pr. Johanna CHLUBA
INSERM U866 Lipides Nutrition Cancer
Université de Bourgogne
Dijon, France

Co-encadrant de thèse :

Dr. Remko A. BAKKER
CardioMetabolic diseases research department
Boehringer Ingelheim Pharma GmbH & Co. KG
Biberach an der Riss, Allemagne

Composition du jury :

Rapporteur	Dr. Ralf JOCKERS, INSERM U1016/UMR8104 CNRS/Université Paris Descartes, Institut Cochin, Paris, France
Rapporteur	Pr. Peter GIERSCHIK, Institut für Pharmakologie und Toxikologie, Ulm Universität, Ulm, Allemagne
Examinatrice	Pr. Johanna CHLUBA, INSERM U866, Lipides Nutrition Cancer, Université de Bourgogne, Dijon, France
Examinateur	Pr. Bruno VERGÈS, Service Endocrinologie, Diabétologie et Maladies Métaboliques, CHU Le Bocage, Dijon, France

Contact

Elisabeth Moussaud (Lamodière)
13 avenue du Château
21800 Quetigny
- France -
elamodiere@wanadoo.fr

Dans la vie, rien n'est à craindre,
tout est à comprendre.

Marie Curie (1867-1934)

Acknowledgments

First of all, I would like to thank Dr. Remko Bakker for his help and guidance during the four years of my PhD thesis. I would like to express my gratitude to Dr. Michael Mark for having given me the opportunity to work in his research department.

I thank Pr. Johanna Chluba for having been my supervisor at the University of Burgundy, Pr. Peter Gierschik, Dr. Ralf Jockers and Pr. Bruno Vergès for having accepted to be part of my PhD dissertation committee. I also thank Pr. Michel Narce for having been part of my progress committee.

I would like to thank my colleagues from the laboratory, Julia Dennenmoser, Eva Hammer, Andrea Lorenz and Oscar McCook for having been intent on keeping a good atmosphere and cohesion in the lab and for their excellent assistance. I had a great time working with you every day. I also thank all the other persons from the CardioMetabolic diseases department I worked with.

I would like to thank Dr. Christofer Tautermann for his very helpful contribution to the structural biochemistry and Karoline Schwarz, Werner Rust, Dagmar Knebel and Dr. Detlev Mennerich from the Genomics group for their help for the gene expression analysis, and also Silke Hobbie's laboratory for their help with the CellKey instrument.

This work would not have been possible without the support of Dr. Marcus Kostka and Pr. Alain Pugin, who both actively contributed to the collaboration between Boehringer Ingelheim Pharma GmbH & Co. KG and the Université de Bourgogne.

I finally thank Simon who encouraged me in this way and always supported me.

Abstract

Metabolic diseases, such as diabetes, dyslipidemia or obesity, are more and more weighing on public health expenses in developed countries. Despite active research, these widespread diseases remain difficult to handle. Promising new therapeutic strategies against metabolic diseases include the development of drugs targeting the free fatty acid receptors, as key players in metabolism homeostasis.

In this context, the current PhD thesis focuses on the study of two G protein-coupled receptors, namely the short-chain free fatty acid receptors 2 (FFA2) and 3 (FFA3).

First, we investigated the expression of the two receptors of interest in a variety of cell types. Then, in order to study the pharmacology and the binding mode of endogenous and synthetic agonists on FFA2 and FFA3, we established stable cell lines expressing each receptor. Once we identified the signaling pathways engendered in response to receptor activation, we showed that synthetic agonists were allosteric activators of the receptors, in the sense that they bind to the receptors at a distinct site from short-chain fatty acids, i.e. the endogenous agonists. To identify the aminoacid residues that were involved in ligand binding, we generated a variety of point mutated receptors by site-directed mutagenesis. By analyzing the effects of the mutations in functional tests, we determined precisely the aminoacid residues that were essential for ligand binding. From these results, we designed *in silico* structural models which may aid future drug design efforts for the discovery of new FFA2 and FFA3 agonists.

Key words : metabolic diseases; obesity; dyslipidemia; diabetes; G protein coupled receptors; short-chain free fatty acids; free fatty acid receptors; pharmacology; site-directed mutagenesis; structural model.

Résumé

Les maladies métaboliques, comme le diabète, la dyslipidémie ou l'obésité, constituent un problème majeur de santé publique dans les pays développés. Ces maladies très répandues restent encore difficiles à traiter malgré une recherche active. Les stratégies thérapeutiques contre ces maladies incluent le développement de nouvelles molécules ciblant les récepteurs aux acides gras, étant donné leur rôle essentiel dans l'homéostasie du métabolisme.

C'est dans ce contexte que s'inscrit ce travail portant sur deux récepteurs couplés aux protéines G, les récepteurs aux acides gras à courte chaîne 2 et 3 ou *free fatty acid receptors* 2 (FFA2) et 3 (FFA3).

Nous avons tout d'abord cherché à déterminer le profil d'expression des deux récepteurs. Ensuite, nous avons établi des lignées cellulaires stable exprimant FFA2 ou FFA3 afin d'étudier la pharmacologie d'agonistes synthétiques et endogènes de ces récepteurs. Après avoir identifié les voies de signalisation engendrées par l'activation des récepteurs, nous avons démontré que les agonistes synthétiques étaient des activateurs allostériques, c'est-à-dire qu'ils se liaient aux récepteurs sur un site distinct de celui des ligands endogènes. Pour identifier les résidus d'acides aminés nécessaires à la reconnaissance des ligands, nous avons généré une gamme de mutants ponctuels de ces récepteurs par mutagénèse dirigée. En analysant l'effet des mutations dans des tests fonctionnels, nous avons pu déterminer avec précision où se liaient les ligands et ainsi pu dessiner par informatique des modèles structuraux des récepteurs qui pourront être utilisés pour le *drug design* de futures molécules agonistes de ces récepteurs.

Mots-clés : maladies métaboliques ; diabète ; dyslipidémie ; obésité ; récepteurs couplés aux protéines G ; acides gras à chaîne courte ; récepteurs aux acides gras ; pharmacologie ; mutagénèse à site dirigé ; modèle structural.

Résumé substantiel en français

Au cours des dernières décennies, l'incidence des maladies métaboliques telles que l'obésité, le diabète ou la dyslipidémie a augmenté à un rythme soutenu et ceci en particulier dans les pays industrialisés. En plus de peser de plus en plus lourd sur les dépenses de santé publique, ces maladies restent difficiles à traiter, les médicaments actuellement sur le marché restant peu efficaces ou ayant des effets secondaires problématiques.
De nouveaux espoirs de thérapie concernent les récepteurs aux acides gras libres. En effet, ces récepteurs découverts récemment jouent un rôle crucial dans la régulation du métabolisme des sucres et des graisses. Parmi eux se trouvent les récepteurs aux acides gras à chaîne courte ou *free fatty acid receptors* (FFA) 2 et 3, récepteurs qui font l'objet de ce travail de thèse.

FFA2 et FFA3 ont donc pour ligands des acides gras à chaîne courte, tels que le propionate, l'acétate ou le butyrate. Ces molécules de petite taille sont libérées dans la lumière intestinale comme produits de fermentation des fibres alimentaires par la microflore intestinale. Les acides gras à chaîne courte sont ensuite transportés dans les entérocytes où ils sont utilisés comme source d'énergie, ou bien rejoignent le flux sanguin pour être distribués de façon systémique et servir, entre autres, de molécules de signalisation renseignant l'organisme sur ce qui a été ingéré.

Les rôles physiologiques précis de FFA2 et FFA3 n'ont cependant pas encore été élucidés. D'une part, de récentes publications suggèrent que ces récepteurs seraient impliqués dans la régulation de la lipolyse et stimuleraient la sécrétion de la leptine, un peptide anorexigène, par les adipocytes. D'autre part, FFA2 et FFA3 semblent être exprimés dans l'intestin, plus précisément dans les cellules entéroendocrines, et stimuleraient la sécrétion d'un certain nombre d'hormones peptidiques, dont certaines comme le peptide YY ou la cholécystokinine ont un pouvoir anorexigène. FFA2

interviendrait également sur le système immunitaire. En effet, lors d'une inflammation du système digestif, les acides gras à chaîne courte réduisent l'inflammation via FFA2 en stimulant la production de cytokines anti-inflammatoires et en inhibant la sécrétion de cytokines pro-inflammatoires par les monocytes.

Au niveau moléculaire, FFA2 et FFA3 appartiennent à la grande famille des récepteurs couplés aux protéines G (RCPG). Les RCPG sont des cibles thérapeutiques particulièrement attractives pour les entreprises pharmaceutiques car ils sont accessibles à la surface des cellules et sont facilement modulables par l'action de petites molécules synthétiques. Ainsi, plus de la moitié des médicaments actuellement sur le marché ont pour cible un RCPG. De par leur appartenance à la famille des RCPG et leur fonction physiologique présumée, FFA2 et FFA3 seraient de bons candidats pour le développement de nouveaux médicaments contre les maladies métaboliques.

C'est dans contexte que se positionne ce travail de thèse portant sur la caractérisation des voies de signalisation cellulaire de FFA2 et FFA3 et sur la pharmacologie de ces récepteurs.

Etant donné les données parcellaires et divergentes décrites dans la littérature sur les sites d'expression de nos récepteurs d'intérêt, nous avons tout d'abord cherché à déterminer dans quels tissus et quels types cellulaires FFA2 et FFA3 étaient exprimés. Ainsi, nous avons trouvé de hauts niveaux d'ARNm des gènes codant pour FFA2 et FFA3 dans les lignées de cellules β-pancréatiques, ainsi que, dans une moindre mesure, dans des lignées de cellules entéroendocrines et d'adipocytes.
Ensuite, afin d'obtenir un modèle biologique pour l'étude de la pharmacologie des récepteurs d'intérêt, nous avons cloné les ADN complémentaires codant pour FFA2 et FFA3 humains, puis établi des lignées cellulaires exprimant chacun de ces récepteurs de manière stable. Nous avons ensuite recherché les voies de signalisation engendrées par l'activation de ces récepteurs par un agoniste naturel, le propionate, et par des agonistes synthétiques mis au point par d'autres groupes pharmaceutiques et décrits dans des brevets. Dans les modèles cellulaires que nous avons établis, l'activation de FFA2 par ses ligands endogènes et synthétiques entraîne de manière dose-dépendante une

diminution de la concentration intracellulaire d'adénosine monophosphate cyclique (AMPc) ainsi qu'une augmentation de la concentration en calcium cytosolique, tandis que l'activation de FFA3 entraîne une diminution de la concentration intracellulaire d'AMPc, mais pas d'augmentation de la concentration en calcium cytosolique. De plus, la stimulation des récepteurs par les ligands endogènes ou synthétiques induit la phosphorylation de la *mitogen-activated protein kinase* ERK (*extracellular signal-regulated kinase*) 1/2. Nous avons également étudié l'effet de l'activation des récepteurs sur les changements cellulaires globaux grâce à la nouvelle technique de mesure de l'impédance cellulaire. Là encore, les cellules répondent aux ligands, qu'ils soient endogènes ou synthétiques, et ceci en fonction de leur concentration. Les réponses cellulaires obtenues dans ce test sont cependant légèrement différentes selon que les cellules sont stimulées par un agoniste endogène ou un agoniste synthétique.

Bien que leurs structures moléculaires soient très différentes, les ligands synthétiques empruntent des voies de signalisation cellulaire globalement similaires à celle des ligands endogènes. Les ligands synthétiques sont en effet des molécules cycliques, de plus grande taille que les acides gras à chaîne courte, et ne présentent pas de fonction acide carboxylique, alors que cette fonction semble essentielle à la liaison des ligands endogènes aux récepteurs. Nous avons donc voulu vérifier l'hypothèse selon laquelle les ligands synthétiques étaient des activateurs allostériques des récepteurs, c'est-à-dire qu'ils se lient aux récepteurs en des sites distincts de celui des ligands endogènes. Pour cela, nous avons conduit deux types d'expériences.

Premièrement, nous avons mis en compétition les ligands dans un test fonctionnel de dosage d'AMPc. La concentration de ligand endogène pour laquelle on obtient 50% de son effet maximal (pEC_{50}) est diminuée en présence de ligand synthétique, et vice versa. En d'autres mots, le ligand endogène devient de plus en plus puissant au fur-et-à-mesure que la concentration en ligand synthétique augmente, et inversement. Cette expérience démontre que les ligands synthétiques sont des activateurs ago-allostériques des récepteurs FFA2 et FFA3.

Deuxièmement, nous avons recherché les résidus d'acides aminés nécessaires à la liaison des ligands en analysant dans des tests fonctionnels la réponse des récepteurs mutés en un point précis. Pour cela, nous avons généré des lignées cellulaires exprimant

chacune un mutant ponctuel de FFA2 ou FFA3 de façon stable. Pour vérifier la fonctionnalité de chaque récepteur muté, nous avons testé ces lignées cellulaires dans des dosages d'AMPc. Nous avons ainsi pu localiser les sites de liaison des ligands synthétiques et ceux des ligands endogènes, sur chacun des récepteurs. A partir de ces résultats, nous avons pu dessiner par bioinformatique des modèles structuraux des récepteurs, outils essentiels à la mise au point de nouveaux agonistes de FFA2 ou FFA3, médicaments potentiels contre les maladies métaboliques.

Table of contents

Part 2

List of figures

List of tables

Abbreviations

B **BSA**, bovine serum albumin
BMI, body mass index
C **cAMP**, cyclic adenosine monophosphate
CCK, cholecystokinine
Compound A, 4-furan-2-yl-2-methyl-5-oxo-1,4,5,6,7,8-hexahydro-quinoline-3-carboxylic acid-o-tolylamide
Compound B, 2-(4-chloro-phenyl)-3-methyl-N-thiazol-2-yl-butyramide
D **DAG**, diacylglycerol
DMEM, Dulbecco's modified Eagle's medium
E **EDTA**, ethylene diamine tetraacetate
EL, extracellular loop
ER, endoplasmic reticulum
ERK, extracellular signal-regulated kinase
F **6-FAM**, 6-carboxy fluorescein
FCS, fetal calf serum
FFA, free fatty acid
FFA1 (=GPR40), free fatty acid receptor 1
FFA2 (=GPR43), free fatty acid receptor 2
FFA3 (=GPR41), free fatty acid receptor 3
FLIPR, fluorescence image plate reader
G **$G\alpha_i$**, inhibitory G protein alpha
$G\alpha_q$, calcium-inducing G protein alpha
$G\alpha_s$, stimulatory G protein alpha
GDP, guanosine diphosphate
GLP-1, glucagon-like peptide 1
GPCR, G protein coupled receptor
GTP, guanosine triphosphate
GTPγS, guanosine-5'-O-(3-thio)triphosphate
H **HBSS**, Hank's balanced salt solution
Hek, human embryonic kidney
HEPES, 4-(2-hydroxyethyl)-1-piperazineethanesulfonic acid
HRP, horseradish peroxidase
5-HT, 5-hydroxytryptamine (=serotonin)
I **IBMX**, 3-isobutyl-1-methylxanthine
IP3, inositol-1,4,5-triphosphate
M **MAPK**, mitogen-activated protein kinase
MOE, molecular operating environment
P **PBS**, phosphate buffer saline
PCR, polymerase chain reaction
PLC, protein kinase C
PMSF, phenylmethanesulfonyl fluoride
PTX, pertussis toxin
PYY, peptide YY
R **RPMI**, Roswell Park Memorial Institute
RT, room temperature
S **SCFA**, short-chain fatty acid
T **T2D**, type 2 diabetes
6-TAMRA, 6-carboxytetramethylrhodamine
TM, transmembrane domain
Tween, polyoxyethylenesorbitan monolaurate
W **wt**, wild type

Part 1

Introduction

This PhD work has been conducted under the direction of Dr. Remko Bakker, from 2007 to 2011, in the CardioMetabolic disease research department of the pharmaceutical company Boehringer Ingelheim Pharma GmbH & Co. KG in Biberach an der Riss (Germany). In this context, it aspires to achieve a better understanding of the biology and the pharmacology of two receptors that are potential therapeutic targets for the treatment of metabolic disorders. We will first provide the scientific background of our research concerning metabolic diseases and the unique drug target family that constitute G-protein coupled receptors (GPCRs). We will then make a literature review of the current knowledge about the two receptors of interest, the free fatty acid receptors 2 and 3. Finally, we will present and discuss the novel original data that we have gained regarding these two receptors.

1. Metabolic disorders

Primary causes for metabolic disorders are a positive energy balance, i.e. a reduced physical activity, in combination with excessive food intake. However, these disorders can be greatly influenced by the genetic background of the patient (Bougnères, 2002). The most prevalent metabolic diseases are diabetes, dyslipidemia and obesity. Although these three diseases are distinct pathologies, they show a high interconnectivity (Fig. 1). For instance, obesity is a major risk factor for developing type 2 diabetes (T2D) and dyslipidemia (Narayan *et al.*, 2007). These disorders often lead to the formation of atherosclerotic plaques and other life-threatening cardiovascular diseases.

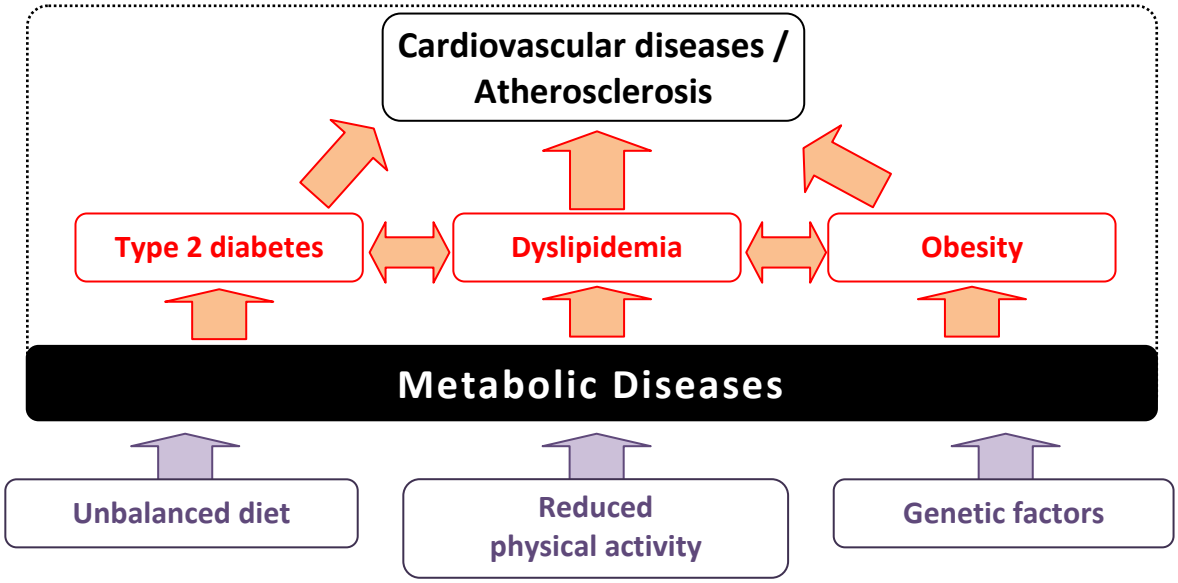

Fig. 1 : Origin and connectivity of metabolic diseases.

All together, unbalanced diet, reduced physical activity and genetic background are risk factors for the development of metabolic diseases, like type 2 diabetes, dyslipidemia and obesity. Metabolic diseases are highly interconnected in the sense that one disease increases the risk for one of the other diseases. The major complications of metabolic diseases are life-threatening cardiovascular diseases, mostly via the formation of atherosclerotic plaques.

All metabolic diseases are in constant progression in developed countries and represent a growing society burden. However, only a few therapeutic tools to improve efficiently patients' metabolic condition are available to date.

In this manuscript, we will focus our interest on the study of short-chain free fatty acid receptors 2 and 3 (FFA2 and FFA3) as potential therapeutic targets for the treatment of metabolic diseases.

1.1. Diabetes

Diabetes is now one of the most common non-communicable diseases globally. It is the fourth or fifth leading cause of death in most high-income countries and there is substantial evidence that it is epidemic in many low- and middle-income countries (Sicree *et al.*, 2010).

Diabetes is a diagnostic term regrouping several disorders characterized by abnormal glucose homeostasis resulting in elevated blood glucose. They are two main types of diabetes, distinguished by their origin (Sicree *et al.*, 2010).

Type 1 diabetes is caused by the destruction of the insulin-producing pancreatic beta cells, typically due to an autoimmune reaction. The disease can affect people of any age,

but usually occurs in children or young adults. Type 1 diabetes is one of the most common endocrine and metabolic conditions diagnosed in childhood (Sicree *et al.*, 2010).

Conversely, the diagnosis of type 2 diabetes usually occurs after the age of 40. T2D accounts for 90-95% of all diabetes cases diagnosed worldwide (Sicree *et al.*, 2010). It is characterized by a systemic insulin resistance : insulin is still produced but the target tissues do not respond to it anymore.

The prevalence of T2D has strongly risen during the last decades (Ahren, 2009). In Europe, around 6.9% of the adult population suffer from T2D in 2010 and this number is projected to increase to 8.1% by 2030 (Sicree *et al.*, 2010). Complications from diabetes, such as coronary artery and peripheral vascular disease, stroke, diabetic neuropathy, amputations, renal failure and blindness result in increasing disability, reduced life expectancy and enormous public health costs (Sicree *et al.*, 2010).

Besides complications, other serious metabolic disorders are actually often diagnosed in association with T2D. These metabolic disorders include dyslipidemia, obesity and cardiovascular diseases.

1.2. Dyslipidemia

Dyslipidemia is characterized by an abnormal blood lipid profile, namely a high triglyceride (TG) concentration, a low high-density lipoprotein (HDL) cholesterol concentration and a high low-density lipoprotein (LDL) cholesterol concentration. Causes for dyslipidemia may be genetic but seem to be in most cases related to lifestyle and unbalanced diet (Bougnères, 2002; Mooradian, 2009).

This imbalanced lipid profile contributes to the development of atherosclerosis. Rupture of atherosclerotic plaques and subsequent acute thrombosis are key events in the mortality associated with acute coronary syndromes.

Dyslipidemia is one of the major risk factors for cardiovascular diseases in patients affected by T2D (Mooradian, 2009). Indeed, T2D alters function of multiple cell types in the vascular system, including endothelium, smooth muscle cells and platelets and thereby promotes atherosclerotic plaque formation in the inner walls of the blood vessels (Beckman *et al.*, 2002) .

1.3. Obesity

Obesity is the result of complex disease involving environmental, psychological, behavioral, and metabolic components. It is associated with a number of debilitating and life-threatening disorders, in particular with T2D and dyslipidemia (Bagchi and Preuss, 2007).

The incidence of obesity has been increasing worldwide at an alarming rate over the last two decades and around 300 million people were diagnosed as obese in 2007 (Bagchi and Preuss, 2007). The WHO projects that by 2015 approximately 2.3 billion adults will be overweight and more than 700 million will be obese. The body mass index (BMI), defined as the individual's body weight divided by the square of his or her height, is commonly used to distinguish between overweight and obesity. A person is considered as overweight when BMI is equal to or more than 25, and obese when BMI is equal to or more than 30.

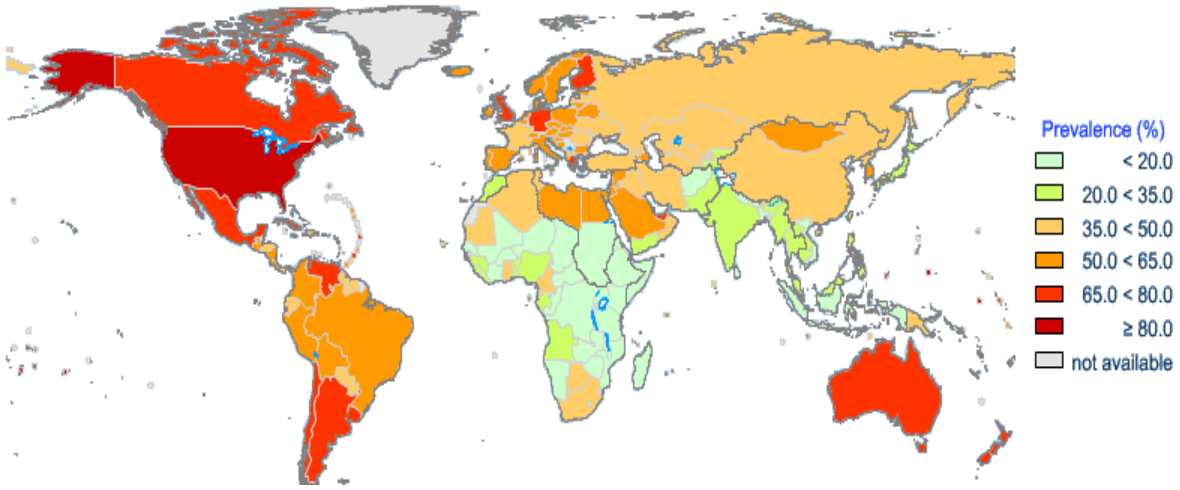

Fig. 2 : Estimated global overweight and obesity prevalence in 2010.

WHO estimated prevalence (in percentage) of overweight and obesity (BMI>25) among men older than 15, calculated for each country for year 2010 (Ono *et al.*, 2005).

1.4. Cardiovascular diseases

Cardiovascular diseases are disorders of the heart and blood vessels and include coronary heart disease, cerebrovascular disease, peripheral arterial disease and pulmonary embolism. If not handled rapidly, all these diseases can be lethal. The most common reason for the lack of blood flow and the subsequent ischemia observed in the

affected tissues is the formation of a thrombus from a ruptured atherosclerotic plaque (Chapman *et al.*, 2010). Abnormal lipid profiles observed in patients affected by dyslipidemia, obesity or T2D promote lipid deposition in the inner wall of blood vessels, thus increasing the risk of formation of atherosclerotic plaques.

1.5. Available treatments

General treatment for patients afflicted by one or several metabolic disorders first consists in dietary modifications and increased physical activity. However, when lifestyle changes are not sufficient anymore, chirurgical and/or pharmacological intervention could be required.

For the treatment of T2D, several drugs have been developed throughout the years. These include metformin, sulfonylurea, thiazolidinediones, meglitinides, α-glucosidase inhibitors, an amylin analogue, exogenous insulin injection, as well as therapies based on activation of glucagon-like peptide 1 (GLP-1) receptors by GLP-1-receptor agonists, or on prevention of the degradation of GLP-1 by inhibiting DPPIV, the enzyme that hydrolyses GLP-1 (Nathan *et al.*, 2009).
However, an issue in the treatment of T2D is that, despite therapy, glycemic control may still deteriorate over time. Furthermore, current therapies against T2D are often associated with weight gain, hypoglycemia or other unpleasant side effects, such as gastrointestinal discomfort, flushing or edema (Nathan *et al.*, 2009).

For the treatment of dyslipidemia, current pharmacotherapies generally include statins, fibrates, or nicotinic acid, in monotherapy or in association with each other (for review, see Chapman *et al.*, 2010).
Nicotinic acid exerts a valuable anti-dyslipidemic effect by attenuating the release of free fatty acids from adipocytes into the blood flow, but causes a disturbing flushing and some of its metabolites can be hepatotoxic (Chapman *et al.*, 2010).
Fibrates lower plasma triglycerides levels and raise HDL by inducing the up- or down-regulation of a variety of genes related to lipid transport and metabolism. However, fibrates may cause renal dysfunctions (Chapman *et al.*, 2010).

A combination therapy associating nicotinic acid or fibrates with statins can counteract such residual non-LDL lipid risk factors (Chapman *et al.*, 2010).

Presently, physical activity and balanced diet remain the best way to handle obesity. Although a few drugs exist to help weight loss, their use is often in debate due to their relative low efficiency and their pronounced side effects.
Among them, orlistat is a potent inhibitor of gastric and pancreatic lipases. It reduces fat absorption by inhibiting hydrolysis of triglycerides in monoacylglycerides and free fatty acids (Guerciolini, 1997). However, it causes adverse gastrointestinal side effects, such as oily stools, fecal spotting and fecal incontinence (Powell and Khera, 2010).
In some cases, anorectic drugs are also used. They include mazindol and amphetamine derivatives, such as diethylpropione, fenproporex and sibutramine. Sibutramine, for instance, blocks presynaptic uptake of norepinephrine and serotonin, thus potentiating the anorectic effects of these neurotransmitters (Flier, 2004). However, sibutramine can also provoke high blood pressure, insomnia, nausea, dry mouth and constipation (Powell and Khera, 2010). Recently, two amphetamine derivatives [sibutramine (Sibutral™) and benfluorex (Mediator™)] were subjected to market withdrawal in some countries due to deleterious side effects.

In conclusion, to fight against obesity, T2D, dyslipidemia, and cardiovascular diseases as well, new therapies that would improve patients' metabolic condition without causing adverse side effects are highly desirable. A number of potential novel targets for the treatment of metabolic disorders concern the best drugable class of receptors, namely the GPCR family.

2. G protein-coupled receptors

2.1. Generalities about GPCRs

GPCRs are among the largest and most diverse protein families in mammalian genomes and genes coding for GPCRs account for around 2% of the human genome (Lagerström and Schiöth, 2008). Around 800 genes encoding GPCRs have been identified so far in the

human genome and around half of them are olfactory or gustative receptors (Harmar *et al.*, 2009). GPCRs have evolved to allow cellular systems to sense their environment through selective recognition of a multitude of external stimuli, such as light, odorant molecules, nucleotides, proteins, peptides or fatty acids (Marinissen and Gutkind, 2001).

Numerous pathologies are associated with defects in GPCRs, including metabolic diseases (Milligan and Kostenis, 2006). Their involvement in key biological processes and their good accessibility at the outer side of the cell make them of great pharmaceutical interest. GPCRs constitute currently the largest family of therapeutic targets, with more than 40% of marketed drugs targeting a GPCR (Wang *et al.*, 2009a).

Receptors of the GPCR family share two main features, relative to their early signaling pathway and their structure. First, GPCRs are constituted of seven transmembrane domains (TM) arranged in α-helices that span from one side to the other of the plasma membrane, allowing the N-terminus to point at the extracellular side and the C-terminus to be in the cytosol (Fredriksson *et al.*, 2003). Second, GPCRs interact, as their name implies, with so-called G proteins, some heterotrimeric proteins that are able to hydrolyze GTP in GDP (Fredriksson *et al.*, 2003). However, some GPCRs are also able to couple with other proteins than heterotrimeric G proteins (Patel, 2004), whereas some G proteins are also able to bind to receptors that are not heptahelical and that are not related to GPCRs in function and evolution (Kristiansen, 2004). In consequence, some authors prefer the term of "seven-transmembrane receptors". In this study, we will however conserve the widely used term of GPCRs to designate this family of receptors.

The GPCR superfamily can be subdivided in different classes, based on similarities in aminoacid sequences, on analysis of clustering of genes and on mechanism of activation. Mammalian GPCRs are classically divided into five families, namely the rhodopsin-like receptor class, the secretin receptor-like class, the glutamate receptor class, the adhesion class and the Frizzled/Taste2 class (Lagerström and Schiöth, 2008).
The free fatty acid receptors belong to the largest GPCR family, namely the rhodopsin-like receptor class or class A. This class counts approximately 700 members, of which around 400 olfactory receptors (Lagerström and Schiöth, 2008). It is the most diverse

GPCR family regarding the nature of its ligands, which include visual pigments, odorants, peptides, biogenic amines, nucleotides and other small molecules (Kristiansen, 2004).

Some crystallography studies show that the seven α-helices of the receptor form a barrel through the membrane, the N-terminus being at the extracellular side and the C-terminus at the intracellular side of the receptor (Fig. 3). The main binding site for small ligands in rhodopsin-like GPCRs is located within the central crevice of the bundle formed by the seven TM domains (Jacoby *et al.*, 2006). The extracellular loops (EL) have been identified as a region of great variability between receptors and are therefore believed to play an important role in ligand recognition (Rosenbaum *et al.*, 2009). Other features specific to rhodopsin-like receptors include a short N-terminus, the presence of leucine-rich repeats in the C-terminus and conserved cysteine residues that are predicted sites for disulphide bounds between EL1 and EL2 (Lagerström and Schiöth, 2008).

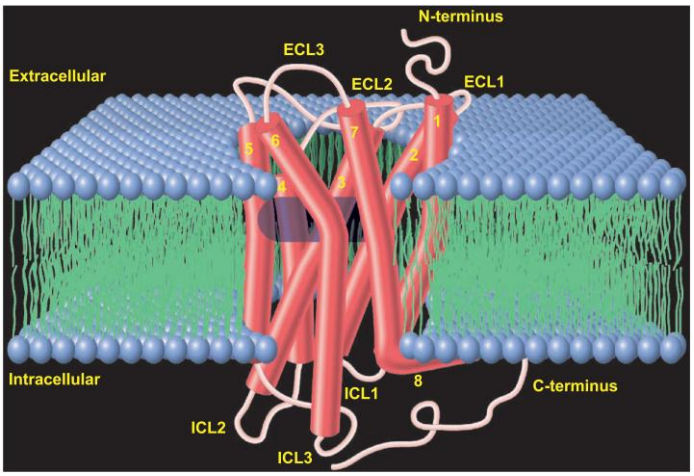

Fig. 3 : Schematic representation of a rhodopsin-like receptor.

This model is based on the crystal structure of the rhodopsin receptor (pdb code 1L9H). Transmembrane domains are represented as cylinders; ribbons represent extracellular loops (ECL) or intracellular loops (ICL).

(Extracted from Kristiansen, 2004)

The first high-resolution crystal structure of a GPCR was elucidated ten years ago, revealing the structure of the bovine rhodopsin and thus confirming the seven helices structure (Palczewski *et al.*, 2000; Fig. 3). However, GPCR crystallization is a so harsh that, to date, the crystal structures of only a few additional rhodopsin-like GPCRs, namely the β1 and β2 adrenergic receptors, the adenosine A2A receptor, the dopamine D3 receptor, and the CXCR4 receptor, have been published (Bokoch *et al.*, 2010; Cherezov *et al.*, 2007; Chien *et al.*, 2010; Jaakola *et al.*, 2008; Rasmussen *et al.*, 2007;

Warne *et al.*, 2008; Warne *et al.*, 2011, Wu *et al.*, 2010). These models have been extensively used as basis to predict the structure of many GPCRs using bioinformatics algorithms. Even if bioinformatics tools achieve good predictions, the large diversity of the GPCR family makes it difficult to elucidate the exact structure of a given receptor. In consequence, additional techniques such as site-directed mutagenesis are still needed to unravel the exact structure of receptors.

2.2. GPCR signaling

2.2.1. G proteins as primary signaling for GPCRs

At the intracellular side of the receptor, the response owed to the activation of a GPCR is mediated by G proteins that undergo activation/inactivation cycles (Fig. 4). G proteins are composed of three subunits, from one part the α subunit, and from the other part the β and γ subunits that form an undissociable complex. In the absence of ligand, the Gα subunit is bound to GDP and is closely associated with the Gβγ heterodimer (Fig. 4A). This Gα-GDP/Gβγ complex interacts with the cytosolic loops of the GPCR. Gβγ facilitates the coupling of Gα to the receptor and acts as a guanine nucleotide dissociation inhibitor for Gα-GDP, slowing the spontaneous exchange of GDP by GTP (Wettschureck and Offermanns, 2005).

Ligand binding to the receptor induces a conformational change in the Gα subunit, allowing the exchange of GDP by GTP (Fig. 4B). Gβγ dissociates from Gα-GTP (Fig. 4C), Gα-GTP and Gβγ are free to interact with their respective effectors (Fig. 4D). Signaling is terminated when GTP returns to GDP by the GTPase activity of the Gα subunit (Fig. 4A). The resulting GDP-bound Gα protein can enter a new cycle, form again a heterotrimer with Gβγ subunits and interact with a receptor (Fig. 4A; McCudden *et al.*, 2005; Wettschureck and Offermanns, 2005).

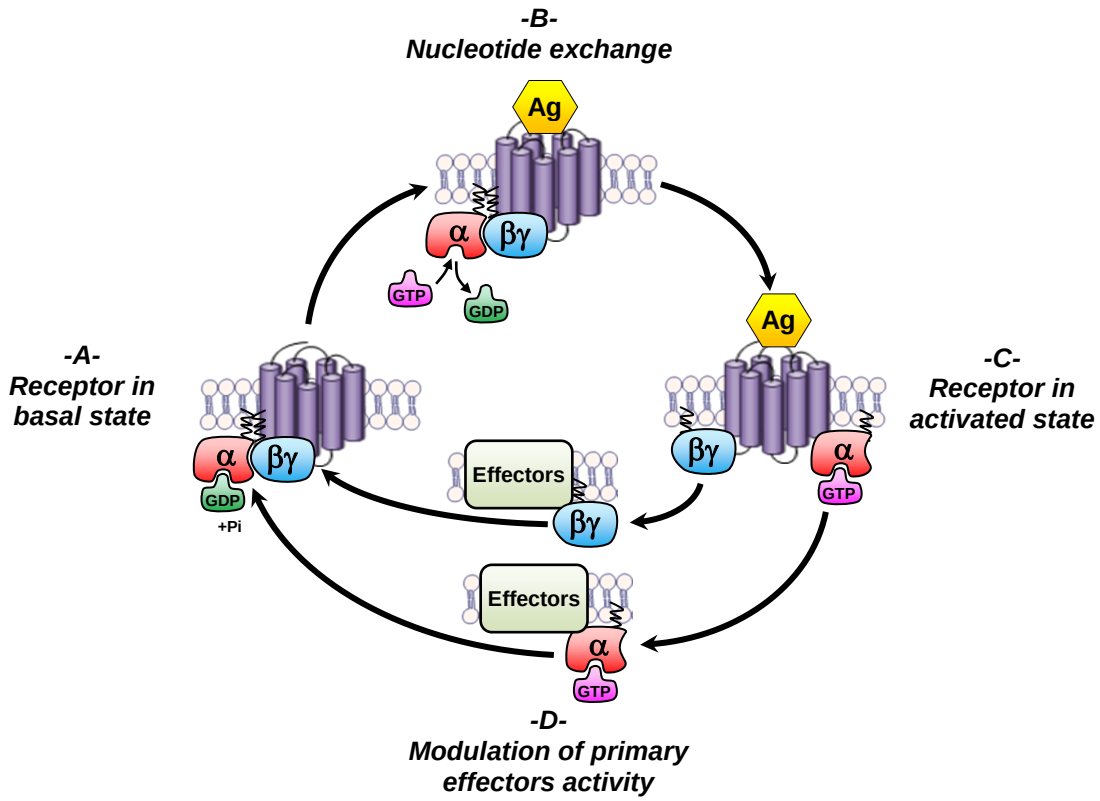

Fig. 4 : Exchange cycle of GDP to GTP under GPCR activation.

A. In basal state, a GPCR binds to membrane-anchored Gα (in red) and Gβγ (in turquoise blue) G protein subunits, Gα carrying a GDP molecule. **B.** The binding of an agonist (Ag, in yellow) to the receptor promotes the exchange of GDP by GTP on the Gα-subunit. **C.** The receptor is then in an activated state : Gα-GTP dissociates from Gβγ. **D.** Gα-GTP and Gβγ are free to interact with primary effectors and thus to activate or inhibit their activity. The receptor returns to its basal state when GTP is spontaneously hydrolyzed to GDP and inorganic phosphate (Pi). GDP, guanosine diphosphate; GTP, guanosine triphosphate. Adapted from Wettschureck and Offermanns (2005).

Depending on the type of G protein that interacts with the receptor, the signal will be transduced to different effectors (Fig. 5). Gα proteins are usually classified according to aminoacid sequence similarities and cellular effects in three major families, namely $G\alpha_s$, $G\alpha_i$ and $G\alpha_q$. Stimulation of $G\alpha_s$ leads to the activation of the adenylyl cyclase resulting in an increase of the cytosolic concentration of cAMP. Conversely, activation of $G\alpha_i$ leads to the inhibition of the adenylyl cyclase, resulting in decreasing cAMP concentrations. Besides, the $G\alpha_q$ protein activates the membrane-bound phospholipase C β (PLCβ) that hydrolyzes phosphatidyl-inositol-4,5-biphosphate (PIP_2) in inositol-1,4,5-triphosphate (IP_3) and diacylglycerol (DAG). IP_3 triggers the release of Ca^{2+} from the endoplasmic reticulum (ER) into the cytosol, thereby increasing the cytosolic Ca^{2+} concentration (Marinissen and Gutkind, 2001). The freed Gβγ dimer is also able to activate or inhibit a range of effectors, including PLCβ, adenylyl cyclase, phosphoinositide-3-kinase (PI3K), and K^+ and Ca^{2+} channels (Milligan and Kostenis, 2006; Smrcka, 2008).

In a physiological context, the intracellular effects of a given receptor will depend on the environment of the receptor, namely the subtypes of the G proteins that are available in the cell and that can specifically couple to the receptor and on the effectors that are present in the cell (Milligan and Kostenis, 2006; Wettschureck and Offermanns, 2005).

A common way to assess GPCR activation in biological models is to measure changes in the concentration of second messengers, classically cAMP or Ca^{2+}, or to study downstream cellular events, such as the phosphorylation of mitogen-activated protein kinases (MAPK), induction of gene expression or cell proliferation.

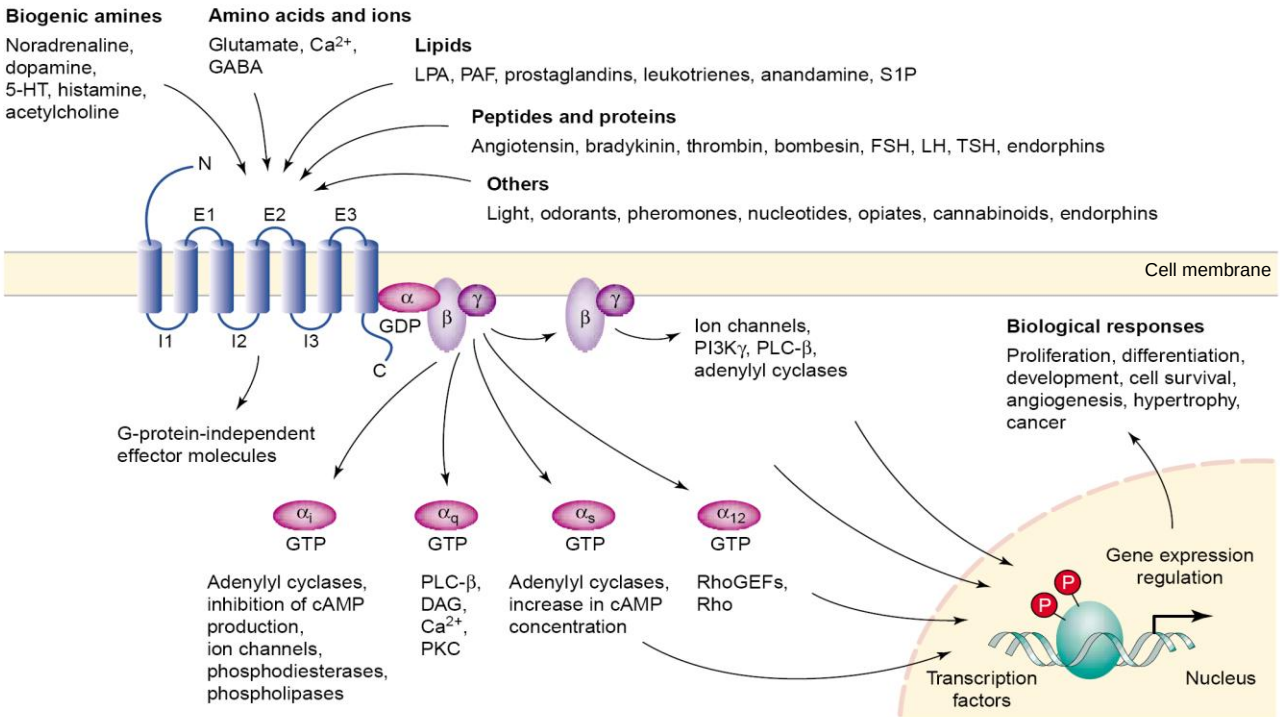

Fig. 5 : Diversity of ligands and of downstream signaling upon GPCR activation.

Various kinds of ligands can activate GPCRs, including biogenic amines, aminoacids, ions, lipids, peptides, nucleotides or light. The stimulation of the GPCR by an agonist results in the activation of G protein α-, *β*- and γ-subunits. G protein subunits interact subsequently with cellular effectors, finally leading to a global response of the cell to its environment. Adapted from Marinissen and Gutkind (2001).

2.2.2. Cellular effectors : example of the ERK1/2 MAPK

Downstream in the activation cascade of GPCRs is a class of protein of first importance : the mitogen-activated protein kinase (MAPK) family. MAPK are involved in the transduction of extracellular signals regulating cell proliferation, differentiation and apoptosis. The extracellular signal-regulated kinase (ERK) 1/2 MAPK is in particular responsible for the transduction of mitogenic signals. Once activated by phosphorylation, ERK1/2 is translocated to the nucleus where it phosphorylates transcription factors involved in the control of cell division and DNA synthesis (Roux and Blenis, 2004). GPCR activation can lead to ERK1/2 phosphorylation via various pathways, depending mainly on the G proteins the receptor couples to (Fig. 6). It can involve classical GPCR effectors, such as the protein kinase C (PKC), but also some more unusual pathways, through tyrosine kinase phosphorylation and activation of small G proteins, for instance belonging to the Ras family (Luttrell and Luttrell, 2003). Despite of the variability of the signaling pathways involved in GPCRs response transduction, ERK1/2 acts as a signaling node where inputs from a variety of pathways converge.

Thereby, ERK1/2 phosphorylation has been considered as an integrated marker of GPCR activation and used for instance in compound library screening studies (Osmond *et al.*, 2005).

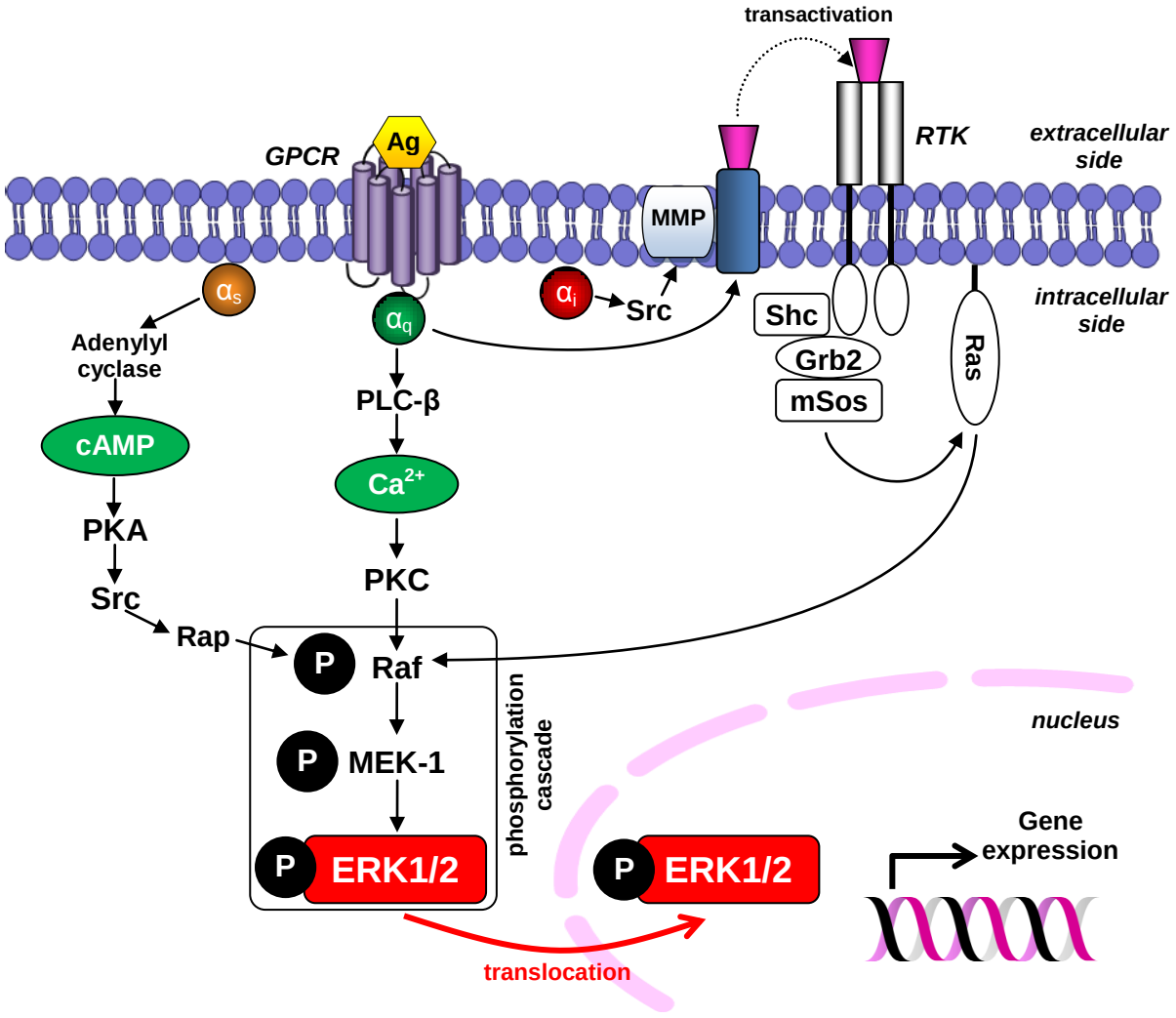

Fig. 6 : Phosphorylation of ERK1/2 in response to GPCR activation.

Whatever the type of the Gα subunit ($G\alpha_s$, $G\alpha_i$ or $G\alpha_q$), signaling pathways in response to activation of a GPCR converge to the activation of Raf and finally of ERK1/2. Depending on the cell type, receptors and G proteins, signaling will be transduced by one or the other signaling pathway. $G\alpha_s$ and $G\alpha_q$ proteins activate ERK1/2 trough relatively straightforward pathways, often via phosphorylation cascades. In contrast, activation of ERK1/2 in response to $G\alpha_i$-coupled receptors involves indirect signaling pathway, for instance through "inside-out" transactivation of another receptor (here, a receptor tyrosine kinase,RTK) for growth factors. Adapted from Osmond *et al.* (2005)

3. The short-chain free fatty acid receptors family

In the last decades, a large effort has been undertaken to identify ligands for orphan GPCRs. This led to the identification of a novel subfamily of GPCRs that were receptors for free fatty acids, of which FFA2 and FFA3. These receptors constitute interesting new therapeutic targets against metabolic diseases.

3.1. Gene identification and genomic structure

In an effort of cloning a gene encoding a receptor for galanin, a new cluster of four intronless genes has been identified in the human genome (Sawzdargo *et al.*, 1997). This cluster was located on the chromosome 19q13 and contained genes that were predicted to be rhodopsin-like receptors, namely GPR40, GPR41, GPR42 and GPR43 (Sawzdargo *et al.*, 1997; Fig. 7A).

In 2003, these genes were deorphanized : GPR40 was found to be a receptor for medium- and long-chain fatty acids, whereas GPR41 and GPR43 were identified as receptors for short-chain fatty acids (Briscoe *et al.*, 2003; Brown *et al.*, 2003). These receptors were consequently renamed free fatty acid receptor 1 (=FFA1 =GPR40), free fatty acid receptor 2 (=FFA2 =GPR43) and free fatty acid receptor 3 (=FFA3 =GPR41). Although these receptors are closely related together, they exhibit some dissimilarity. FFA2 and FFA3 share together 43% aminoacid homology whereas FFA1 shares 33% and 35% aminoacid homology with FFA2 and FFA3, respectively (Stoddart *et al.*, 2008a; Fig. 7B).

Intriguingly, an additional gene called GPR42 is present in the human and the chimpanzee genomes, but not in the mouse, rat and bovine genomes (Brown *et al.*, 2003). In human, GPR42 is localized in the FFA receptors cluster and shares 98% aminoacid homology with FFA3 (Fig.7). Since it did not show activity in functional assays, it has been long considered a pseudo-gene (Sawzdargo *et al.*, 1997) and has been therefore only little studied. The major difference between GPR42 and FFA3 resides in position 174, where GPR42 has a Trp residue whereas FFA3 has an Arg residue [see Appendix #1 for further information about the aminoacid nomenclature]. A Trp174Arg substitution in GPR42 was sufficient to restore the ability of the receptor to respond to short-chain fatty acids (Brown *et al.*, 2003). Moreover, a population study showed that

61% of the genotyped individuals exhibited an Arg at position 174, indicating that variability between GPR42 and FFA3 at position 174 in human may be polymorphism rather than gene-specific variability (Liaw and Connoly, 2009). Therefore, GPR42 may be active in a significant part of the human population and should not be simply classified as a pseudo-gene (Liaw and Connoly, 2009).

Phylogenetic analysis confirmed that FFA receptors belong to the rhodopsin-like GPCR class. Like the majority of rhodopsin-like receptors, FFA1, FFA2 and FFA3 present Cys residues in EL1 and EL2 that are likely to be involved in the formation of an intramolecular disulphide bound, but this remains to be demonstrated experimentally. FFA2 shows a Glu-Arg-Tyr motif at the bottom of TM3 that is conserved among the others rhodopsin-like GPCRs. FFA3 contains at this location a similar motif, Glu-Arg-Phe. The Glu/Asp-Arg-Tyr is known to play a pivotal role in regulating GPCR conformational state (Rovati *et al.*, 2007).

Homologue genes for human FFA2 and FFA3 were also cloned from three other species, namely mouse, rat and bovine (Karaki *et al.*, 2006; Senga *et al.*, 2003; Wang *et al.*, 2009b). The GenBank nucleotide and protein databases also reference putative sequences for FFA2 and/or FFA3 in chimpanzee, rhesus monkey, goat, dog, horse, chicken and zebra fish.

Although the genomic structure of FFA2 and FFA3 is quite similar among mouse, rat and primates, it differs substantially in the bovine genome. In bovine, FFA2 contains an intron placed at the beginning of the gene, whereas FFA3 contains two alternatively spliced introns (Wang *et al.*, 2009b). However, the two different messengers for FFA3 would encode the same protein because the initiation codon is situated in the common second exon (Wang *et al.*, 2009b).

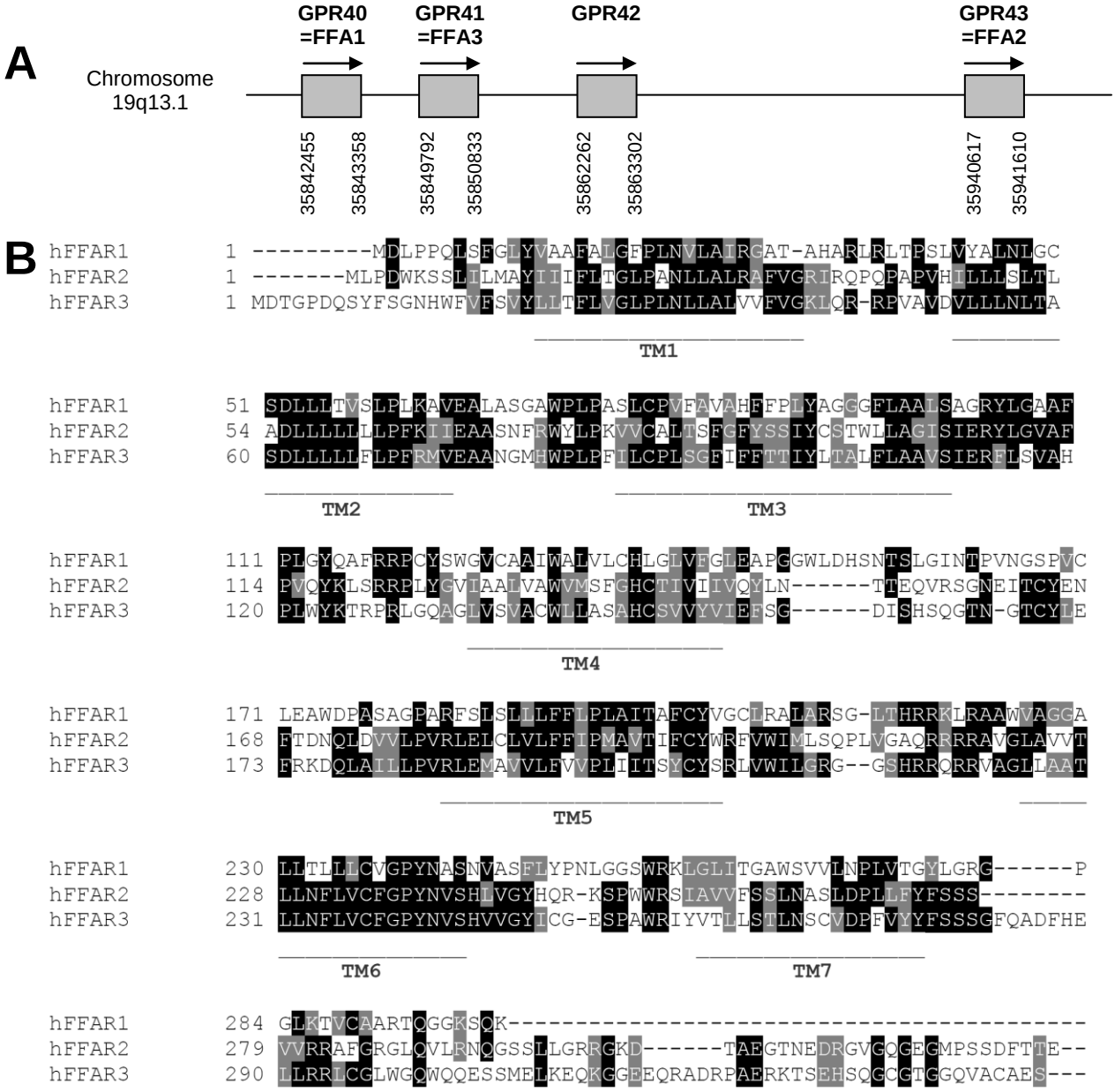

Fig. 7 : The FFA receptors gene family in human.

A. Schematic organization of the genes encoding FFA receptors in the human genome. Contig sequences were aligned to generate a comprehensive map of the human genome. The sequences of the FFA genes are shown as boxes. Numbering gives the position of the genes in the human genome, 1 being the first nucleotide of the p arm of chromosome 19. Drawing is not to scale. Arrows indicate direction of transcription. Adapted from Sawzdargo *et al.* (1997). **B. Alignment of FFA receptors aminoacid sequences.** Sequence alignment of FFA1 (NP_005294.1; 300 aa; 31kDa), FFA2 (NP_005297.1; 330 aa; 37kDa) and FFA3 (NP_005295.1; 346 aa; 39kDa) from human, was computed using the ClustalW2 algorithm (Thompson *et al.*, 1994). In black boxes, the conserved residues. In grey boxes, residues of similar physicochemical properties. TM1-7: predicted location of transmembrane domains (TM).

3.2. Ligands and ligand-binding sites of FFA2 and FFA3

In the search for ligands for FFA2 and FFA3, compound library screenings were performed. Unexpectedly, all compounds formulated as acetate ions were found to be able to stimulate human FFA2 (=hFFA2; Brown *et al.*, 2003). Further experiments by Brown *et al.* (2003), where sodium acetate or ammonium acetate were tested by themselves, showed that acetate was sufficient to activate hFFA2. Other SCFAs such as propionate or butyrate were also found to be ligands not only for hFFA2, but also for human FFA3 (=hFFA3), while a range of saturated and unsaturated medium- and long-chain free fatty acids failed to activate hFFA2 and hFFA3 (Brown *et al.*, 2003; Xiong *et al.*, 2004). Noteworthy, whereas all three SCFAs showed a similar potency on hFFA2, acetate was almost inactive on hFFA3 (Brown *et al.*, 2003).

SCFAs are the main end product of bacterial metabolism in the human large intestine (Fig. 8). They derive principally from the anaerobic fermentation of carbohydrate fibers by the gut microflora. In human, the total SCFA concentration in the colon lumen fluctuates between 60 and 130mM, with a ratio of 60:20:20 for acetate:propionate:butyrate (Cummings *et al.*, 1987). SCFAs are then absorbed in the colon and end up in blood (Topping and Clifton, 2001). Whereas SCFA blood levels vary considerably throughout the day, they usually reach a peak 1h after meal ingestion and are therefore a kind of marker to the whole organism that a fiber-rich meal has been ingested (Wolever *et al.*, 1997). Finally, the postprandial concentration of acetate in human peripheral is around 150µM, 3µM for butyrate and 6µM for propionate (Wolever *et al.*, 1997).

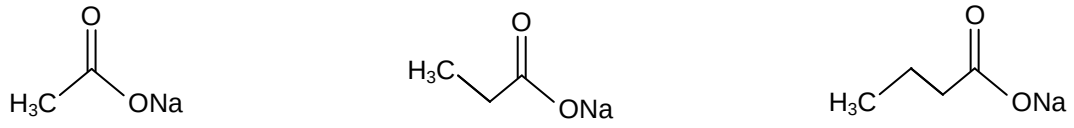

Fig. 8 : Structure of the endogenous ligands for the short-chain fatty acid receptors 2 and 3.

The SFCAs propionate and butyrate are ligands for both FFA2 and FFA3, whereas acetate is more specific to FFA2. SCFAs are represented here as sodium salts.

High-throughput screening campaigns for drug discovery allowed the identification of several molecules that were exogenous ligands for FFA2 or FFA3 (Lee *et al.*, 2008;

Leonard *et al.*, 2007). In our study, we will focus on two of them, that we will thereafter designate as Compound A and Compound B (Fig. 9). Compound A and Compound B are specific agonists for FFA2 and FFA3, respectively, and both are of relatively low molecular weight (around 300g/mol).

Compound A

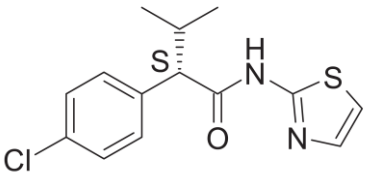

Compound B

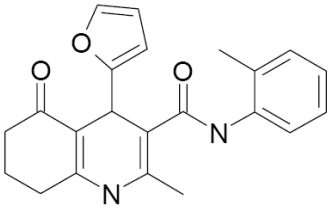

Fig. 9 : Chemical structure of the synthetic ligands for hFFA2 and hFFA3.

Compound A (2-(4-chloro-phenyl)-3-methyl-N-thiazol-2-yl-butyramide) is a specific agonist for hFFA2, while Compound B (4-furan-2-yl-2-methyl-5-oxo-1,4,5,6,7,8-hexahydro-quinoline -3-carboxylic acid o-tolylamide) is a specific agonist for hFFA3.

Interestingly, conversely to the endogenous ligands, Compound A and B present aromatic groups but no carboxylic acid groups (Fig. 8 and 9). The high divergence in chemical structures between the exogenous and the endogenous ligands are in line with the hypothesis that they interact to their cognate receptors at distinct binding sites. Indeed, first hints in the literature support this idea. For instance, a study that used site-directed mutagenesis identified three aminoacid residues in hFFA2 (Arg180, Arg255 and His242) that were crucial for the binding of propionate but not of Compound A (Stoddart *et al.*, 2008b). Further supporting this idea, Lee and colleagues demonstrated that Compound A was an allosteric modulator of FFA2, suggesting that Compound A binds at a different site than the orthosteric ligand propionate (Lee *et al.*, 2008).
However, more precise insights into the pharmacology of FFA2 and FFA3 are needed to confirm the aforementioned hypothesis and to identify more precisely the aminoacid residues of the binding pockets that interact with endogenous and exogenous ligands. These efforts should finally lead to a more exact modeling of the ligand binding sites and to general structures of the both receptors.

Although both FFA2 and FFA3 respond to SCFAs, differences in signal transduction and expression patterns would support the idea that the two receptors play distinct

physiological roles. However, the physiological functions of FFA2 and FFA3 remain to be clearly defined.

The following sections will focus successively on FFA2 and FFA3, and more especially on their coupling with G proteins, their expression sites and their expected physiological functions.

4. The free fatty acid receptor 2

4.1. Signal transduction

Several publications explore the coupling of FFA2 in different cell types and assays. One of the earliest article about FFA2 shows a specific coupling of FFA2 with $G\alpha_{12}$, $G\alpha_{13}$, $G\alpha_{14}$, $G\alpha_{i1}$ and $G\alpha_{i3}$ G proteins using a panel of yeast strains expressing a range of different yeast/mammalian Gα chimeras (Brown *et al.*, 2003). Later studies with CHO and Hek293 cells expressing human FFA2 demonstrated that acetate and propionate were able to induce Ca^{2+} mobilization and to decrease cAMP levels, suggesting a double coupling of the receptor with $G\alpha_i$ and $G\alpha_q$ proteins (Lee *et al.*, 2008; Stoddart *et al.*, 2008b).

4.2. Tissue distribution

FFA2 seems to be expressed in a variety of tissues, including adipocytes, gut and immune cells.

FFA2 mRNA were detected at a high level in subcutaneous, perirenal, mesenteric, parametrial and epididymal adipose tissues in mice (Hong *et al.*, 2005). In these tissues, expression increased significantly under a high-fat diet (1.3 to 3-fold induction), the most drastic effect appearing in mesenteric adipose tissue (Hong *et al.*, 2005). Interestingly, the level of FFA2 mRNA increased in the murine 3T3-L1 cell line as they differentiate from preadipocytes to adipocytes (Hong *et al.*, 2005).

Besides, FFA2 expression was detected by immunohistochemistry in human and rat colon, in particular in enteroendocrine cells that express GLP-1 and PYY (Kaji *et al.*, 2011; Karaki *et al.*, 2006; Karaki *et al.*, 2008; Tazoe *et al.*, 2008; Tazoe *et al.*, 2009). In rat, presence of FFA2 mRNA has been confirmed by real-time PCR in the colon and in the proximal parts of the gut at a lower level (Dass *et al.*, 2007).

FFA2 mRNA were also found in the murine insulinoma cell line Min6 and in pancreatic islets isolated from mice (Kedebe *et al.*, 2009).

Human FFA2 mRNA were also detected in various immune cells, such as peripheral blood leukocytes, neutrophils, monocytes and in the spleen (Brown *et al.*, 2003; Cox *et al.*, 2009; Maslowski *et al.*, 2009; Nilsson *et al.*, 2003).

Taken together, these different results may suggest a role for FFA2 in the gut, the adipose tissue and the immune system.

4.3. Physiological functions

4.3.1. Stimulation of adipogenesis and inhibition of lipolysis

The effects of SCFAs on adipocytes and lipolysis have been explored using three kinds of models, namely 3T3-L1 cells, mouse primary adipocytes and *in vivo* in mice.

3T3-L1 mouse cells are commonly used as *in vitro* model for preadipocytes and can be easily differentiated into adipocytes in seven days under treatment including insulin, 3-isobutyl-1-methylxanthine (IBMX) and dexamethasone (Ge *et al.*, 2008; Hong *et al.*, 2005; Lee *et al.*, 2008). Treatment of 3T3-L1 cells with propionate or acetate at 0.1µM during the whole process of differentiation elevates their degree of differentiation into adipocytes (Hong *et al.*, 2005). mRNA analysis during the differentiation process shows an increased expression of FFA2 after treatment with SCFAs (Hong *et al.*, 2005). Moreover, gene silencing of FFA2 using siRNA inhibits differentiation of 3T3-L1 cells (Hong *et al.*, 2005). Taken together, these data suggest that FFA2 is required for the differentiation of 3T3-L1 in adipocytes (Hong *et al.*, 2005).

Besides, in differentiated 3T3-L1, propionate and acetate are able to strongly reduce isoprenalin-induced lipolysis in a dose-dependent manner (Ge *et al.*, 2008; Hong *et al.*, 2005; Lee *et al.*, 2008). The inhibitory effect of propionate and acetate on lipolysis is diminished when FFA2 is silenced by siRNA, suggesting a gene-specific effect of FFA2 on lipolysis (Hong *et al.*, 2005). Acetate-induced inhibition of lipolysis in 3T3-L1 is also sensitive to pertussis toxin (PTX), suggesting that the inhibitory effect of acetate is mediated by the $G\alpha_i$ component of the FFA2 signaling pathway (Ge *et al.*, 2008).

In mouse primary adipocytes, treatment with propionate or acetate at 100µM provokes a 2-fold decrease of glycerol release (Ge *et al.*, 2008). This SCFA-dependent decrease of

glycerol release is abolished in primary adipocytes from FFA2 knockout mice, suggesting a gene-specific anti-lipolytic activity of FFA2 (Ge *et al.*, 2008).

In vivo, an intraperitoneal injection of acetate in a mouse leads to a dose-dependent decrease in the plasmatic free fatty acids (FFA) levels. The maximal effect was observed with a single dose of 500mg/kg sodium acetate, leading to a transient diminution of plasmatic FFA levels of around 30% of the initial level 15min after injection (Ge *et al.*, 2008). In FFA2 knockout mice, the plasma FFA–lowering activity of acetate was not observed, indicating that the effect of acetate is mediated by FFA2 (Ge *et al.*, 2008). Given that dyslipidemia often occurs in patients suffering from obesity, diabetes or insulin resistance, the effects of acetate were also tested on *ob/ob* mice (Ge *et al.*, 2008). *ob/ob* mice are a common *in vivo* model used in metabolic disease research. They are leptin deficient, exhibit hyperphagia, hyperglycemia, hyperinsulinemia and early-onset morbid obesity (Tschöp and Heiman, 2001). In *ob/ob* mice, administration of acetate was able to lower the plasma FFA levels by 30%, suggesting that FFA2 is still functional in obese models (Ge *et al.*, 2008).

4.3.2. Anti-inflammatory effect

FFA2 is suspected to play also a role in the immune system (Nilsson *et al.*, 2003). The expression of FFA2 during the differentiation of murine leukocyte progenitors into monocytes or granulocytes is increased by around 9 times (Senga *et al.*, 2003). In human monocytes, FFA2 mRNA level is increased by around 5 fold after a 3-hour stimulation with bacterial lipopolysaccharide (Senga *et al.*, 2003).

Functions of FFA2 in the immune system have been investigated in more detail in human, rat and mouse immune cells and also on models for inflammatory bowel diseases (Cox *et al.*, 2009; Maslowski *et al.*, 2009; Sina *et al.*, 2009; Tedelind *et al.*, 2007; Vinolo *et al.*, 2009). Thus, SCFAs increased the secretion of anti-inflammatory cytokines, inhibited the secretion of some pro-inflammatory cytokines and acted as chemoattractant for neutrophils to inflammatory sites (Cox *et al.*, 2009; Maslowski *et al.*, 2009; Sina *et al.*, 2009; Tedelind *et al.*, 2007; Vinolo *et al.*, 2009). Since the beneficial effects of SCFAs were lost in FFA2 knockout mice, the observed effects were supposed to

be owed to FFA2 and not to another receptor, like for instance FFA3 (Maslowski *et al.*, 2009).

4.3.3. Additional potential roles for FFA2

Another function for FFA2 in relation to metabolic organs has been suggested. In bovine subcutaneous primary adipocytes, SCFAs would be involved in the induction of the leptin gene (Soliman *et al.*, 2007). Given that acetate is as potent as propionate in increasing leptin expression, this effect is probably due to FFA2 and not to FFA3 (Soliman *et al.*, 2007). However, bovine and human SCFA metabolisms are very different: in ruminants, SCFAs constitute the main source of energy which is not the case in human (Soliman *et al.*, 2007).

In the gut, since FFA2 seems to be colocalized with GLP-1- and PYY-secreting enteroendocrine cells, one can assume that stimulation of FFA2 may enhance the secretion of GLP-1.

5. The free fatty acid receptor 3

Although FFA2 and FFA3 share some similarities regarding their aminoacid sequences and ligands, FFA3 exhibits its own specificity for G proteins, expression pattern and physiological roles.

5.1. Signal transduction

Several reports suggest the coupling of FFA3 solely with the pertussis toxin (PTX)-sensitive $G\alpha_i$ G protein (Brown *et al.*, 2003; LePoul *et al.*, 2003; Xiong *et al.*, 2004). For example, in CHO-K1 cells transiently expressing mouse FFA3, SCFAs were able to suppress forskolin-induced cAMP production and this effect was sensitive to PTX (LePoul *et al.*, 2003). In Hek293T cotransfected with hFFA3 and the $G\alpha_{o1}$ protein, SCFAs were able to activate the receptor in GTPγ[^{35}S] assays (Brown *et al.*, 2003). In *Xenopus* melanophores heterologously expressing hFFA3, stimulation with SCFAs provoked pigment aggregation, which indicates a decrease in cytosolic cAMP concentration (Xiong *et al.*, 2004). In contrast to FFA2, FFA3 was not able to induce Ca^{2+} mobilization, unless it

is artificially coupled to the chimeric Ca^{2+}-inducing $G\alpha_{qG66Di5}$ protein (Stoddart *et al.*, 2008b).

5.2. Tissue distribution

FFA3 seems to have a more widespread expression pattern than FFA2.

High levels of FFA3 expression were detected in the gastrointestinal tract, in particular in the ileum and the colon in mouse and in human (Dass *et al.*, 2007; Gordon *et al.*, 2010; Samuel *et al.*, 2008; Tazoe *et al.*, 2009). More precisely, FFA3 was colocalized with cholecystokinin (CCK)-secreting cells in mouse and with PYY-secreting enteroendocrine cells in human (Gordon *et al.*, 2010; Samuel *et al.*, 2008). Remarkably, FFA2 and FFA3 are not localized in the same colonic enteroendocrine cells in human (Tazoe *et al.*, 2009).

Expression of FFA3 has been also found in adipose tissue, but this finding remains controversial. Some could detect FFA3 mRNA in human adipocytes at high levels (Brown et al, 2003; Xiong *et al.*, 2004) whereas others could only detect low levels of FFA3 mRNA (LePoul *et al.*, 2003; Zaibi *et al.*, 2010). In the murine preadipocytic 3T3-L1 cell line, FFA3 expression increased upon differentiation, although remaining at relatively low levels (Brown et al, 2003). Another study could not detect any FFA3 mRNA in a variety of adipose tissues from mouse or in differentiated 3T3-L1 cells (Hong *et al.*, 2005). FFA3 mRNA has been successfully detected in subcutaneous and perirenal adipose tissues from goat at a substantial level (Mielenz *et al.*, 2008).

In addition, FFA3 is expressed in the murine insulinoma cell line Min6, in mouse islets and in human pancreas (Kedebe *et al.*, 2009; Leonard *et al.*, 2007; Zaibi *et al.*, 2010). Interestingly, the FFA3 gene was found to be upregulated in pancreatic islets from *db/db* diabetic mice compared to wild-type mice (Leonard *et al.*, 2007).

Taken together, these results suggest a role for FFA3 in the gut, adipose tissue, and pancreatic islets.

5.3. Physiological functions

5.3.1. Nutrient sensing and PYY secretion from enteroendocrine cells

FFA3 may be involved in the sensing of SCFAs resulting from the degradation of carbohydrates by the gut microbiota (Karra *et al.*, 2009; Tazoe *et al.*, 2009). Interestingly, in FFA3-knockout mice, PYY secretion from the gut was significantly

reduced in comparison with the wild-type mice (Gordon *et al.*, 2010; Samuel *et al.*, 2008). Moreover, PYY secretion is increased by 4 folds when mice are inoculated with gut bacteria vs. germ-free mice (Gordon *et al.*, 2010; Samuel *et al.*, 2008). These results are in line with the finding that FFA3 expression is colocalized with PYY in enteroendocrine cells (Tazoe *et al.*, 2009). Moreover, butyrate and propionate, but not acetate, induce the release of PYY from rat colon (Plaisancié *et al.*, 1996). PYY has been shown to inhibit a range of biological processes, including food intake, gastric emptying, pancreatic and intestinal secretions and gut motility (Karra *et al.*, 2009). FFA3 would then be involved in energy balance via an enhanced PYY secretion, but this theory remains to be verified.

5.3.2. Leptin secretion from adipocytes

Leptin is a circulating peptide hormone that is secreted mainly by white adipose tissue. Homozygous mutation of the *ob* leptin gene leads to hyperphagia, extreme obesity, diabetes, neuroendocrine abnormalities and infertility (Kelesidis *et al.*, 2010). Therefore, leptin is considered a key player in regulation of energy homeostasis, metabolism, neuroendocrine function and reproduction (Kelesidis *et al.*, 2010).

FFA3 stimulation with SCFAs enhanced leptin production and leptin gene expression in the Ob-luc murine adipocyte cell line and in murine primary adipocytes (Xiong *et al,* 2004). Propionate-induced stimulation of leptin gene expression in Ob-luc cells could be knocked down by infection with a virus containing FFA3-specific siRNA (Xiong *et al,* 2004). Moreover, *in vivo* acute administration of propionate increases circulating leptin levels in mice (Xiong *et al,* 2004). SCFAs were also able to increase leptin secretion from bovine primary adipocytes (Soliman *et al.*, 2007).

Collectively, these facts support a possible role of FFA3 in PYY and leptin secretion. However, no data about the effect of SCFAs on human adipocytes or enteroendocrine cells are available to date.

6. FFA2 and FFA3 as potential therapeutic targets for metabolic diseases

Based on the possible physiological roles listed above, FFA2 and FFA3 have gained interest as potential therapeutic targets for several diseases related to metabolic disorders. In association with an appropriate diet, modification of lifestyle, or with other medicines, agonists for FFA2 or FFA3 would probably help improving metabolic conditions.

Indeed, agonists for FFA2 would theoretically lower free fatty acid levels in blood, thus ameliorating an eventual dyslipidemia. Actually, promising new synthetic agonists for FFA2 exhibit pronounced anti-lipolytic and plasma free fatty acid-lowering effects in mouse (Ge *et al.*, 2008). Besides, a treatment with FFA2 agonists would possibly reduce intestinal inflammation, thus reducing the risk of colitis, as proposed by Cox *et al.* (2009). Expected effects of FFA2 agonists would also concern an enhanced leptin secretion from adipocytes that would decrease appetite and stimulate energy expenditure.

Concerning agonists for FFA3, they would allow a better control of appetite and obesity via the enhancement of the secretion of two key hormones in the regulation of energy homeostasis, namely leptin and PYY.

7. Problematic and aims of the study

As previously mentioned, FFA2 and FFA3 receptors have become attractive therapeutic targets, mainly due to their potential beneficial effects against a variety of metabolic diseases. However, scientific knowledge on FFA2 and FFA3 remains limited.

For instance, available data about FFA2 and FFA3 expression is inconsistent. In this study, we will first attempt to clarify the expression pattern of the receptors in a variety of cell lines and tissues.

Moreover, although several endogenous and exogenous ligands for FFA2 and FFA3 have been described so far, little is known about the pharmacology of the receptors. The second aim of this study will be to dissect the signaling pathways engendered in response to endogenous and synthetic agonists in established cell lines and to determine if the synthetic agonists act as allosteric or orthosteric agonists.

To complete the pharmacological profile of the receptors, we will then determine by site-directed mutagenesis which aminoacids residues are required for ligand recognition.

The final purpose of this study will be to design structural models for hFFA2 and hFFA3 that may aid future drug design for these receptors and thus help to generating selective high affinity ligands that could be potential drugs against metabolic disorders.

Part 2

Material and methods

1. Chemicals and reagents

A	Agar	Invitrogen, Karlsruhe, Germany
	Agarose	Biorad, Hercules, CA
	Ampicillin, solution	US Biological, Swampscott, MA
B	Beta-mercaptoethanol	Sigma Aldrich, Steinheim, Germany
	Bovine serum albumin	Sigma Aldrich, Steinheim, Germany
	Bovine serum albumin (fatty-acid free)	Serva, Heidelberg, Germany
C	Calcium chloride	Merck, Darmstadt, Germany
	Chloroform-isoamylalcohol	Sigma Aldrich, Steinheim, Germany
	Collagenase II	Serva, Heidelberg, Germany
	Corticosterone	Sigma Aldrich, Steinheim, Germany
	Cyclopropanecarboxylate	Acros organics, Geel, Belgium
D	Dexamethasone	Sigma Aldrich, Steinheim, Germany
	Dimethylsulfoxide	Serva, Heidelberg, Germany
E	Ethanol	Sigma Aldrich, Steinheim, Germany
	Ethidium bromide, solution	Sigma Aldrich, Steinheim, Germany
F	Forskolin	Sigma Aldrich, Steinheim, Germany
G	Glucose (α-D-glucose)	Sigma Aldrich, Steinheim, Germany
H	Hank's balanced salt solution (HBSS)	Invitrogen, Karlsruhe, Germany
	HEPES, solution	Invitrogen, Karlsruhe, Germany
	Hydrochloric acid	Merck, Darmstadt, Germany
	Hygromycin B, solution	Invitrogen, Karlsruhe, Germany
I	Insulin (from bovine pancreas)	Sigma Aldrich, Steinheim, Germany
	Ionomycin	Sigma Aldrich, Steinheim, Germany
	3-isobutyl-1-methylxanthine (IBMX)	Sigma Aldrich, Steinheim, Germany
	Isopropanol	Sigma Aldrich, Steinheim, Germany
K	Kanamycin, solution	Sigma Aldrich, Steinheim, Germany
L	Luria-Bertoni (LB) Miller's medium	US Biological, Swampscott, MA
M	Magnesium sulfate	Merck, Darmstadt, Germany
	Methanol	Sigma Aldrich, Steinheim, Germany
	Milk powder	Sigma Aldrich, Steinheim, Germany
N	Non-enzymatic cell dissociation buffer	Sigma Aldrich, Steinheim, Germany
	Nuclease-free water	Qiagen, Hilden, Germany

P	Pertussis toxin (PTX), solution	Sigma Aldrich, Steinheim, Germany
	Phenol-chloroform-isoamylalcohol	Sigma Aldrich, Steinheim, Germany
	Phenylmethanesulphonylfluoride (PMSF)	Serva, Heidelberg, Germany
	Phorbol myristate acetate	Sigma Aldrich, Steinheim, Germany
	Phosphate buffered saline (PBS)	Invitrogen, Karlsruhe, Germany
	Ponceau-S solution	Sigma Aldrich, Steinheim, Germany
	Potassium chloride	Merck, Darmstadt, Germany
	Potassium dihydrogen phosphate	Merck, Darmstadt, Germany
	Probenecid	Sigma Aldrich, Steinheim, Germany
S	Sodium acetate	Serva, Heidelberg, Germany
	Sodium bicarbonate	Merck, Darmstadt, Germany
	Sodium butyrate	Sigma Aldrich, Steinheim, Germany
	Sodium chloride	Merck, Darmstadt, Germany
	Sodium dodecyl sulphate (SDS)	Serva, Heidelberg, Germany
	Sodium hydrogenphosphate	Sigma Aldrich, Steinheim, Germany
	Sodium hydroxide, solution	Carl Roth, Karlsruhe, Germany
	Sodium propionate	Sigma Aldrich, Steinheim, Germany
	Sodium pyruvate, solution	Lonza, Verviers, Belgium
T	Tris-borate-EDTA (TBE) buffer	Carl Roth, Karlsruhe, Germany
	Transfer buffer for Western Blot	Serva, Heidelberg, Germany
	Tris-(hydroxymethyl)-amino-methane (Tris)	Sigma Aldrich, Steinheim, Germany
	Trypan blue, solution	Serva, Heidelberg, Germany
	Trypsin-EDTA, solution	Lonza, Verviers, Belgium
	Tween-20	Sigma Aldrich, Steinheim, Germany
Z	Zeocin™ (=phleomycin D1)	Invitrogen, Karlsruhe, Germany

All cell culture media were purchased from Lonza (Belgium) and fetal bovine serum from Biological Industries (Beit Haemek, Israel).

Rosiglitazone, Compound A and Compound B were synthesized by the chemistry department of Boehringer Ingelheim GmbH & Co. KG in Biberach an der Riss, Germany.

2. Cell culture and cell differentiation

2.1. Generalities

All cell types were cultured in an incubator at 37°C, 5% CO_2 and 95% humidity. For passaging, we washed the cells with sterile phosphate buffered saline (PBS) without calcium and magnesium, let them sit in a trypsin/EDTA solution at 37°C for 1 to 3min, centrifuged them at 200*g* for 5min and replate a part of the resuspended pellet in the desired medium and dish. When needed, cells were counted either manually in a Fuchs-Rosenthal chamber or with a Countess device (Invitrogen). In brief, cells were pelleted,

resuspended in medium, diluted 1:10 in PBS, then 1:2 in Trypan blue solution and counted. For PTX treatments, cells were incubated overnight (13-18h) in the appropriate medium supplemented with 100ng/ml PTX.

2.2. Hek293 Flpin

Hek293 Flpin cells are widely used cells derived from human embryonic kidney. They were purchased from Invitrogen. Untransfected cells were cultured in Dulbecco's modified Eagle's Medium (DMEM) supplemented with 10% FCS and 100µg/ml Zeocin, whereas recombinant cells were grown in DMEM supplemented with 10% (v:v) FCS and 100µg/ml Hygromycin B.

2.3. Ins1E

The Ins1E cell line derives from cells isolated from a rat insulinoma, i.e. a pancreatic islet β-cell tumor. They were cultured in Roswell Park Memorial Institute (RPMI) 1640 medium, supplemented with 10% FCS, 50µM β-mercaptoethanol, 10mM HEPES and 1mM sodium pyruvate, in collagen I-coated flasks.

2.4. Min6C4

Min6C4 cell line is a subclone of Min6 mouse insulinoma cell line that has been selected for its capacity to secrete high amounts of insulin. Min6C4 were cultured in DMEM supplemented with 15% FCS and 50µM β-mercaptoethanol. We obtained them from Dr. Jun-Ichi Miyazaki (Osaka, Japan).

2.5. STC-1

STC-1 cells derive from a mouse enteroendocrine tumor. They were cultured in DMEM supplemented with 10% FCS.

2.6. NCI-H716

NCI-H716 cells derive from human enteroendocrine cells. They were cultured in RPMI 1640 supplemented with 10% FCS. Cell differentiation was promoted by culturing the

cells for 9 days on a plate coated with a thin layer of Matrigel™ matrix (Becton Dickinson, Cat. 354603).

2.7. THP-1

THP-1 is a human monocytic cell line. THP-1 cells were cultured in RPMI 1640 supplemented with 10% FCS. Cells were differentiated into macrophages by culturing in medium containing 20ng/ml phorbol myristate acetate for 2 days.

2.8. 3T3-L1

3T3-L1 is a mouse preadipocytic cell line. 3T3-L1 cells were cultured in DMEM supplemented with 10% FCS. The cells were differentiated following a previously described protocol (Hong *et al.*, 2005). In brief, the cells were treated upon confluency for 2 days with 0.5mM IBMX, 1µM dexamethasone and 1.7µM insulin in DMEM supplemented with 10% FCS. After 48h, medium was replaced by DMEM supplemented with 10% FCS and cells were maintained in this medium until differentiation (for at least 7 days).

2.9. Isolation and differentiation of rat adipocytes

Rat preadipocytes were isolated from male Wistar rats, mainly as previously described (Rodbell, 1964). Epididymal and perirenal fat tissues were collected, finely minced in a sterile environment and digested with 1g/l collagenase II in Krebs Ringer buffer (118mM NaCl, 1.18mM KH_2PO_4, 4.83mM KCl, 1.18mM $MgS0_4$, 2.54mM $CaCl_2$, 25mM $NaHCO_3$, 11.1mM glucose, 20g/l bovine serum albumin) by incubation at 37°C for 1h under stirring. The fat cell homogenate was then filtered through a gauge and preadipocytes were pelleted by centrifugation at 400*g* for 10min. Preadipocytes were then seeded in DMEM + 5% FCS in 6-well plates at $3.5x10^5$ cells/well.

Two days after seeding, preadipocytes were confluent. They received a first treatment for 2 days consisting of 0.5mM IBMX, 100nM corticosterone, 1µM insulin in DMEM supplemented with 5% FCS. Medium was then changed and the cells received a second treatment consisting of 100nM corticosterone and 1µM insulin in DMEM supplemented with 5% FCS until the end of the experiment.

2.10. Preparation of peripheral blood mononuclear cells

Peripheral blood mononuclear cells were isolated from human blood by density gradient centrifugation using Lymphoprep tubes (Axis shield, Oslo, Norway). Erythrocytes and granulocytes are trapped at the bottom of the tube, whereas blood mononuclear cells (mainly containing lymphocytes, macrophages and monocytes) float at the interphase between Ficoll-Isopaque and plasma. The content of the final fraction was checked under microscope before use.

3. Molecular biology

3.1. General molecular biology techniques

3.1.1. Culture medium for bacteria

To grow bacteria, we routinely used Luria-Bertoni (LB) Miller-modified medium, consisting of 10g/l peptone, 5g/l yeast extract, 10g/l NaCl. Solidified medium for plates were obtained by addition of 5g/l agar to liquid LB Miller-modified medium prior to sterilization.

3.1.2. Bacterial transformation

For molecular biology purposes, we routinely used thermocompetent TOP10 *Escherichia coli* bacteria (Invitrogen) with the following transformation protocol. Bacteria were thawed on ice and 0.1-2µg DNA were added to the bacteria for an additional 30min-period on ice. Bacteria were then heat shocked from ice to 42°C for 30s in a heat-block, then placed back on ice for 2min. Bacteria were able to recover from the transformation by incubation at 37°C for 1h, 150rpm, in 500µl SOC medium (Invitrogen). Bacteria were then spread on LB-plates containing the appropriate antibiotic.

3.1.3. Expansion and preparation of plasmidic DNA

For cloning and sequencing purposes, plasmidic DNA was extracted from 1ml- to 10ml-overnight liquid cultures using a RNeasy Miniprep kit (Qiagen). For transfection purposes, endotoxin-free plasmidic DNA was obtained from larger overnight culture volumes (50 to 250ml) using an EndoFree Plasmid Maxi kit (Qiagen).

3.1.4. Standard polymerase chain reaction

For cloning purposes, PCR were performed using the high-fidelity AccuPrime *Pfx* DNA polymerase (Invitrogen). Classically, we used 0.1 to 100ng DNA template, 0.3µM of each primer, 1U AccuPrime *Pfx* polymerase and 1X AccuPrime *Pfx* reaction mix, in a total volume of 20µl. PCR program was the following : first, at 95°C for 2min to denature the DNA template, then 15 to 30 cycles consisting of periods at 95°C for 15s, 55-75°C (depending on the size and the GC content of the primers) for 30s for the annealing step, 68°C for 1min/kb for the extension phase, and finally an additional step at 68°C for 2min to terminate the reaction.

3.1.5. Standard DNA restriction

Classically, 0.1 to 10µg DNA was restricted with 1-10U endonuclease in a 20µl reaction volume for 15min to 4h at 37°C in a heat block. If required, restriction enzymes were heat inactivated by incubating at 65°C or 80°C for 20min, as per the manufacturer's instructions. If the enzyme could not be heat inactivated, DNA was purified using the QIAquick nucleotide removal kit (Qiagen). All restriction enzymes and reaction buffers were purchased from New England BioLabs (Ipswich, MA).

3.1.6. Agarose gel electrophoresis

DNA was routinely loaded in 1X Blue Juice (Invitrogen) on precast 1.2% agarose E-Gels (already containing 0.1-0.3mg/l ethidium bromide; Invitrogen), and run for 30min at 70V before imaging under UV light.

For preparative gels, we prepared gels containing 0.6-2% agarose (depending on the size of the band to extract) in 1X TBE buffer (0.1mM Tris-borate pH 8.3, 2mM EDTA). 1X TBE buffer was also used as running buffer for the electrophoresis. Gels were then incubated for 5min in a 1mg/l ethidium bromide bath before imaging under UV light. DNA fragments were then extracted from preparative agarose gels using the QIAQuick gel extraction kit (Qiagen) as per the manufacturer's instructions.

3.1.7. Dephosphorylation of DNA fragments

To avoid self-ligation of vectors, we used the shrimp alkaline phosphatase (Roche Applied Science). We incubated 20-50ng DNA for 15min at 37°C with 1U alkaline

phosphatase in 1X dephosphorylation buffer (Roche Applied Science). The enzyme was then inactivated by incubation at 65°C for 15min.

3.1.8. Ligation

For ligation of DNA fragments, we used the Rapid DNA ligation kit from Roche. Typically, we incubated 50ng of dephosphorylated vector with 150ng insert, with 5U T4 DNA ligase in 1X ligation buffer. We performed ligation for 1h at room temperature (RT) for sticky-ended fragments and overnight at 4°C for blunt-ended fragments.

3.1.9. DNA sequencing

After each cloning or subcloning step and prior to transfection, gene coding sequences were checked by sequencing with adequate vector- or gene-specific primers (Operon, Ebersberg, Germany).

3.2. Cloning of hFFA2 and hFFA3

3.2.1. Cloning of hFFA2

The coding sequence of hFFA2 (NM_005306) was amplified by PCR from a commercial DNA template (Multispan, Hayward, CA) using the forward primer 5'-AAAAAGCAGGCTTCGAAGGAGATAGAACCATGCTGCCGGACTGG-3' and the reverse primer 5'-GAAAGCTGGGTCCTACTCTGTAGTGAAGTC-3'. A second PCR was ran to add Gateway adapters to the product of the first PCR, with the forward primer 5'-GGGGACAAGTTTGTACAAAAAAGCAGGCT-3' and the reverse primer 5'-GGGGACCACTTTGTACAAGAAAGCTGGGT-3'. The amplified product was then inserted by B/P Gateway recombination in the donor vector pENTR221 (Invitrogen). We performed the L/R Gateway recombination in pEF5/FRT/V5DEST (Invitrogen).

3.2.2. Cloning of hFFA3

The coding sequence of hFFA3 (NM_005304) was amplified by PCR from a commercial DNA template (Multispan, Hayward, CA) using the forward primer 5'-ACTATGCTCGAGGGATCTGGAGATACAGGCCC-3' and the reverse primer 5'-CTGCGCGGATCTAAGCTTCTAGCTTTCAGCACAGGCC-3'. The amplified product was then

subcloned in the pGA7 vector (Geneart, Regensburg, Germany), flanked by *allL* recombination cassettes. We performed the L/R Gateway recombination in pEF5/FRT/V5-DEST (Invitrogen).

3.3. Site-directed mutagenesis

We generated point mutations in hFFA2 and hFFA3 using the QuikChange site-directed mutagenesis kit (Stratagene). We performed the PCR with 50ng DNA template, 125ng of each primer, 2.5U *PfuTurbo* DNA polymerase, 1X dNTP mix, 1X buffer (Invitrogen) in a final volume of 50µl/tube. The PCR program was the following : 95°C for 30s, then 18 cycles at 95°C for 30s, 55°C for 60s and 68°C for 70s. The remaining methylated, non-mutated template was digested by incubation with DpnI (10U/tube; Stratagene) at 37°C for 1h. Mutagenesis reaction product (1µl) was then used to transform 50µl supercompetent XL1-Blue bacteria (Stratagene; see section 3.1.3 for transformation protocol).

FFA3 mutation	Primer sequence
M72A	GTTCCTGCCTTTCCGC**GC**GGTGGAGGCAGCCAATG CATTGGCTGCCTCCACC**GC**GCGGAAAGGCAGGAAC
F96A	CTCTCTGGATTCATCTTC**GC**CACCACCATCTATCTCAC GTGAGATAGATGGTGGTG**GC**GAAGATGAATCCAGAGAG
Y100A	CTTCTTCACCACCATC**GC**TCTCACCGCCCTCTTCC GGAAGAGGGCGGTGAGA**GC**GATGGTGGTGAAGAAG
R185A	GCCATCCTCCTGCCCGTG**GC**GCTGGAGATGGCTGTGGT ACCACAGCCATCTCCAGC**GC**CACGGGCAGGAGGATGGC
R185K	GCCATCCTCCTGCCCGTG**AA**GCTGGAGATGGCTGTGGT ACCACAGCCATCTCCAGC**TT**CACGGGCAGGAGGATGGC
N242A	GTCTGCTTTGGGCCCTAC**GC**CGTGTCCCATGTCGTGG CCACGACATGGGACACG**GC**GTAGGGCCCAAAGCAGAC
H245A	CTGCTTTGGGCCCTACAACGTGTCC**GCA**GTCGTGGGCTATATCTGCGGT ACCGCAGATATAGCCCACGAC**TGC**GGACACGTTGTAGGGCCCAAAGCAG
H245N	GGCCCTACAACGTGTCC**A**ATGTCGTGGGCTATATC GATATAGCCCACGACAT**T**GGACACGTTGTAGGGCC
H245F	CTGCTTTGGGCCCTACAACGTGTCC**TT**TGTCGTGGGCTATATCTGCGGT ACCGCAGATATAGCCCACGACA**AA**GGACACGTTGTAGGGCCCAAAGCAG
R258A	TATCTGCGGTGAAAGCCCGGCGTGG**GC**GATCTACGTGACGCTTCTCAGCA TGCTGAGAAGCGTCACGTAGATC**GC**CCACGCCGGGCTTTCACCGCAGATA
R258K	CTGCGGTGAAAGCCCGGCGTGG**AA**GATCTACGTGACGCTTCTCA TGAGAAGCGTCACGTAGATC**TT**CCACGCCGGGCTTTCACCGCAG

Table 1 : Sequences of the primers used for site-directed mutagenesis of hFFA3.

Each primer is given in 5'-3' direction, the top primer being the forward primer and the bottom primer being the reverse primer. Mutated nucleotides appear in bold and underlined.

FFA2 mutation	Primer sequence
I66A	GCTGCTGCCCTTCAAG**GC**CATCGAGGCTGCGTCGAAC GTTCGACGCAGCCTCGATG**GC**CTTGAAGGGCAGCAGC
S86A	GGTCGTCTGCGCCCTCACG**GC**TTTTGGCTTCTACAGCAGC GCTGCTGTAGAAGCCAAAA**GC**CGTGAGGGCGCAGACGACC
S86G	GGTCGTCTGCGCCCTCACG**G**GTTTTGGCTTCTACAGCAGC GCTGCTGTAGAAGCCAAAAC**C**CGTGAGGGCGCAGACGACC
F89A	CCTCACGAGTTTTGGC**GC**CTACAGCAGCATCTACTG CAGTAGATGCTGCTGTAG**GC**GCCAAAACTCGTGAGG
Y90A	CTCACGAGTTTTGGCTTC**GC**CAGCAGCATCTACTGC GCAGTAGATGCTGCTG**GC**GAAGCCAAAACTCGTGAG
Y94A	GCTTCTACAGCAGCATC**GC**CTGCAGCACGTGGCTCC GGAGCCACGTGCTGCAG**GC**GATGCTGCTGTAGAAGC
S96A	ACAGCAGCATCTACTGC**GC**CACGTGGCTCCTGGCGG CCGCCAGGAGCCACGTG**GC**GCAGTAGATGCTGCTGT
H140A	GGGTTATGTCCTTTGGT**GC**CTGCACCATCGTGATCA TGATCACGATGGTGCAG**GC**ACCAAAGGACATAACCC
R180A	ACGTGGTGCTGCCCGTG**GC**GCTGGAGCTGTGCCTG CAGGCACAGCTCCAGC**GC**CACGGGCAGCACCACGT
R180K	ACGTGGTGCTGCCCGTG**AA**GCTGGAGCTGTGCCTG CAGGCACAGCTCCAGC**TT**CACGGGCAGCACCACGT
Y238A	TGGTGTGCTTCGGACCT**GC**CAACGTGTCCCACCTGG CCAGGTGGGACACGTTG**GC**AGGTCCGAAGCACACCA
N239A	GTGTGCTTCGGACCTTAC**GC**CGTGTCCCACCTGGTG CACCAGGTGGGACACG**GC**GTAAGGTCCGAAGCACAC
H242N	GACCTTACAACGTGTCC**A**ACCTGGTGGGGTATCACC GGTGATACCCCACCAGGT**T**GGACACGTTGTAAGGTC
R255A	AGAAAAAGCCCCTGGTGG**GC**GTCAATAGCCGTGGTGTTC GAACACCACGGCTATTGAC**GC**CCACCAGGGGCTTTTTCT
R255K	AGAAAAAGCCCCTGGTGG**AA**GTCAATAGCCGTGGTGTTC GAACACCACGGCTATTGAC**TT**CCACCAGGGGCTTTTTCT
S256A	GCCCCTGGTGGCGG**G**CAATAGCCGTGGTGTTCAG CTGAACACCACGGCTATTG**C**CCGCCACCAGGGGC
S262A	CAATAGCCGTGGTGTTC**GC**TTCACTCAACGCCAGTC GACTGGCGTTGAGTGAA**GC**GAACACCACGGCTATTG
S263A	TAGCCGTGGTGTTCAGT**G**CACTCAACGCCAGTCTGG CCAGACTGGCGTTGAGTG**C**ACTGAACACCACGGCTA
H242A	GGACCTTACAACGTGTCC**GC**CCTGGTGGGGTATCACCAG CTGGTGATACCCCACCAGG**GC**GGACACGTTGTAAGGTCC
H242F	GGACCTTACAACGTGTCC**TT**CCTGGTGGGGTATCACCAG CTGGTGATACCCCACCAGG**AA**GGACACGTTGTAAGGTCC

Table 2 : Sequences of the primers used for site-directed mutagenesis of hFFA2.

Each primer is given in 5'-3' direction, the top primer being the forward primer and the bottom primer being the reverse primer. Mutated nucleotides appear in bold and underlined.

3.4. Principle of the Flpin system and establishment of stable cell lines

3.4.1. Principle and advantages of the Flpin system

The Flpin system allows the integration of the gene of interest (GOI) at a specific location in the genome of mammalian cells thanks to Flp Recombination Target (FRT) cassettes (Fig. 10).

It ensures the generation of an isogenic recombinant cell line, i.e. the GOI is inserted at the same site in every cell, therefore eliminating the necessity to test the GOI expression level in each cell clone. One can pool the cells together directly after clone selection und use them for further experiments.

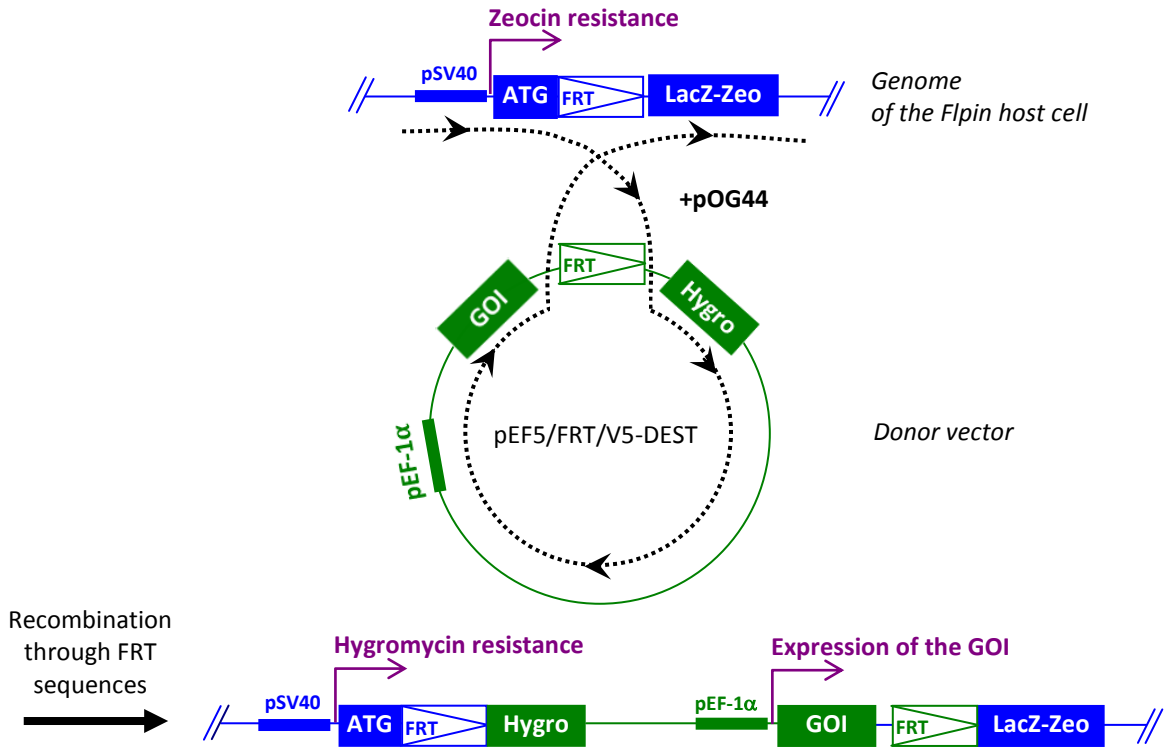

Fig. 10 : Principle of the Flpin system.

The genome of the Flpin cell lines contains a LacZ-Zeo gene in frame with a start codon (ATG) and a FRT cassette, conferring the Zeocin resistance on untransfected cells. Cells are then cotransfected with pOG44 and pEF5/FRT/V5-DEST containing the gene of interest (GOI). pOG44 encodes for the enzyme that ensures the recombination between the FRT cassette from the cell line and the FRT cassette from the pEF5/FRT/V5-DEST vector. After recombination, the GOI is inserted in the genome and its expression is under the control of the elongation factor-1α promoter (pEF-1α); the start codon (ATG) is no longer in frame with the Zeocin resistance but with the Hygromycin resistance.

3.4.2. Stable transfection and selection of recombinant cells

Hek293 Flpin cells were seeded in collagen I-coated 6-well plates in DMEM supplemented with 10% FCS, to be 50 to 80% confluent on the next day. Cells were transfected using Polyfect (Qiagen) as per the manufacturer's instructions. Two days after transfection, transfected cells were selected with DMEM supplemented with 10% FCS and 100µg/ml HygromycinB. Two days later, untransfected cells started dying and medium was then replaced every day. Around 2 weeks later, visible clones appeared. Cell clones were pooled, thoroughly resuspended by pipetting up and down and further maintained in culture in selection medium.

3.5. Gene expression analysis

3.5.1. RNA extraction

The RNA extraction protocol that we used is based on the RNA binding properties of a silica gel membrane. Biological samples were first lysed in RLT buffer (Qiagen). This buffer contains β-mercaptoethanol and guanidium isothiocyanate, both highly denaturing agents, that degrade RNases, thus ensuring isolation of intact RNA. Lysates were then homogenized through QiaShredder columns (Qiagen) at 20000*g* for 1min in order to reduce their viscosity by shearing the genomic DNA and remove any insoluble material. One volume 70% ethanol was added to the lysates to provide appropriate binding conditions. Contaminants were washed away with buffer RW1 (Qiagen), DNA traces were digested with RNAse-free DNAse set (Qiagen) and RNA was finally eluted in nuclease-free water. RNA samples were stored at -80°C.

For fat cells, we also used a RNeasy kit, but with the following modifications. Once differentiated, fat cells were lysed in a 1:1 (v:v) mix of RLT buffer and phenol-chloroform-isoamylalcohol (25:24:1; v:v). Lysates were subsequently centrifuged at 10000*g* for 5min, then 1 volume of chloroform-isoamylalcohol (24:1; v:v) was added to the upper aqueous phase and thereafter re-centrifuged at 10,000*g* for 5min. RNA was precipitated by addition of 1 volume of 70% ethanol and purified using a RNeasy Mini kit, following the manufacturer's instructions.

3.5.2. Reverse transcription

To synthesize complementary DNA (cDNA) from mRNA templates, we used the High capacity reverse transcription kit (Applied Biosystems). Each reaction tube contained 1X RT buffer, 4mM dNTP mix, 1X RT random primers, 2.5U Multiscribe reverse transcriptase from the kit and 0.5-2µg total RNA in a total reaction volume of 50µl. The random primers consisted of a mix of random hexamers that permitted the reverse transcription of the total RNA content, including mRNA, tRNA and rRNA.

The reverse transcription program was the following : 10min at 25°C (initiation step), 120min at 37°C (elongation step) and 5s at 85°C (enzyme denaturation step). cDNA samples were stored at -20°C.

3.5.3. Real-time polymerase chain reaction

We performed real-time PCR with 10-50ng cDNA per tube in 1X Universal PCR Master Mix (consisting of *Taq* polymerase, buffer and dNTP mix at non-disclosed concentrations; Applied Biosystems) with 200nM forward primer, 200nM reverse primer and 100nM TaqMan probe. TaqMan probes are modified oligonucleotides that are labeled with FAM in 5' and with 6-TAMRA in 3'. All primers and TaqMan probes were synthesized by Operon (Ebersberg, Germany). As house-keeping gene, we used RNA polymerase II from the respective species. RNA levels were quantified by extrapolation from a standard curve.

		Reference	Forward primer 5'-3'	Reverse primer 5'-3'	TaqMan probe 5'6-FAM-3'6-TAMRA
FFA2	*human*	NM_005306	GCTTTCCCCGTGCAGTACAA	CCAGAGCTGCAATCACTCCAT	CTCTCCCGCCGGCCTCTG
	mouse	NM_146187	CATCAGCATGGAACGCTACCT	TGGCCGGCGGGATAA	AGTGGCCTTCCCGGTGCAGTACAA
	rat	NM_001005877	CCGCCGGCCACTGTAC	TGCAATGGCCAAAGGACAT	AGTGATCGCTGCTCTGGTGGCCTG
FFA3	*human #1*	NM_005304	GCTTTGGGCCCTACAACGT	CACGCCGGGCTTTCAC	TCCCATGTCGTGGGCTATATCTG
	human #2	NM_005304	GAGATGGCTGTGGTCCTCTTT	CCAGGCGGCTGTAGCAGTA	TGGTCCCGCTGATCATCACCAG
	mouse	NM_001033316	GCTTTGGGCCCTACAACGT	CACGCCGGGCTTTCAC	TCCCATGTCGTGGGCTATATCTG
	rat	NM_001108912	TGGTGTTCCTCGTGGGACTAC	GCGGCGACGCAGCTT	CAACGTGATGGCCCTGGTGGTCTT
RNA pol II	*human*	NM_000937	GCAAGCGGATTCCATTTGG	TCTCAGGCCCGTAGTCATCCT	AAGCACCGGACTCTGCCTCACTTCATC
	mouse	NM_009089	GCCAAAGACTCCTTCACTCACTGT	TTCCAAGCGGCAAAGAATGT	TGGCTCTTTCAGCATCTCGTGCAGATT
	rat	XM_001079162	GCAGGCGAGAGCGTTGAG	CATTGGTATAATCAAAACGGAACTTC	CTGGCTACACTTAAGCCTTCTAATAAAGC

Table 3 : Sequences of the primers used for real-time PCR.

6-FAM= 6-carboxyfluoresceine, TAMRA= 6-carboxytetramethylrhodamine, RNA pol II= RNA polymerase II

For human FFA3, set#2 was used for FFA3-expressing stable cell lines and set#1 was used for all other cell lines and tissues.

4. Functional assays for FFA2 and FFA3

4.1. cAMP assays

To monitor receptor activation upon stimulation with ligands, we used various functional cellular assays. A first one was the measurement of cAMP cellular levels. To do so, we developed a method in our laboratory, using Amplified Luminescence Proximity Homogeneous Assay (ALPHA) Screen from PerkinElmer. This method is based on the energy transfer from donor beads to acceptor beads and on the competition between biotinylated cAMP from the kit and endogenous cAMP produced in the cell (Fig. 11).

Assay buffer consisted of HBSS (1.26mM $CaCl_2$, 0.49mM $MgCl_2.6H_2O$, 0.41mM $MgSO_4.7H_2O$, 5.33mM KCl, 0.44mM KH_2PO_4, 4.17mM $NaHCO_3$, 137.93mM NaCl, 0.34mM Na_2HPO_4, 5.56mM D-glucose), 5mM HEPES, 0.1% (w:v) fatty acid free BSA, pH 7.4. Cells were washed with PBS, detached from the bottom of the flask with Non-enzymatic cell dissociation buffer (Sigma), counted in a Fuchs-Rosenthal chamber and seeded in assay buffer at 14000 cells per well in 384-well white Optiplates, together with 1U/well acceptor beads. Cells were stimulated for 1h at 37°C, 5% CO_2, 95% humidity, simultaneously with compounds at the desired concentration and 10µM forskolin (end concentration). After stimulation, cells were then lysed in detection buffer (5mM HEPES, 0.3% (v:v) Tween 20, 0.1% (w:v) BSA, pH 7.4) containing 1U/well donor beads and 1U/well biotinylated cAMP. Plates were subsequently incubated for 2h at RT in the dark and finally measured using an EnVision plate reader (PerkinElmer).

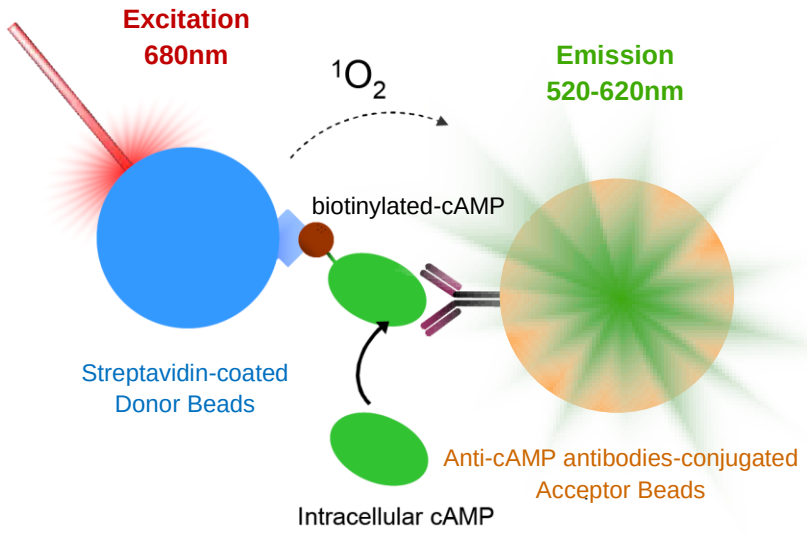

Fig. 11 : Principle of cAMP ALPHAScreen assay.

In the absence of endogenous cAMP, the streptavidin-coated donor beads (in blue) bind to the biotinylated cAMP (in grey, with biotin in brown). Biotinylated cAMP is recognized by the anti-cAMP antibodies that coat the acceptor beads (in orange), bringing in proximity the donor beads and the acceptor beads. Upon excitation at 680nm, singlet oxygen molecules are expulsed from donor beads and diffuse to the proximate acceptor beads. The excited acceptor beads generate emission of light between 520 and 620nm.
In the presence of intracellular non-biotinylated cAMP, endogenous cAMP competes with the biotinylated cAMP and disrupts the complex. The beads are not close one from the other anymore and no singlet oxygen transfer occurs.
Thus, the less endogenous cAMP in the cell, the more light emission we measure, and reciprocally.

4.2. Calcium assay

To monitor cytosolic Ca^{2+} influxes, we used a fluorescence image plate reader (FLIPR) and a Calcium4 kit (both from Molecular Devices). Before the assay, the Ca^{2+}-sensitive dye Calcium4 is in the form of a non-fluorescent ester. Once inside the cells, the ester group is cleaved by intracellular esterases, resulting in a negatively charged fluorescent dye that stays inside the cells and that strongly fluoresces upon binding with Ca^{2+}.

Cells were seeded in collagen I-coated black clear-bottom 384-well plates, at a density of 25000 cells/well and incubated overnight at 37°C, 5% CO_2, 95% humidity. On assay day, medium was removed from the wells and replaced by assay buffer (HBSS, 20mM HEPES, pH 7.4). Cells were then incubated for 90min at RT with the no-wash Ca^{2+}-sensitive Calcium4 dye, diluted as recommended by the manufacturer in assay buffer supplemented with 2mM probenicid (end concentration). In a FLIPR Tetra device (Molecular Devices), compounds were added to the cells and changes in fluorescence were measured over time (λ_{exc}=470-495nm; λ_{em}=515-575nm).

4.3. Detection of phosphorylated ERK1/2 by Western Blot

Western Blots were performed to detect the phosphorylation of ERK1/2.

Cells were seeded in collagen I-coated 6-well plates in growth medium. Once confluent, cells were serum-starved overnight in DMEM without FCS. Cells were then stimulated for 10min at 37°C with ligands diluted in prewarmed serum-free DMEM and lysed on ice with 250µL/well 1X Lysis buffer (Cell Signaling), freshly supplemented with 1mM phenylmethanesulphonylfluoride (PMSF). Cell membrane debris were eliminated by centrifugation at 20000*g* for 30min at 4°C and the protein content of the supernatant was determined using a BCA Protein assay kit (Pierce). Samples were denaturated by incubation at 95°C for 5min in loading buffer (62.5mM Tris.HCl pH 6.8, 1.5% (v:v) β-mercaptoethanol, 1.5% (w:v) sodium dodecyl sulphate). Proteins were then loaded on a Criterion Tris.HCl precast 10% polyacrylamide gel (Biorad) at 80µg proteins/well and transferred to a NC2 nitrocellulose membrane (Serva) in cold transfer buffer (250mM Tris, 192mM glycine, 20% (v:v) methanol). Transfer quality was checked by Ponceau S staining (ready-to-use solution of 0.1% (w:v) Ponceau S in 5% (v:v) acetic acid; Sigma). Membranes were then blocked for 1h at RT with 5% (w:v) skim milk powder in 1X TBST

(10mM Tris pH 7.8, 150mM NaCl, 0.1% (v:v) Tween 20), washed with 1X TBST and incubated overnight at 4°C with primary antibodies from rabbit (either anti-ERK1/2 or anti-phospho Tyr^{202}/Tyr^{204}-ERK1/2) in 1X TBST, 5% (w:v) BSA. After washing with TBST, membranes were incubated for 1-3h at RT with secondary antibodies (HRP-coupled anti-rabbit antibodies) in 1X TBST. Membranes were again thoroughly washed with 1X TBST and HRP activity was detected using LumiLight^{PLUS} WesternBlot substrate (Roche) in a LAS 3000 device (Fujifilm).

4.4. CellKey impedance assay

Impedance-based assay systems measure changes in electrical impedance relative to a voltage applied to a cell monolayer. They allow measurement of the activation of all receptor types including G protein-coupled receptors, tyrosine kinase receptors, and some nuclear receptors. Upon activation of cell surface receptors, signal transduction pathways are initiated, causing cellular electrophysiological and morphological changes. Activation of intracellular effectors results in changes in the cellular cytoskeleton, which are reflected in changes in the flow of current across and between the cells. These changes in the flow of current are evinced by an overall change in the impedance in a single well (Fig. 12). Impedance-based assay technologies have the advantage not to require labels or special reagents (McGuinness, 2007).

CellKey plates contain electrodes at the bottom of each well. The apparatus applies small voltages at low frequencies that induce extracellular current that passes around the cells. At high frequencies, an intracellular current is induced (Fig. 12A). Upon receptor stimulation, signal transduction events occur and lead to cellular changes, such as changes in cell adherence, cell shape and volume and cell–cell interaction, and ultimately result in changes in cytoskeletal organization. These cellular changes affect the flow of extracellular and intracellular currents and, therefore, affect the magnitude and characteristics of the measured impedance (Fig. 12B).

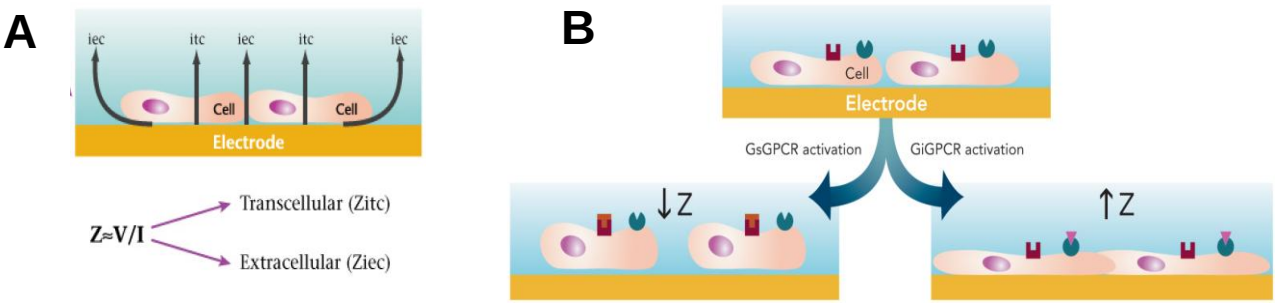

Fig. 12 : Principle of the CellKey impedance assay.

A. According to the Ohm's law, the impedance (Z) equals to the voltage (V) divided by the current (I). The CellKey device applies voltages at different frequencies at the electrode. At low frequencies, the voltages induce extracellular currents (iec) that pass between the cells, whereas at high frequencies, the voltages induce transcellular currents (itc) that pass through the cell layer. **B.** In the case of GPCRs stimulation, changes in Z values depend on the G protein coupling of the receptors. For $G\alpha_s$-coupled receptors, cells tend to become smaller upon stimulation, the impedance (Z) is therefore decreased. On the contrary, if the receptor is $G\alpha_i$-coupled, the cells tend to become larger and the impedance (Z) is increased. Adapted from McGuinness (2007).

Cells were seeded in collagen I-coated 384-well CellKey plates at a density of 20000 cells/well. On assay day, cells were washed 3 times in assay buffer (HBSS containing 5mM HEPES, 1% (v:v) DMSO, 0.1% (w:v) fatty-acid free BSA, pH 7.4) in the CellKey device. After an equilibration phase of 90min, cells were stimulated with compounds and the changes in extracellular impedance were monitored over time.

5. Designing of receptor structural models

We used the homology modeling program Modeller to design the structural models of hFFA2 and hFFA3 on the basis of the recently resolved inactive structures of β2 adrenergic receptor (pdb code: 2RH1; Cherezov *et al.*, 2007) and A_2A adenosine receptor (pdb code: 3EML; Jaakola *et al.*, 2008). Alignment was performed using Molecular Operating Environment (MOE), version 2008.10, with the BLOSUM30 substitution matrix and a gap penalty of 20.

First, an alignment of the FFA receptor family was created, and the β2 and A_2A receptor sequences were subsequently aligned to the FFA receptor family alignment, ensuring the correct positioning of the highly conserved sequence motifs known in class A GPCRs. Based on this alignment, and with the additional constraint of maintaining the conserved disulfide bridge between TM3 and EL2, 100 homology models were

constructed for FFA2 and FFA3. The most appropriate models, based on the presence of a suitable ligand-binding pocket as well as having side-chain orientations in agreement with our experimental findings from single point mutagenesis experiments, were further refined by backbone modifications. In line with the proposed "toggle switch mechanism" of GPCR activation (Schwartz *et al.*, 2006), TM6 was straightened by approximately 15°, to better represent the activated state of the ligand-binding region within the FFA2 and FFA3 receptors. This adjustment brings the essential residue H6.55 closer to the binding cavity. The resulting receptor models get protonated and gradually relaxed with the Amber99 forcefield as implemented in MOE, always keeping spatial restraints on the backbone in the TM region in order to avoid degradation of the receptors. The EL2 region is modeled so that the conserved cysteins are aligned with their cystein counterparts in the templates. By that, the conserved disulfide bond between EL2 and the top of TM3 is enforced. Bearing in mind that the EL2 regions of most structurally resolved GPCRs differ strongly, the EL2 of the final model is subjected to a short molecular dynamics simulation (1000ps, 300K, NVT, Δt=0.002ps, water box) in MOE, where the positions of the TM-backbones are fixed and only the extracellular loops are allowed to move.

6. Ligand docking

The ligands were flexibly docked into the receptor model employing GOLD (Verdonk *et al.*, 2003) with flexible side-chains in the proposed ligand binding region. The side chains of the residues in position 3.32, 3.33, 6.51, 6.55, 7.35, 7.39 and 7.42 were allowed to move and the best 10 top scoring poses were kept and visually inspected. In a last step, the receptor and the ligand poses were manually readjusted to be in accordance with mutagenesis data and the resulting complex underwent gradual minimization with the MMFF94x forcefield as implemented in MOE with a tethered protein backbone. To crudely check the plausibility of the poses, a short molecular dynamics simulation (1000ps, 300K, NVT, Δt=0.002ps) was performed in MOE with constrained backbone positions. However, no significant ligand shifts has been observed, suggesting stability of the ligand-receptor complexes.

7. Data analysis

All linear and non-linear regression fittings, calculations of pEC_{50} and extrapolations from standard curves were performed using GraphPad Prism 5.02 software (San Diego, CA). Values are given as mean ± SEM, unless otherwise stated. Quantification of the Western Blot analysis was performed by densitometric analysis using Advanced Image Data Analyzer (AIDA, version 4.15.205, Raytest, Straubenhardt, Germany).

Part 3

Results and discussion

1. Expression pattern of FFA2 and FFA3

Given the discrepancy in the literature concerning the expression of FFA2 and FFA3, we performed real-time PCR experiments on a variety of cell lines or tissues that were susceptible to express FFA2 and/or FFA3 (Fig. 13).

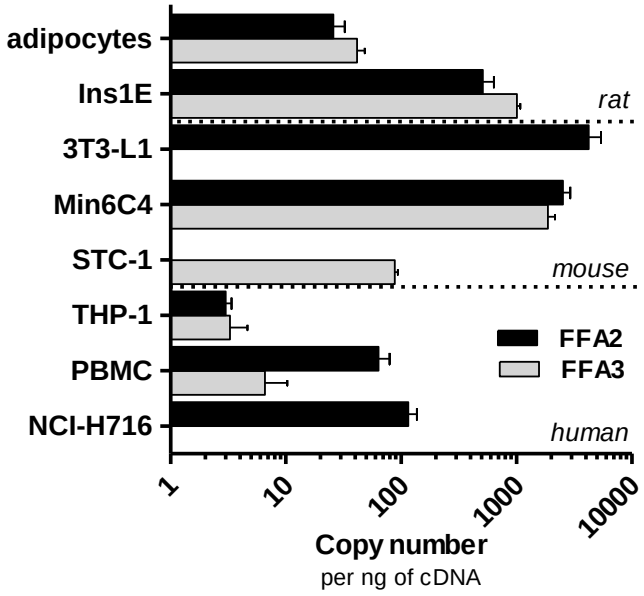

Fig. 13 : Gene expression of FFA2 and FFA3 in various cell lines or tissues.

Absolute mRNA level was determined using TaqMan real-time polymerase chain reaction by extrapolation of gene- and species-specific standard curves. RNApolII was used as endogenous control. Expression is given in number of copies per ng of cDNA. Some cells underwent differentiation process before experiment : rat preadipocytes were differentiated for 9 days, 3T3-L1 for 10 days, and NCI-H716 for 9 days, THP-1 for 2 days. Error bars represent SEM, n=3-6. PBMC : peripheral blood mononuclear cells.

The highest expression of FFA2 was found in differentiated 3T3-L1 murine adipocytes (n_{copies}/ng_{cDNA}=4227±1183). A notable amount of FFA2 mRNA was also present in Min6C4 (n_{copies}/ng_{cDNA}=2528±390) and Ins1E cells (n_{copies}/ng_{cDNA}=512±126), which are both pancreatic insulinoma cell lines from mouse and rat, respectively. A low expression

of FFA2 was found in NCI-H716 human enteroendocrine cells (n_{copies}/ng_{cDNA}=115±21), human PBMC (n_{copies}/ng_{cDNA}=64±16) and rat adipocytes (n_{copies}/ng_{cDNA}=26±6). Inexistent or very low expression of FFA2 was found in STC-1 mouse enteroendocrine cells and in THP-1 human macrophages.

A high level of expression of FFA3 was detected in Min6C4 (n_{copies}/ng_{cDNA}=1870±291) and in Ins1E cells (n_{copies}/ng_{cDNA}=1010±68). A moderate expression of FFA3 was found in mouse enteroendocrine STC-1 cells (n_{copies}/ng_{cDNA}=88±6) and in rat differentiated adipocytes (n_{copies}/ng_{cDNA}=41±7). However, a low or very low mRNA level for FFA3 was found in 3T3-L1 adipocytes, NCI-H716, human PBMC or THP-1 macrophages.

These data show that the insulinoma cell lines Min6C4 and Ins1E express both FFA2 and FFA3 at a high level, supporting a role for FFA2 and FFA3 in pancreatic β-cells. This result is in line with the results of Kebede *et al.* (2009) who found expression of FFA2 and FFA3 in mouse pancreatic islets and Min6 cells.

Adipocytes isolated from rat also showed appreciable levels of both FFA2 and FFA3 (Fig. 13), suggesting a role for both FFA2 and FFA3 in adipocytes. Nevertheless, in murine 3T3-L1 adipocytes, we were able to detect the expression of FFA2 at a high level, but not of FFA3 (Fig. 13), in accordance with a previous study (Hong *et al.*, 2005).

We found a relatively high expression of FFA2 but no FFA3 in the human NCI-H716 cell line and, conversely, a high expression of FFA3 but not FFA2 in the murine STC-1 cell line (Fig. 13). Previous studies showed expression of both FFA2 and FFA3 in enteroendocrine cells from human colon (Gordon *et al.*, 2010; Karaki *et al.*, 2008; Samuel *et al.*, 2008; Tazoe *et al.*, 2009). However, in double-immunostained human gut slices, FFA2 and FFA3 appeared not to be colocalized (Tazoe *et al.*, 2009). We did not find precise data in the literature concerning the expression of FFA2 in mice, but FFA3 was found to be expressed in mouse enteroendocrine cells (Gordon *et al.*, 2010; Samuel *et al.*, 2008).

Consistently with the study of LePoul *et al.* (2003), we found a modest expression of FFA2 and FFA3 in human peripheral blood mononuclear cells (PBMC), the expression level of FFA3 being lower than that of FFA2 (Fig. 13). PBMC actually consist of a mix of lymphocytes, monocytes and macrophages. However, the THP-1 monocytic cell line that we tested, although differentiated into macrophages, expressed FFA2 and FFA3 at only very low levels (Fig. 13). These results are in accordance with the study by Brown *et al.* (2003).

It is noteworthy that our data reflect only the mRNA levels of the FFA2 and FFA3 genes, but do not give information about the protein expression level.
As a control, we also checked the expression of the FFA2 and FFA3 from the cell lines that we established : they exhibited a high level of expression (n_{copies}/ng_{cDNA}=13042±1466 for FFA2 and n_{copies}/ng_{cDNA}=6959±3181 for FFA3) and the real-time PCR primers showed specificity for hFFA2 or hFFA3, respectively (data not shown). Moreover, untransfected Hek293 Flpin cells did not show expression of FFA2 or FFA3.

2. Characterization of the Hek293 Flpin expressing hFFA2 or hFFA3

2.1. Functional assays for $G\alpha_i$- and $G\alpha_q$-coupled receptors

In the present study, we established cellular models that stably expressed either hFFA2 or hFFA3. In order to study these receptors in these biological systems, we performed a variety of assays reflecting the cellular events owed to receptor activation.
We assumed that FFA2 coupled to both $G\alpha_i$ and $G\alpha_q$, and that FFA3 coupled solely to $G\alpha_i$, like suggested by LePoul *et al.* (2003). We evaluated the $G\alpha_i$-coupling by measuring cAMP levels using the ALPHAScreen technology and the $G\alpha_q$-coupling by monitoring the Ca^{2+} fluxes using a FLIPR platform (Fig. 14). Moreover, we detected the phosphorylation of the mitogen-activated protein kinase ERK1/2, considered a marker for GPCR activation, by Western Blot (Fig. 14). An additional functional assay utilizes a new method for studying global cellular changes in response to GPCR activation, the CellKey

impedance-based assay. Indeed, GPCR activation can deeply modify the cytoskeletal organization, for instance via the activation of ERK1/2 (Huang *et al.*, 2004).

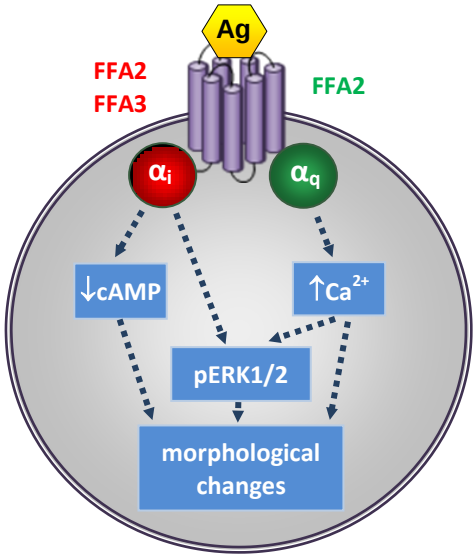

Fig. 14 : Expected cellular events in response to activation of FFA2 or FFA3.

In response to agonist (Ag) binding, FFA2 and FFA3 are both supposed to couple to $G\alpha_i$ proteins. Thus, one can assess cAMP contents to visualize receptor activation. FFA2 is also supposed to couple to $G\alpha_q$ proteins, which are responsible for Ca^{2+} elevation in the cytosol. Activation of GPCRs also induces phosphorylation of ERK1/2 and morphological changes that one can evaluate by Western Blot and by impedance-based assay, respectively.

2.2. cAMP assays

2.2.1. Endogenous and synthetic agonists for FFA2

In order to study the cAMP response of FFA2 to agonists, we tested the hFFA2-expressing cell line that we established in a heterogeneous ALPHAScreen cAMP assay.

To be able to identify a $G\alpha_i$-dependent decrease in cAMP, we first had to raise the basal cAMP concentration artificially with forskolin, a well-known activator of the adenylyl cyclase (Seamon *et al.*, 1981). Stimulation of the receptor with the naturally occurring ligands propionate, acetate and butyrate or with the synthetic Compound A led to a decrease of the forskolin-induced cAMP production, indicating a $G\alpha_i$-coupling of FFA2 (Fig. 15A). Endogenous ligands displayed similar potencies at FFA2, while Compound A was much more potent that SCFAs, being around 100 times more potent than propionate (Fig. 15A). Interestingly, all ligands that we tested brought the cAMP concentration down to the same level (Fig. 15A). The pEC_{50} and efficacy values that we found are in line with the published literature (Lee *et al.*, 2008; Wang *et al.*, 2010). Moreover, propionate and Compound A did not show effect on non-transfected parental cells, proving that the cAMP lowering effect observed in the FFA2-expressing cell lines was specific to FFA2. Taken together, our results confirm the natural coupling of FFA2 to

$G\alpha_i$ proteins that has been previously documented in other biological systems (Brown *et al.*, 2003; Lee *et al.*, 2008).

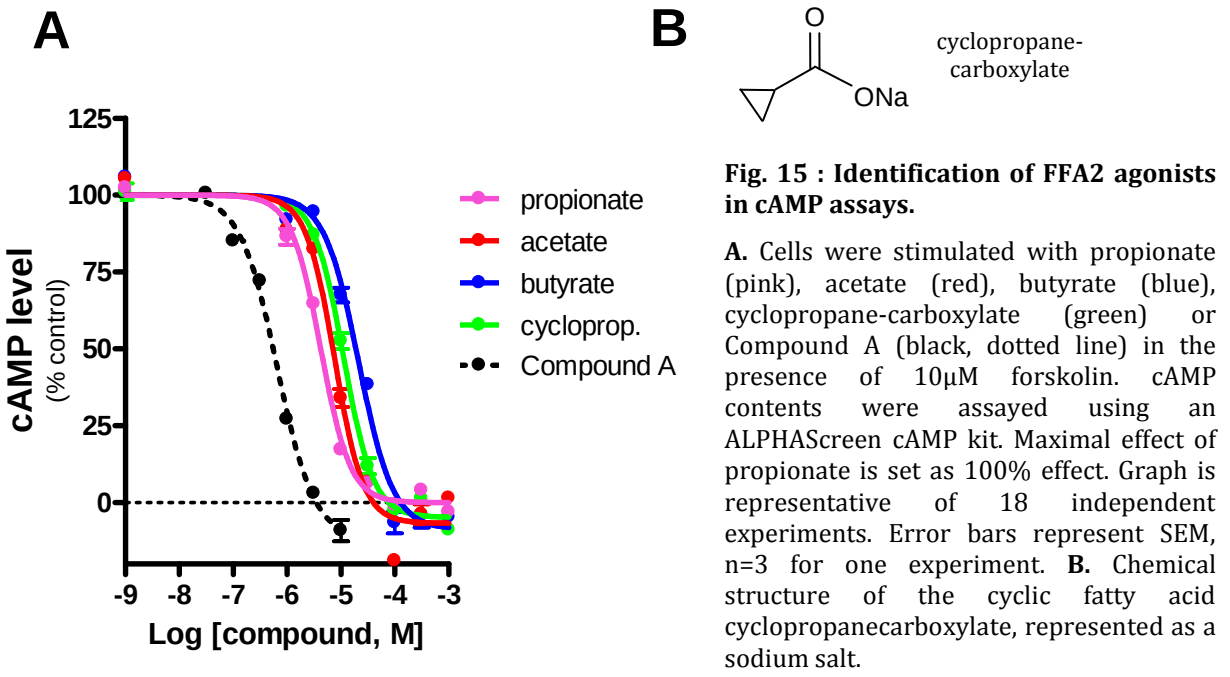

Fig. 15 : Identification of FFA2 agonists in cAMP assays.

A. Cells were stimulated with propionate (pink), acetate (red), butyrate (blue), cyclopropane-carboxylate (green) or Compound A (black, dotted line) in the presence of 10µM forskolin. cAMP contents were assayed using an ALPHAScreen cAMP kit. Maximal effect of propionate is set as 100% effect. Graph is representative of 18 independent experiments. Error bars represent SEM, n=3 for one experiment. **B.** Chemical structure of the cyclic fatty acid cyclopropanecarboxylate, represented as a sodium salt.

Ligand	pEC_{50}	% Effect	n
acetate	5.1±0.1	94±4	14
propionate	4.6±0.1	100±1	18
butyrate	4.8±0.1	70±3	10
cyclopropanecarboxylate	4.9±0.1	95±2	8
Compound A	6.5±0.1	110±10	16

Table 4 : Potency and efficiency of FFA2 ligands in cAMP assays.

Additionally, we found that the small cyclic fatty acid cyclopropanecarboxylate (Fig. 15B) was an agonist for FFA2 (Fig. 15A), at a similar efficacy and potency to propionate. This is line with a recent publication (Schmidt *et al.*, 2011).

Collectively, our data demonstrate that we have successfully established a cellular model to test hFFA2 function in cAMP assays. We were able to confirm the results of other groups regarding the activity of the SCFAs and of Compound A (Lee *et al.*, 2008; Wang *et al.*, 2010).

Regarding the structure of the endogenous agonists, the small size and the carboxyl group seem to be essential features to ensure binding of the ligand to the receptor. It has been previously shown that replacement of the carboxyl moiety of a SCFA by an amide moiety, for instance the exchange of acetate by acetamide, abolished the ability of the SCFAs to activate FFA2 (Stoddart *et al.*, 2008b). This result suggests that the carboxyl moiety is required to activate the receptor. On the other hand, Compound A does not exhibit a carboxyl moiety, although being also an allosteric activator of FFA2 (Lee *et al.*, 2008). Therefore, there may be one binding site where SCFAs bind to the receptor thanks to their carboxyl moiety, and a second binding site where Compound A binds to the receptor but that does not require a carboxyl group.

From a physiological point of view, the decrease of the second messenger cAMP can be decisive. For instance, in rat adipocytes, a decrease in cAMP leads to the inhibition of lipolysis, via the inhibition of the cAMP-dependent protein kinase (PKA), that in turn is not able to activate the hormone-sensitive lipase (HSL), an enzyme that catalyses the hydrolyzation of triglycerides into glycerol and free fatty acids (Duncan *et al.*, 2007). In 3T3-L1 cells and primary mouse adipocytes, propionate and Compound A are able to inhibit lipolysis, presumably by lowering the cytosolic cAMP concentration and via the same mechanisms as in rat adipocytes (Ge *et al.*, 2008; Lee *et al.*, 2008).
Moreover, it has been shown that SCFAs were able to inhibit glucose-induced insulin secretion from rat pancreatic islets and Min6 insulinoma cells (Leonard *et al.*, 2006; Ximenes *et al.*, 2007). This is in line with the hypothesis that a decrease in cAMP contents via $G\alpha_i$-coupled receptors would inhibit the cAMP–dependent glucose-stimulated insulin secretion process (Kebede *et al.*, 2009). A diminution of the secretion of insulin would lead to a lower fat storage in adipocytes, thus contributing to a weight loss.

2.2.2. Endogenous and synthetic ligands for hFFA3

We conducted the same kind of experiments with the hFFA3-expressing Hek293 Flpin cell line that we established. We found that, in our model, the SFCA propionate and butyrate were able to lower the forskolin-induced cAMP production via FFA3, at potencies comparable to that we found for FFA2 (Fig. 16). In contrast, acetate was much less potent on FFA3 than on FFA2, consistently with previous reports (LePoul *et al.*, 2003; Stoddart *et al.*, 2008b; Fig. 16).

Interestingly, cyclopropanecarboxylate is not only an agonist of FFA2, but also of FFA3, with similar potencies on the two receptors (Fig. 16).

In our hands, the synthetic agonist Compound B described in the patent by Leonard *et al.* (2007) was able to decrease intracellular cAMP concentration via hFFA3, with a mean pEC_{50} value of 4.8 (Fig. 16). This value is line with what has been documented in the patent (Leonard *et al.*, 2007). Untransfected parental Hek293 Flpin cells did not respond to Compound B, indicating that the response observed with FFA3-expressing cells was specific to FFA3. We also observed that Compound B was active on the mouse and the rat FFA3 stably expressed in Hek293 Flpin cells, with similar potency and efficacy to the human receptor (data not shown).

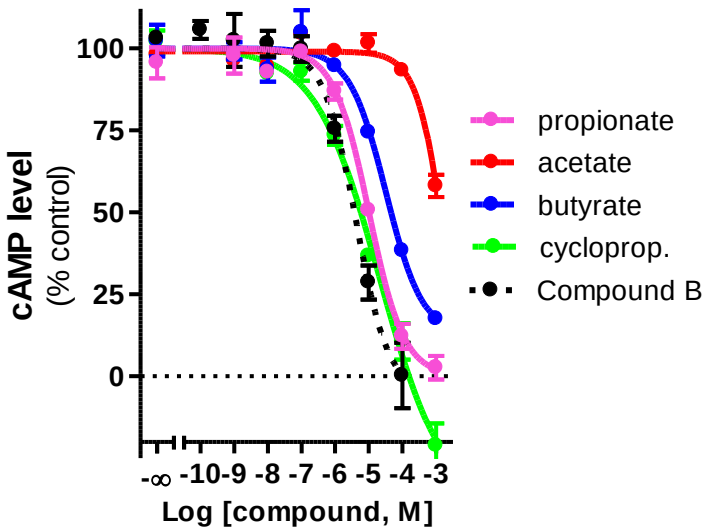

Fig. 16 : Identification of FFA3 agonists in cAMP assays.

Cells were stimulated with propionate (pink), acetate (red), butyrate (blue), cyclopropane-carboxylate (green) or Compound B (black, dotted line) in the presence of 10µM forskolin. Cytosolic cAMP concentration was measured using the ALPHA Screen technology. Effect of propionate is set as 100% effect. Graph is representative of 12 independent experiments. Error bars represent SEM, n=3 for one experiment.

Ligand	pEC_{50}	% Effect	n
acetate	3.9±0.1	27±3	8
propionate	4.3±0.1	100±1	8
butyrate	4.3±0.1	74±5	8
cyclopropanecarboxylate	4.7±0.1	116±4	8
Compound B	4.8±0.1	103±5	10

Table 5 : Potency and efficiency of hFFA3 ligands in cAMP assays.

Taken together, our results indicate a coupling of FFA3 to cAMP-lowering $G\alpha_i$ proteins. However, the physiological relevance of a such a coupling is not clear. We can speculate that FFA3 would play the same role as FFA2, namely to inhibit lipolysis in adipocytes and to inhibit glucose-induced insulin secretion from β-cells, but this remains to be clarified.

2.3. Calcium signaling

2.3.1. Ligand binding triggers calcium influx in FFA2 expressing cells but not in FFA3 expressing cells

Several articles report a coupling of FFA2 with $G\alpha_q$ proteins (Brown *et al.*, 2003; LePoul *et al.*, 2003; Nilsson *et al.*, 2003; Stoddart *et al.*, 2008b). Therefore, we wanted to check whether the hFFA2-expressing cell line that we established was also able to induce a rise in cytosolic Ca^{2+} (Fig. 18). To do so, we performed fluorometric imaging plate reader (FLIPR)-based Ca^{2+} assays, recording the total fluorescence from whole wells.

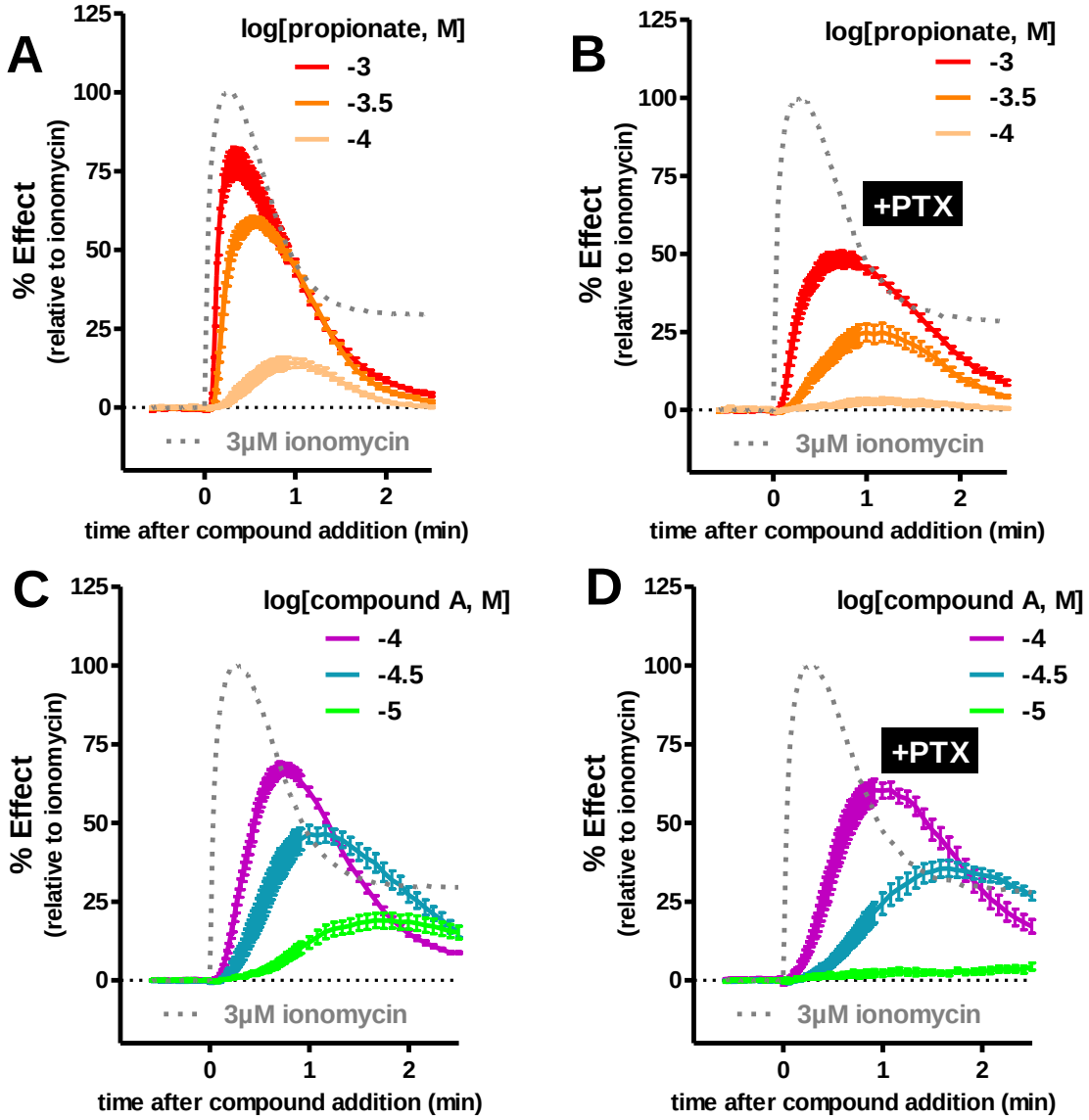

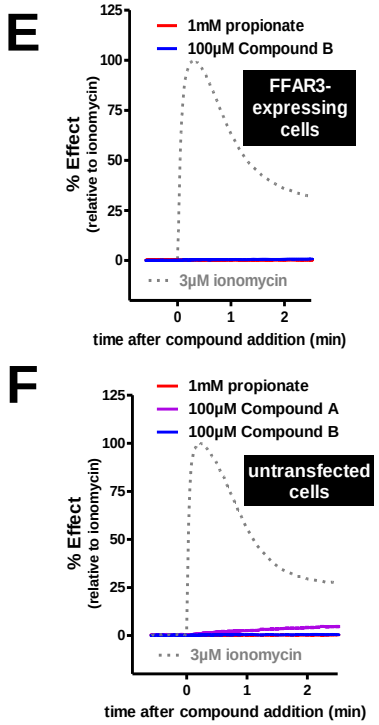

Fig. 17 : FFA2 but not FFA3 induce an increase of cytosolic calcium levels upon stimulation with propionate or synthetic compounds.

Hek293 Flpin cells expressing hFFA2 wild type were stimulated with various doses of propionate (**A and B**) or Compound A (**C and D**) with (**A and C**) or without (**B and D**) pertussis toxin (PTX) pretreatment o/n at 100ng/ml. Hek293 Flpin cells expressing hFFA3 were also challenged with propionate and the FFA3-specific Compound B (**E**). As a control, untransfected parental Hek293 Flpin cells were challenged with propionate, Compound A or Compound B (**F**). The maximal cellular response obtained with 3µM ionomycin was set as 100% effect (grey dotted line). Graphs are representative of 4 experiments. Error bars represent SEM, n=8 for one experiment.

We found that in the FFA2-expressing Hek293 Flpin cells, propionate was able to provoke a dose-dependent increase in cytosolic Ca^{2+} concentration, with a maximum peak reached around 20s after addition of the highest concentration of propionate (Fig. 17A). Remarkably, the maximal height of the peak diminished and the response was delayed while the propionate concentration decreased (Fig. 17A). Moreover, in our cellular model, propionate appeared somewhat less potent than in cAMP assays : using 100µM propionate, we hardly detected a signal in Ca^{2+} assays (Fig. 17A), whereas in cAMP assays, this concentration was sufficient to obtain the maximal effect (Fig. 15A). The shape of the tracings and the kinetics that we obtained with propionate was similar to that reported from single-cell Ca^{2+} assays (Stoddart *et al.*, 2008b).

We showed that Compound A was also able to trigger a dose-dependent Ca^{2+} mobilization (Fig. 17C). These results are in line with a previous report, in which FFA2 was transfected in aequorin-containing CHO-K1 cells (Lee *et al.*, 2008). In our FLIPR assay, the peak obtained with the highest concentration of Compound A was reached around 40s after compound addition, i.e. twice as late as with the highest concentration of propionate (Fig. 17C). This delay may be the result of different signaling pathways induced by either propionate or Compound A. However, the areas under curve calculated for the highest concentrations of propionate and Compound A remained equivalent (data not shown). In a similar manner to propionate, the peak induced by Compound A came later and became broader with decreasing concentrations of Compound A (Fig. 17C). Like propionate, Compound A is less potent in calcium assays than in cAMP assays, 10µM Compound A triggering a weak response in calcium assays (Fig. 17C), but a maximal response in cAMP assays (Fig. 15A).

Moreover, untransfected and hFFA3-expressing Hek293 Flpin cells did not respond to propionate, Compound A or Compound B in Ca^{2+} FLIPR assays (Fig. 17E and F). These results show that the Ca^{2+} mobilization that we observed in FFA2-expressing cells was specific to FFA2 and confirm that FFA3 does not couple to $G\alpha_q$.

Aside from $G\alpha_q$, it has been described that some subtypes of $G\alpha_i$ and $G\beta\gamma$ proteins were also able to provoke a Ca^{2+} response in the cytosol by activating PLC (Hur and Kim, 2002; Quiterrer and Lohse, 1999). To determine if the Ca^{2+} wave that we observed in hFFA2-expressing cells had a $G\alpha_i$ component, we tested the effect of PTX. PTX selectively

inhibits $G\alpha_i$ proteins by ADP-ribosylation, thus preventing the interaction of the $G\alpha_iGDP/\beta\gamma$ heterotrimer with the activated receptor (Smrcka, 2008). We observed a mild overall decrease of Ca^{2+} responses after PTX treatment (Fig 17B and D). Remarkably, the Ca^{2+} response induced by propionate was more sensitive to PTX than the response induced by Compound A (Fig. 17B and D). This result suggests that at least a part of the Ca^{2+} response that we observed was owed to $G\alpha_i$ and/or $G\beta\gamma$ proteins and that this additional component was more relevant for propionate than for Compound A. This observation supports the idea that Compound A may induce different signaling pathways than propionate.

From a physiological point of view, the coupling of FFA2 with Ca^{2+} responses can be linked to many processes.

For instance, in isolated human neutrophils, stimulation with propionate or acetate induced a robust intracellular Ca^{2+} flux (Cox *et al.*, 2009; LePoul *et al.*, 2003). It is also known that transient increases in cytosolic Ca^{2+} are necessary for initiation of the proinflammatory activities in these cells (Tintinger *et al.*, 2009). However, treatment of human neutrophils with acetate markedly reduced the surface expression of the proinflammatory receptors CXCR2 and C5aR (Maslowski *et al.*, 2009), indicating that *in vivo* FFA2 would rather have an anti-inflammatory effect on neutrophils.

In enteroendocrine cells, the secretion of hormones that control the metabolism of glucose and fat, such as CCK, GLP-1 and glucose-dependent insulinotropic peptide (GIP) upon stimulation of GPR40 or GPR120 with medium- and long-chain fatty acids is mediated by a transient increase in cytosolic Ca^{2+} concentration (Hirasawa *et al.*, 2005; Tanaka *et al.*, 2008). Consequently, we can hypothesize that a Ca^{2+} elevation in enteroendocrine cells in response to a stimulation of FFA2 would lead to an enhanced secretion of CCK, GIP and GLP-1.

In human adipocytes, an elevation of the intracellular Ca^{2+} activates the phosphodiesterase 3B that hydrolyses cAMP, finally leading to the inhibition of lipolysis via the inhibition of the hormone sensitive lipase (Xue *et al.*, 2001). FFA2 agonists may then inhibit lipolysis through the $G\alpha_q$-pathway, in complement to the $G\alpha_i$-pathway.

2.3.2. Synergistic effects of a simultaneous stimulation by Compound A and propionate

To further explore the Ca^{2+} responses triggered by propionate and Compound A, we decided to test both ligands together. We observed that a simultaneous addition of 1mM propionate with 0.1mM Compound A provoked a marked and early rise in Ca^{2+} concentration, slightly stronger than with 1mM propionate or 0.1mM Compound A alone (Fig. 18). Moreover, propionate and Compound A at concentrations that provoked only a poor Ca^{2+} response in single-addition experiments induced a prominent and early response when added simultaneously (Fig. 18). This synergistic effect may reflect an allosteric regulation of the receptor by Compound A : the simultaneous binding of both ligands to the receptor may keep it in an activated state.

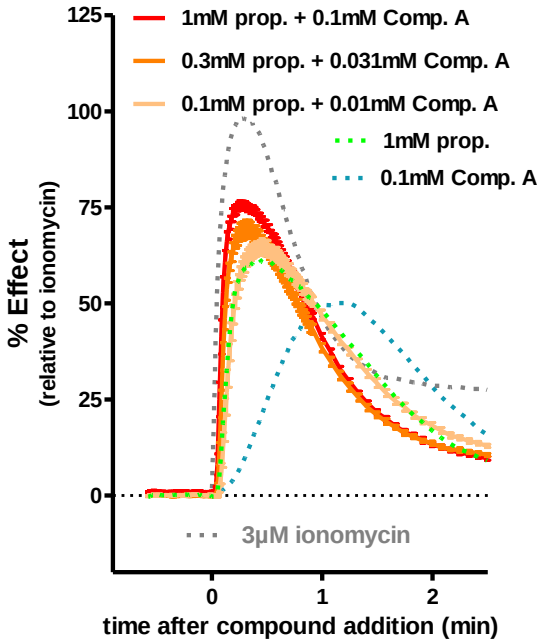

Fig. 18 : Simultaneous stimulation with propionate and Compound A leads to a synergic increase in cytosolic Ca^{2+} concentration.

Hek293 Flpin cells expressing hFFA2 wild type were challenged with a mix of propionate (prop.) and Compound A (Comp. A) at various concentrations. Kinetics of ionomycin (grey dotted line), propionate alone (green dotted line) and Compound A alone (blue dotted line) are represented with dotted lines. The maximal cellular response obtained with 3µM ionomycin was set as 100% effect. Graph is representative of 3 independent experiments. Error bars represent SEM, n=8.

2.3.3. Activitability after a first stimulation

In order to know if the receptor was still re-activable after a first stimulation, we stimulated the receptor with a subsequent dose of ligand 4min after the first one. We observed that the second stimulation still induced a Ca^{2+} response, but of lower intensity (Fig. 19). A possible explanation to that would be that the first stimulation caused the emptying of the intracellular Ca^{2+} stores and that their regeneration was not immediate.

However, we demonstrated here that the receptor was still able to respond to a second stimulation.

This result is in partial contradiction with a previous study where human neutrophils were challenged twice with 30mM acetate (LePoul *et al.*, 2003). In this experiment, the first addition of acetate did provoke a Ca^{2+} elevation, but not the second one. However, the second stimulation was applied only 90s after the first stimulation, at a time where the intracellular stores might be completely empty.

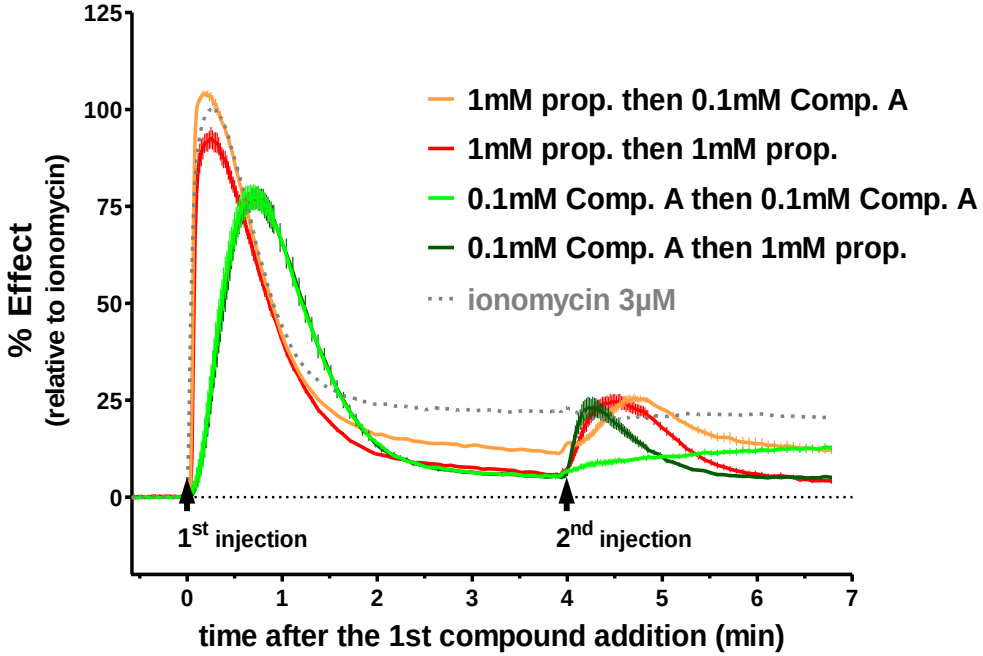

Fig. 19 : Sequential stimulation with propionate and Compound A leads twice to an increase in cytosolic Ca^{2+} concentration.

Hek293 Flpin cells expressing hFFA2 wild type were challenged at t=0 with 1mM propionate (prop.) or 0.1mM Compound A (Comp. A). At t=4min, cells underwent a second stimulation with 1mM propionate (prop.) or 0.1mM Compound A (Comp. A). Arrows indicate the time of compound addition. DMSO concentrations were adjusted to remain constant in all wells. Ionomycin response (grey dotted line) is set as 100% effect; buffer was used for second addition of the ionomycin control. Graph is representative of 3 independent experiments. Error bars represent SEM, n=8.

2.4. Phosphorylation of extracellular signal-regulated kinase (ERK) 1/2

In addition to the cAMP and Ca^{2+} second messengers, GPCRs can activate kinases, and more particularly extracellular signal-regulated kinase (ERK) 1/2.

The ERK1/2 mitogen-activated kinase acts as a signaling node that is activated in response to a variety of extracellular events (Luttrell and Luttrell, 2003). It is admitted that activation of GPCRs generally results in the activation of ERK1/2 by phosphorylation, whatever the type of G protein that is associated to the receptor (Osmond *et al.*, 2005). We performed here Western Blots to determine whether stimulation of FFA2 or FFA3 induced phosphorylation of ERK1/2 in our cellular models. The ERK and phosphoERK antibodies that we used recognize the two ERK isoforms : one of 44kDa, also referred to as ERK1, and one of 42kDa, also referred to as ERK2 (Fig. 20).

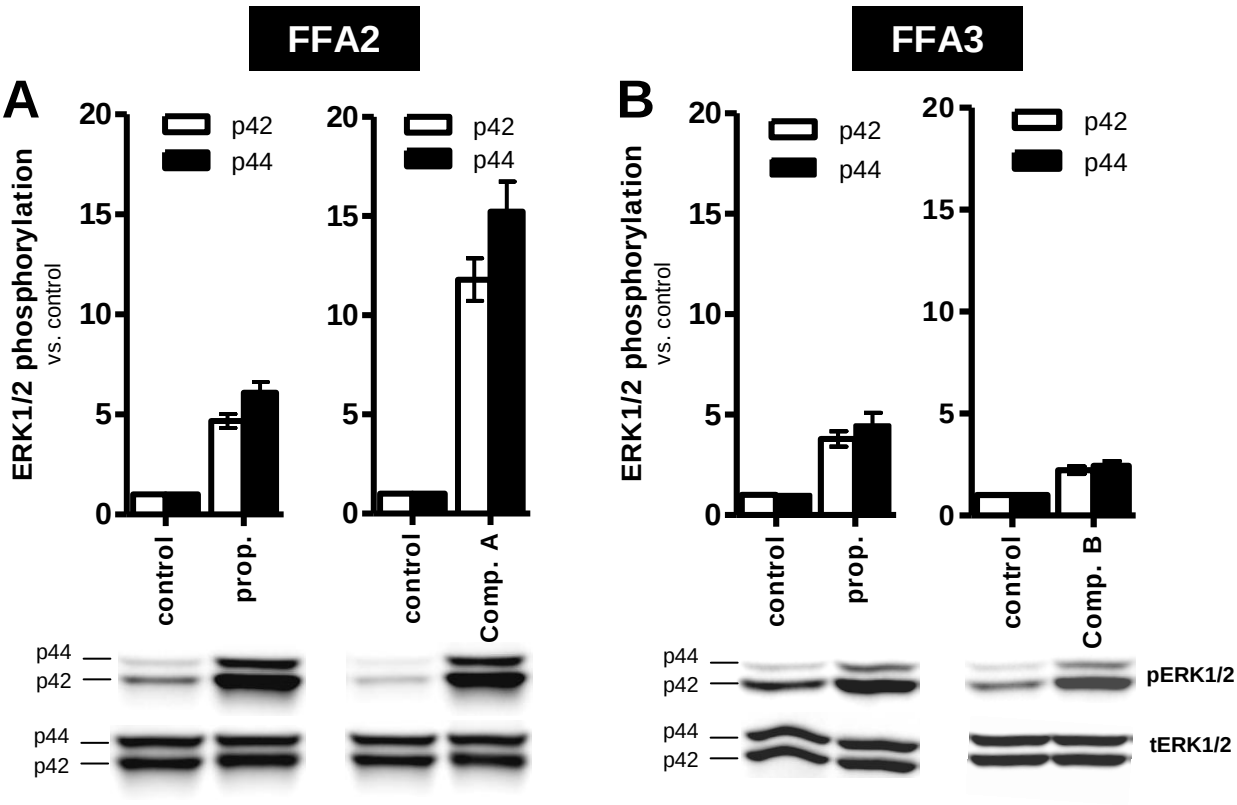

Fig. 20 : Detection of the phosphorylation of ERK1/2 by Western Blot.

A. Phosphorylation of ERK1/2 in Hek293 Flpin cells expressing hFFA2. **B.** Phosphorylation of ERK1/2 in Hek293 Flpin cells expressing hFFA3. Cells were serum-starved overnight before stimulation for 10min at 37°C with 1mM propionate (prop.), 0.1mM Compound A (Comp. A) or 0.1mM Compound B (Comp. B). Controls for propionate and synthetic agonists consisted of either water or DMSO, respectively. Primary antibodies detect either total ERK1/2 (tERK1/2) or ERK 1/2 phosphorylated on positions Thr202/Tyr204 (pERK1/2). Relative light density from the Western Blots was calculated using AIDA software and normalized to the control values. Pictures are representative of 6-9 independent experiments. Error bars represent SEM, n=6-9.

In Hek293 Flpin cells expressing hFFA2, stimulation with 1mM propionate generated a robust induction of ERK 1/2 phosphorylation, p44 being preferred to p42 (6.1±0.5 and 4.7±0.4-fold induction, respectively). Compound A also provoked a very strong induction of ERK1/2 phosphorylation, with an induction fold of 15.2±1.5 for p42 and 11.8±1.1 for p44 (Fig. 20A).

A weaker induction of ERK 1/2 phosphorylation was observed in Hek293 Flpin cells expressing hFFA3 in response to 1mM propionate (3.8±0.4-fold induction of p42 and 4.5±0.6-fold induction of p44) and to the synthetic agonist Compound B (2.2±0.2 for p42 and 2.5±0.2 for p44, respectively; Fig. 20B).

Untransfected cells did not exhibit responses to propionate or synthetic compounds (data not shown), suggesting that the ERK1/2 phosphorylation was specifically mediated by the FFA2 or FFA3 receptors.
Although the induction of the phosphorylation of ERK1/2 in response to the stimulation with agonists is obvious, the numbers should be carefully considered. Indeed, the basal levels obtained for the DMSO control were very low for both cell lines, in particular for the p44 band, giving a very high fold increase between basal and stimulated states.

It is also important to consider that although our experiment assesses the phosphorylation level ERK1/2, it is not sufficient to predict the complete biological activity of ERK1/2. Once activated, cytoplasmic ERK1/2 can in turn phosphorylate a variety of cytoplasmic, membrane, nuclear and cytoskeletal substrates. However, to be able to activate transcription factors that control DNA synthesis and cell division, phosphorylated ERK1/2 must be first translocated to the nucleus (Luttrell and Luttrell, 2003).

Additionally, the physiological effects of ERK1/2 phosphorylation are cell type-dependent.
For instance, activation of ERK1/2 is essential for the initiation of the differentiation of preadipocytes into adipocytes. Indeed, phosphorylated ERK1/2 activates cAMP-responsive element-binding protein (CREB), which in turn induces the expression of adipogenic genes, such as PPARγ and CEB/P genes (Petersen *et al.*, 2008). This process would then permit the storage of FFA in adipocytes instead of getting high levels of FFA in the blood.
FFA2 and FFA3 are also expressed in insulinoma cell lines. In the Ins1 rat pancreatic *β*-cell line, phosphorylation of ERK1/2 is promoted by a high concentration of glucose (15mM) via the activation of PKC by Ca^{2+} (Briaud *et al.*, 2003). Downstream in the signaling pathway, ERK1/2 activates CREB, improving cell survival in the Min6 pancreatic *β*-cell line and *ex vivo* in rat islets (Costes *et al.*, 2006).
Finally, in enteroendocrine cells, phosphorylation of ERK1/2 is associated with secretion of GLP-1 (Lim *et al.*, 2009).

Taking these results together, we may assume that administration of agonists for either FFA2 or FFA3 would potentially promote the phosphorylation of ERK1/2 in pancreas, enteroendocrine cells and adipose tissue, thus improving beta-cell survival, enhancing GLP-1 secretion from enteroendocrine cells, and scavenging fatty acids in adipocytes. All these effects are in line with the hypothesis that FFA2 and FFA3 activation would be beneficial for treatment of metabolic disorders.

2.5. CellKey impedance assay

In addition to cAMP assays, Ca^{2+}-mobilization assays and ERK1/2 phosphorylation by Western Blot, we also used a novel label-free live-cell technique, based on the measurement of cellular dielectric spectroscopy to assess comprehensive cellular events upon receptor stimulation : the CellKey impedance assay.

When cells are exposed to a stimulus, signaling events engender changes in cell electrophysiology, morphology, volume, adherence and cell-cell interactions. All these changes affect the flow of extracellular and transcellular currents and induce variations in impedance. The CellKey instrument measures the cellular impedance (for further information, see Material and Methods section). The CellKey technique has been proven particularly useful for the study of GPCRs. Indeed, based on the shape of the kinetics response, one can have an idea of the kind of Gα protein a GPCR couples to (Verdonk *et al.*, 2006).

2.5.1. CellKey assay with Hek293 Flpin-hFFA2 cells

We previously showed that FFA2 was coupled with both $G\alpha_i$ and $G\alpha_q$ proteins. We meant to use the CellKey technology to discriminate between couplings upon stimulation of FFA2 by propionate or Compound A.

Stimulation of hFFA2-expressing Hek293 Flpin cells with 1mM propionate led to a dip of the cellular impedance occurring in the first minute after compound addition, down to a minimal level of around -150Ω. After the dip, the impedance markedly increased to then stabilize (Fig. 21A). The same kind of response profile has been observed upon stimulation of the muscarinic m_1 receptor (Fang *et al.*, 2008), which is known to couple with $G\alpha_q$ proteins. This response profile is actually considered as typical of $G\alpha_q$-coupled GPCRs (McGuinness *et al.*, 2009; Verdonk *et al.*, 2006), and confirms the $G\alpha_q$-coupling of

hFFA2. Although the effect of propionate was dose-dependent, with a pEC_{50} around 4.3 (Fig. 21E), the amplitude of the dip progressively diminished with decreasing concentrations of propionate, to be finally completely abolished by 10µM propionate (Fig. 21A). Moreover, we also tested propionate and Compound A on untransfected cells and did not see any change in impedance (data not shown), demonstrating that the observed response of FFA2-expressing cells to propionate and Compound A was FFA2-specific.

Interestingly, after PTX treatment, the hFFA2-cells responded to propionate but with a pEC_{50} around 3.9. Upon PTX treatment, the amplitude of the dip and the Ziec values at t=9min were diminished by around 30% (Fig. 21B and E). This result is in line with our previous result in Ca^{2+} assays and confirms that a notable part of the response of FFA2 is due to PTX-sensitive $G\alpha_i$ proteins.

Regarding Compound A, it also provokes a $G\alpha_q$-like response at a 10µM-concentration, in a similar fashion to propionate (Fig. 21C). The effect of Compound A was also dose-dependent, with a pEC_{50} around 5.7 (Fig. 21E). The dip obtained with 10µM Compound A was not as deep as that obtained with 1mM propionate, but we could not test higher concentrations of Compound A because of solubility issues (Fig. 21C). PTX treatment reduced the Ziec value of Compound A by half at t=9min (Fig. 21D and E). Taken together, these data are in accordance with the Ca^{2+} assays where we observed that the response to Compound A was more affected by the PTX-treatment than the response to propionate (Fig. 21D).

Thus, thanks to the CellKey technique, we were able to complement the results from the other assay formats.

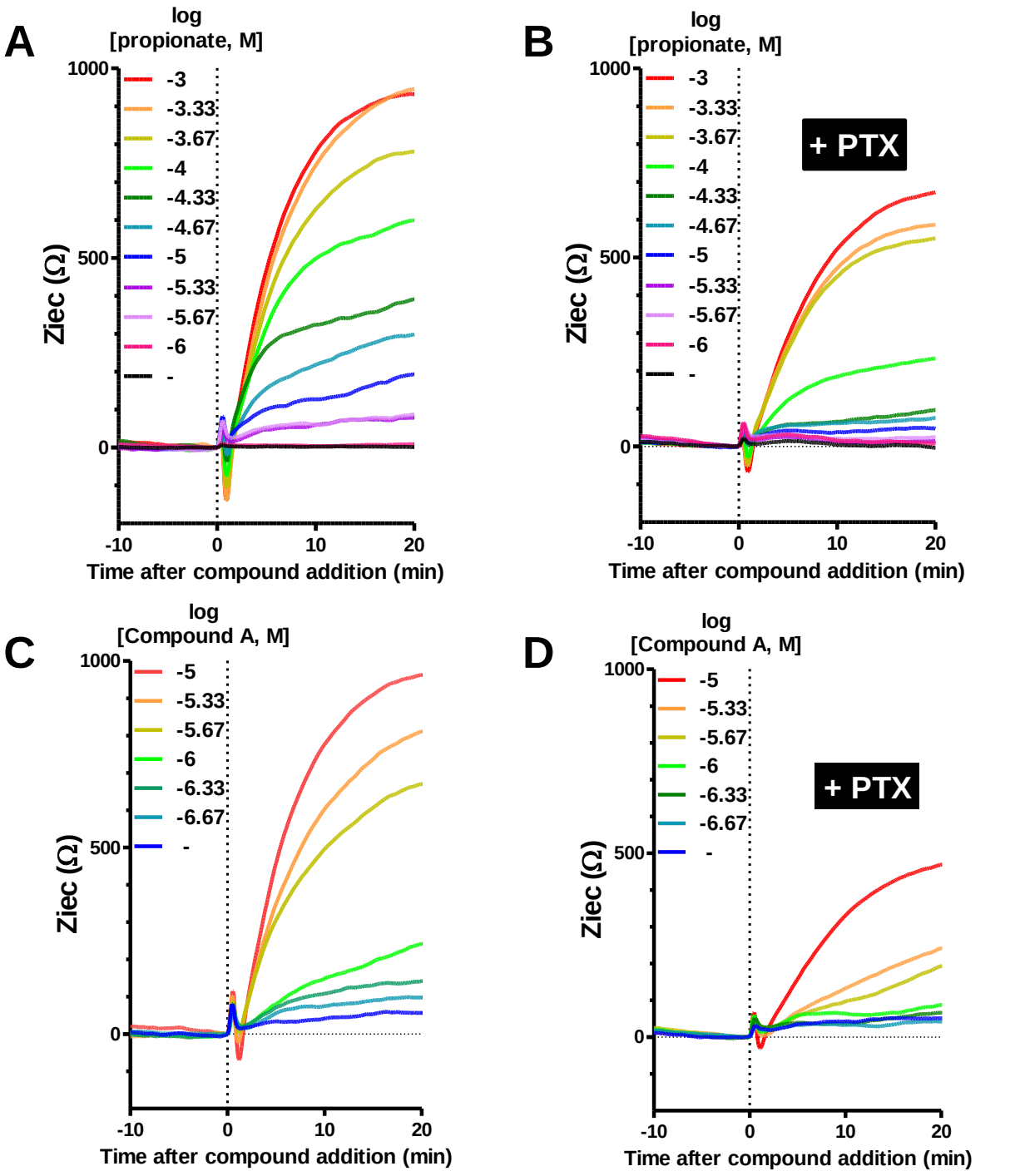

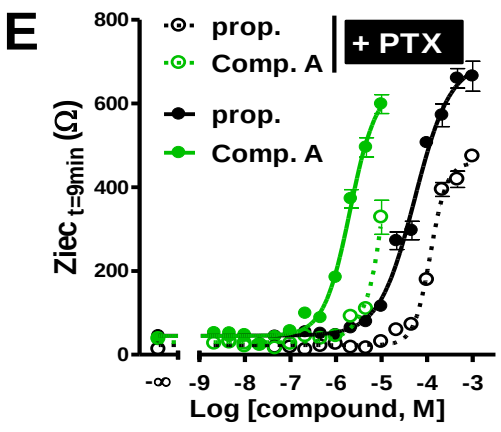

Fig. 21 : Changes of extracellular impedance (Ziec) in Hek293 Flpin cells expressing hFFA2 wild type.

A to D. Kinetics of Ziec (in ohms) upon stimulation with various doses of propionate (A and B) or Compound A (C and D), without (A and C) or with (B and D) 100ng/ml pertussis toxin (PTX) overnight treatment. Concentrations of propionate and Compound A are depicted using a rainbow color scale. Drawings are representative of 3 independent experiments. **E**. Dose-response curves of Ziec at t=9min after addition of propionate (black) or Compound A (green) with (open circles and dotted lines) and without (closed circles) PTX treatment. Error bars represent SEM, n=3-9 from one experiment.

2.5.2. CellKey assay with Hek293 Flpin-hFFA3 cells

We also explored the behavior of FFA3-expressing cells in CellKey experiments. We obtained dose-response curves with propionate and Compound B, although the impedance remained in a lower range than with FFA2-expressing cells, with a maximal value around 300Ω (Fig. 22A and B). In the first 4min after compound addition, we observed a dip of the impedance with propionate, in a similar way to what we observed with FFA2-expressing cells. Interestingly, the impedance dip did not appear with Compound B, even at the highest dose that we were able to test (0.1mM) (Fig. 22B), suggesting distinct signaling pathways for propionate and Compound B. Actually, the shape of the tracing that we obtained with Compound B corresponds to a classical tracing for $G\alpha_i$-coupled receptors, like $5HT_{1B}$ (Fang *et al.*, 2008).

At t=4min, the impedance strongly increased upon receptor activation to reach a maximal impedance value at around t=9min, went then slowly down to then stay quite stable (Fig. 22A and B). This is in contrast with FFA2-expressing cells where impedance continuously slowly increased after the initial dip. However, the last observations are valid only for the highest doses of propionate (0.1 to 1mM) and Compound B (0.1mM), but not for lower doses where the impedance increased slowly and without drawing a peak. Moreover, we also tested Compound B on untransfected cells and did not see any change in impedance (data not shown), demonstrating that the observed response of FFA3-expressing cells to Compound B was FFA3-specific.

In contrast with FFA2-expressing cells, the FFA3-expressing cells did not respond to propionate or Compound B after PTX treatment. This result suggests that FFA3 is exclusively coupled to $G\alpha_i$ PTX-sensitive G proteins, contrary to FFA2 that would be also coupled to both $G\alpha_i$ and $G\alpha_q$ proteins.

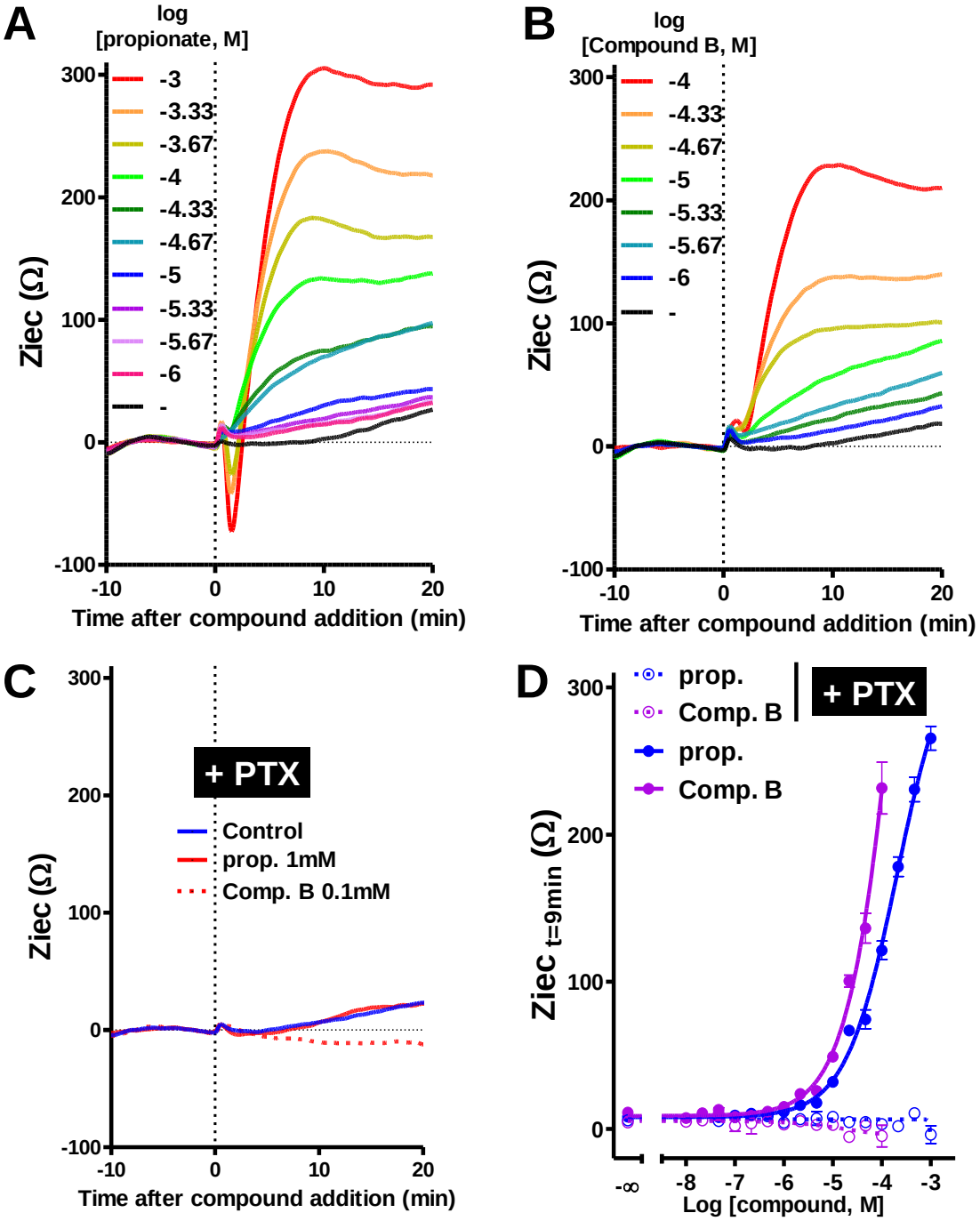

Fig. 22 : Changes of extracellular impedance (Ziec) in Hek293 Flpin cells expressing hFFA3.

A to C. Kinetics of Ziec (in ohms) upon stimulation with various concentrations of propionate (A) or Compound B (B), without (middle A and B) or with (C) pretreatment with pertussis toxin (PTX) overnight at 100ng/ml. Kinetics are representative of 3 independent experiments. **D**. Dose-response curves of Ziec at t=9min after addition of propionate (in blue) or Compound B (in purple) with (open circles and dotted lines) and without (closed circles) treatment with PTX. Error bars represent SEM, n=3-9.

3. Pharmacology of hFFA2 and hFFA3

3.1. Binding mode of FFA2 and FFA3 agonists

It has been previously shown that Compound A was an ago-allosteric activator of hFFA2, i.e. that Compound A interacts with the receptor in a distinct binding pocket from that of propionate (Lee *et al.*, 2008). We were also able to confirm in cAMP assays that Compound A was an ago-allosteric activator of FFA2 (data not shown). However, little is known about the pharmacology of hFFA3. To explore further the binding mode of propionate, cyclopropanecarboxylate and Compound B on FFA3, we tested combinations of these substances in cAMP assays.

In a first set of experiments, we applied fixed doses of cyclopropanecarboxylate to dose-response curves of propionate and observed a decrease of the basal cAMP concentration (i.e. in absence of propionate) without modifying the potency of propionate (Fig. 23C). The decrease of the cAMP content at low concentrations of propionate is due to cyclopropanecarboxylate by itself, and the lack of shift in the potency of propionate indicates that cyclopropanecarboxylate and propionate bind to the same or overlapping site on the receptor. If propionate is defined as an orthosteric agonist of FFA3, then cyclopropanecarboxylate is an orthosteric agonist of the receptor, i.e. both SCFAs bind to the same site.

In a second experiment, we tested dose-response curves of propionate in the presence of various doses of Compound B (Fig. 23D). Compound B reduced the basal cAMP concentration, but at the same time displaced the pEC_{50} of propionate to the left. This shows that propionate and Compound B do not bind to the same or overlapping site, i.e. Compound B is an allosteric agonist of FFA3. In the converse experiment, propionate was able to displace the pEC_{50} of Compound B to the left (Fig. 23B), confirming that propionate and Compound B do not bind to the same site.

Finally, we also tested dose-response curves of Compound B in the presence of various doses of cyclopropanecarboxylate. The potency of Compound B was shifted to the left as the concentration of cyclopropanecarboxylate increased, demonstrating that cyclo-propanecarboxylate does not bind to the same or overlapping site as Compound B (Fig. 23A).

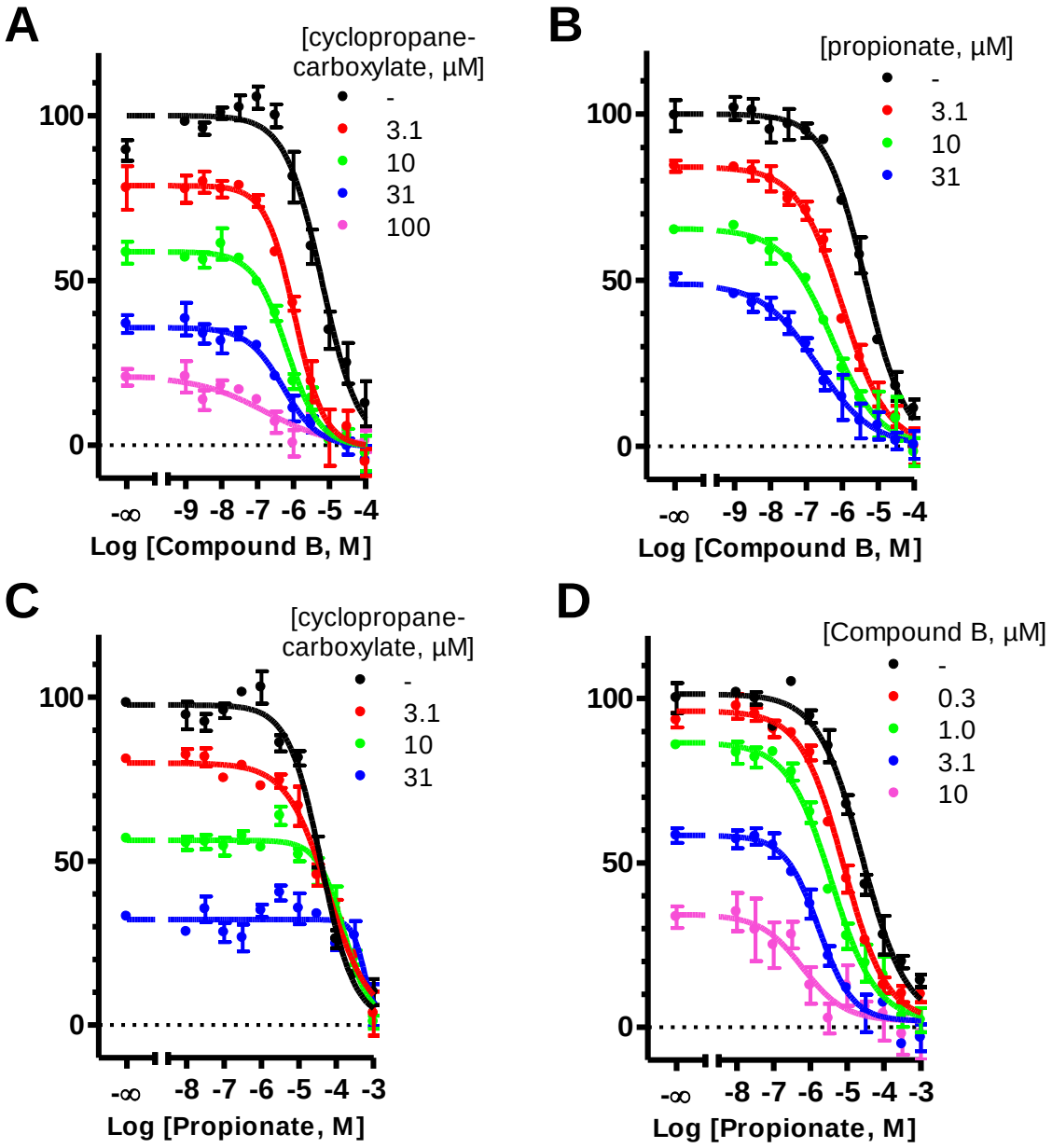

Fig. 23 : cAMP assays on Hek293 Flpin cells expressing hFFA3.

ALPHAScreen cAMP assays with combinations of Compound B with various doses of cyclopropanecarboxylate (**A**), of Compound B with various doses of propionate (**B**), of propionate with various doses of cyclopropanecarboxylate (**C**), of propionate with various doses of Compound B (**D**) were performed in order to determine the binding mode of these FFA3 agonists. In comparison to propionate, cyclopropanecarboxylate acted as an orthosteric agonist, whereas Compound B was an allosteric agonist. Graphs are representative of 7 independent experiments. Errors bars represent SEM, n=3 for one experiment.

3.2. Identification of ligand binding sites by site-directed mutagenesis

Propionate is an orthosteric agonist for hFFA2 and hFFA3, whereas Compound A and B are allosteric agonists for hFFA2 and FFA3, respectively.

However, little is known about the interaction sites of these ligands with the receptors. A way to identify precisely the aminoacid residues that interact with ligands is to modify selectively some aminoacids, one at a time, by site-directed mutagenesis, and to analyze the subsequent effects of the mutations on the receptor functionality.

3.2.1. Selection and location of the mutated aminoacid residues

In this study, we selected some aminoacid residues in the TM regions of the receptors that were possible key residues for ligand binding in GPCRs (see Fig. 24A and B). Visual inspection of primary structural models for the FFA receptor family designed on the basis of two available GPCR structures, namely the β2 adrenergic receptor (Cherezov *et al.*, 2007) and the A_{2A} adenosine receptor (Jaakola *et al.*, 2008), allowed us to select the residues to mutate. In some cases, our choice was comforted by the fact that some of the selected residues have been previously shown to be crucial for ligand recognition in FFA1, FFA2 or FFA3, although in other cellular models and/or other functional assays (Stoddart *et al.*, 2008b; Sum *et al.*, 2007).

In the following sections, we will designate the residues by their absolute position in the protein sequence on their cognate receptor (e.g. I66) and/or, to facilitate comparison between GPCRs, their relative position according to the Ballesteros nomenclature. According to the Ballesteros nomenclature, the first number gives the TM and the second number its position, number 50 being the most conserved residue in one TM (e.g. I2.61; Ballesteros and Weinstein, 1995).

Thus, to explore how FFA2 recognizes its ligands, we mutated selectively and individually the aminoacid residues located in positions I66, S86, F89, Y90, Y94, S96, H140, R180, Y238, N239, H242, R255, S256, S262 and S263 by the small hydrophobic residue alanine (A) (see Fig. 24A for aminoacid position in the receptor and Table 1 in the Appendices section for information about the physicochemical properties of aminoacid residues). Additionally, the two positively charged arginine residues R180

and R255 were substituted by lysines (K), which are also positively charged. The aromatic histamine residue H245 was also substituted by an aromatic phenylalanine (F) residue and an asparagine (N) residue, like in hFFA1. The serine residue S86 was also replaced by a glycine (G) residue, like in the mouse and rat FFA2 sequences.

Likewise, we mutated selectively the hFFA3 residues M72, F96, Y100, R185, N242, H245, R258 to small hydrophobic alanine (A) residues. The R185 and R258 residues were additionally substituted by lysine (K) residues, whereas H245 was also substituted by a phenylalanine (F) and an asparagine (N) residue (Fig. 24B).

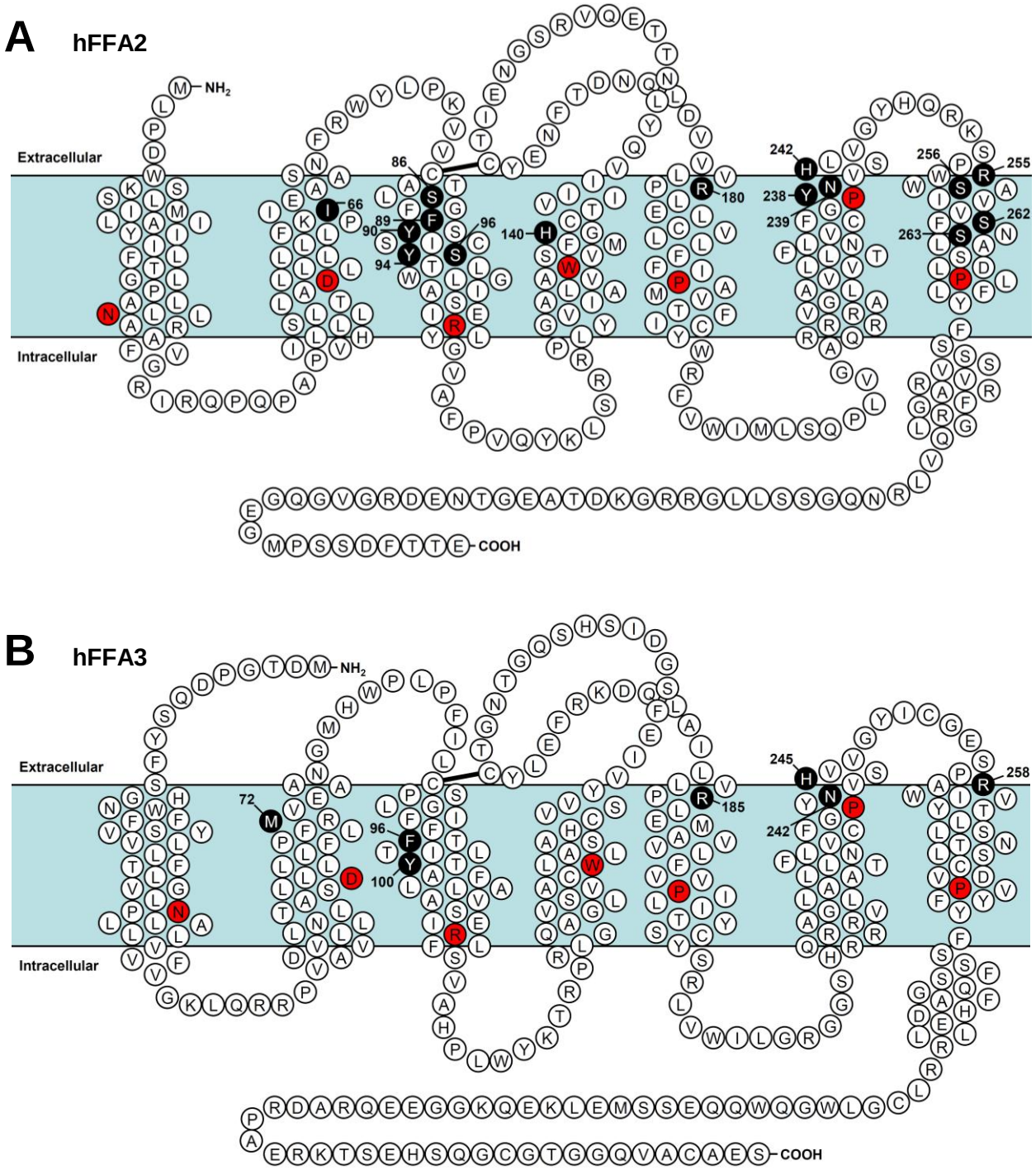

Fig. 24 : Representation of the aminoacid residues sequence of hFFA2 and hFFA3 receptors.

Snake plots of FFA2 (**A**) and FFA3 (**B**) receptors across the membrane. Blue areas represent the cytoplasmic membrane, with the extracellular side being upward and the intracellular side downward. Black bars between cysteine residues represent putative disulfide bridges. Mutated residues in the transmembrane domains are shown in black circles, together with their numbering in the protein sequence. Highly conserved residues, set as number 50 in the Ballesteros nomenclature, are shown in red circles.

3.2.2. Gene expression

Before testing the effects of the mutations, we first checked whether the mutated receptors were expressed in the cell lines that we established to ensure that an absence of response in functional assays would not be simply due to an absence of receptor expression. To do so, we used real-time quantitative PCR and designed specific primer sets that bound outside of the mutated regions.

As we mentioned before, we assessed only at the mRNA levels and not the protein expression on itself because we had no available antibodies specific to our receptors of interest. Besides, antibodies would not have been so useful in our case since they might not have recognized mutated receptors.

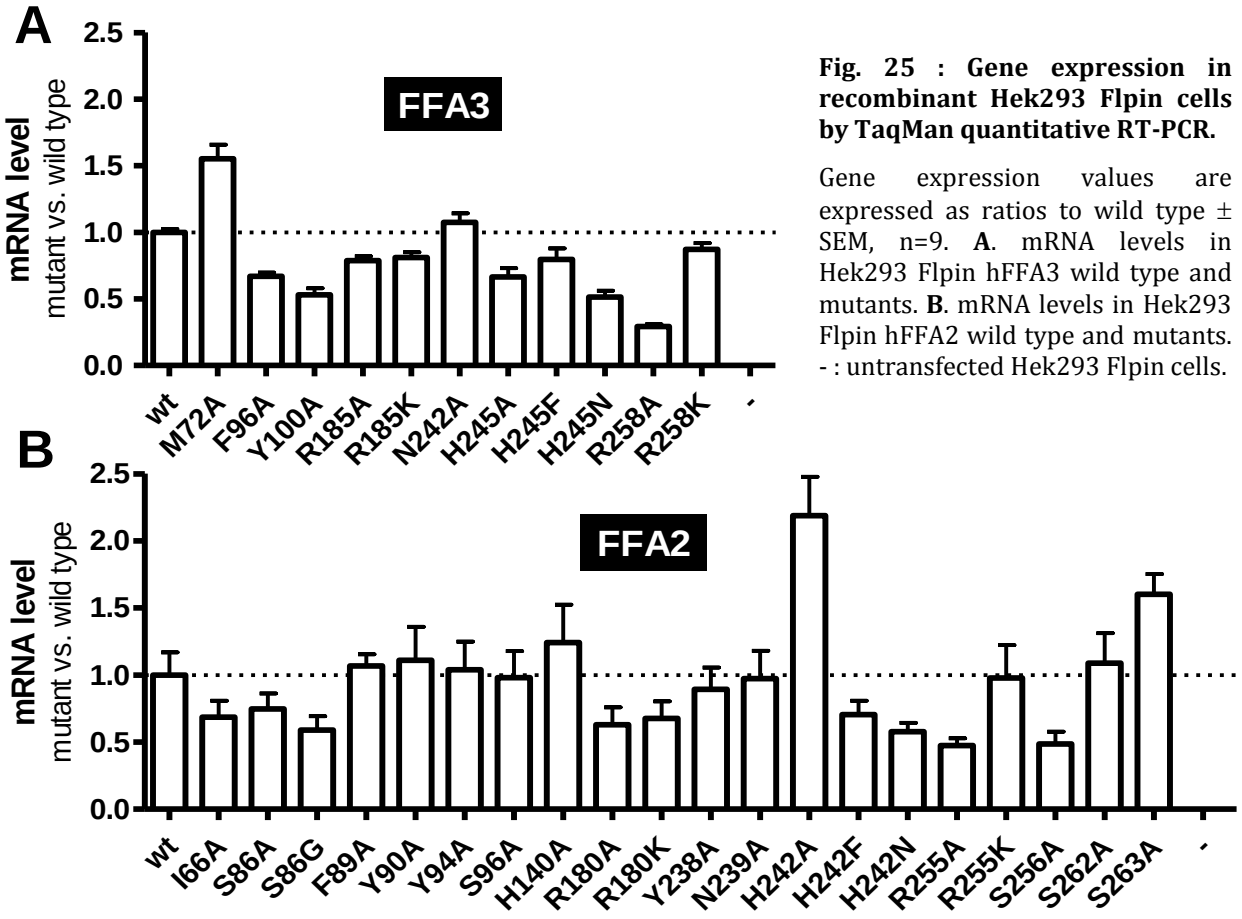

Fig. 25 : Gene expression in recombinant Hek293 Flpin cells by TaqMan quantitative RT-PCR.

Gene expression values are expressed as ratios to wild type ± SEM, n=9. **A**. mRNA levels in Hek293 Flpin hFFA3 wild type and mutants. **B**. mRNA levels in Hek293 Flpin hFFA2 wild type and mutants. - : untransfected Hek293 Flpin cells.

Ratios of mRNA levels were comprised between 0.5 and 2.2 for FFA2 and between 0.3 and 1.6 for FFA3, relatively to the wild-type receptors (Fig. 25A and B). No expression of FFA2 and FFA3 was detected in parental untransfected cells (Fig. 25A and B).

3.2.3. Comparative analysis of hFFA2 mutants in cAMP assays

To evaluate the effects of the mutations on the FFA2 receptor, we tested the ability of the ligands to activate the mutated receptors in cAMP assays. In total, 20 different mutants of FFA2 receptor were generated (Fig. 24A) and were tested in cAMP assays in response to propionate or Compound A. Representative dose-response curves are presented in Fig. 26 and mean values are shown in Table 6.

We did not identify an aminoacid residue mutation that strongly disrupted the receptor response to Compound A. Thus, we based our observations on the responses of the mutated receptors to propionate that, in contrast, were in most cases affected by the mutation.

Substitution of Y90 (3.33), R180 (5.39), Y238 (6.51), H242 (6.55) and R255 (7.35) by an alanine residue resulted in a complete loss of the response to propionate (Fig. 26; Table 6), showing that the aminoacid residues at these positions are essential for the activation of the receptor by propionate.

Mutation of R180 (5.39), H242 (6.55) and R255 (7.35) by an alanine residue totally disrupted the response of the receptor to propionate, but affected only slightly the response of Compound A (Fig. 26; Table 6). Interestingly, the substitution of R180 (5.39) or R255 (7.35) by a positively charged lysine did not restore the response of propionate, indicating that the positive charge in these positions is not sufficient to ensure the function of the receptor (Fig. 26). These results are line with what has been previously described for these mutated receptors, but in other assay formats, such as aequorin, GTPγS or inositol triphosphate assays (Stoddart *et al.*, 2008b; Swaminath *et al.*, 2010). The same was true for the receptor mutated on position H242 (6.55) that did not respond to propionate when this residue was substituted by either the positively charged arginine like in the human FFA1 sequence, or a phenylalanine residue (Fig. 26).

In a attempt to classify GPCRs, Surgand *et al.* (2006) published a computational prediction of 30 TM residues that potentially point inward the ligand binding cavity of GPCRs (Surgand *et al.*, 2006). According to this classification, the positively charged R5.39, H6.55 and R7.35 are conserved among the FFA receptor family, but not among their closely related receptors, like dicarboxylate receptors or purinergic receptors (Surgand *et al.*, 2006). In FFA1, mutagenesis studies showed that the residues R5.39,

H6.55 and R7.35 were necessary for the binding of the carboxyl-containing synthetic ligand GW9508, but less crucial for the binding of the natural ligand linoleate (Sum *et al.*, 2007). These three residues were then proposed to act as an anchor for orienting the carboxyl moiety of the ligands (Sum *et al.*, 2007). For FFA2, whose ligands are much smaller than those of FFA1, the hypothesis is that these three residues form a positively charged environment, which anchors the carboxyl moiety of SCFAs.

The substitution of the tyrosine residues in position 90 (3.33) and 238 (6.51) by an alanine residue disrupted the receptor function as well (Fig. 26 and Table 6). In contrast, in FFA1, mutation of Y240 (6.51) to an alanine or phenylalanine had little effect on the response to its natural or synthetic ligands (Sum *et al.*, 2007). Notably, Y6.51 is well conserved among rhodopsin-like GPCRs, or replaced by a phenylalanine residue, whereas Y3.33 is conserved only among receptors that are close to the FFA family, ie. the purinergic receptors and the dicarboxylate receptors (Surgand *et al.*, 2006). Although located slightly deeper in the orthosteric binding pocket, Y90 and Y238 seem to point to the binding pocket in our primary structural model. They may help stabilizing the binding of the ligand to R180 (5.39), H242 (6.55) and R255 (7.35). Y90 may interact with R180 by hydrogen bonding, whereas Y238 may interact directly with the ligand.

Mutation of F89 (3.32), Y94 (3.37) or N239 (6.52) by an alanine residue also affected the response to propionate, but to a lesser extent than the above described positions (Fig. 26; Table 6). Indeed, these mutants displayed a residual response to high concentrations of propionate (Fig. 26). Similarly, in human FFA1, mutation of H3.32 or Y3.37 by alanine residues also resulted in a partial loss of responsiveness to the endogenous ligand linoleate (Sum *et al.*, 2007). However, mutation of H3.32 or Y3.37 in human FFA1 by phenylalanine residues had little effect on the potency of linoleate (Sum *et al.*, 2007). N6.52 is conserved in the FFA receptor family and some other GPCR subfamilies. The 6.52 position has not been studied in FFA1. Positions 3.32 and 6.52 were predicted to be part of the GPCR binding cavity according to Surgand *et al.* (2006).

The I66A (2.61), S86A (3.29), S86G, S256A (7.36), S262A (7.42), S263A (7.43) mutated receptors displayed no dramatic difference in comparison to the wild-type receptor

regarding the potency or efficacy of propionate (Fig. 26; Table 6), suggesting that these positions do not play a role in ligand binding or that these mutations do not disturb the receptor structure enough to affect the functionality of the receptor.

Intriguingly, the S96A (3.39) and H140A (4.44) mutated receptors responded to propionate with the same potency as the wild-type receptor, but presented a gain of function of Compound A, its potency being increased by around 10 fold in comparison with the wild-type receptor (Fig. 26; Table 6). Regarding the H140 (4.44) position, one can draw a parallel with the observations made by Stoddart *et al.* (2008b) where FFA2 gained the ability of responding to the C6 SCFA caproate when presenting the H140A mutation.

According to Surgand's classification, the binding cavity of the GPR91 receptor is predicted to be close to those of the FFA receptor family (Surgand *et al.*, 2006). GPR91 is a receptor for succinate, a small dicarboxylic acid (He *et al.*, 2004). Mutation of the basic residues R99 (3.29), H103 (3.33), R252 (6.55) and R281 (7.39) by alanine residues totally impaired the function of GPR91, confirming the involvement of these positions in ligand binding (He *et al.*, 2004). These four positively charged residues would provide a binding environment for the two carboxyl moieties of succinate, formed on one side by R99 and H103 on TM3, and on the other side by R252 on TM6 and R281 on TM7 (He *et al.*, 2004). In FFA2, only a part of these positively charged residues are conserved : 3.29 is a serine, 3.33 a tyrosine, 7.39 a valine and only 6.55 is still positively charged, since it is an histidine residue.

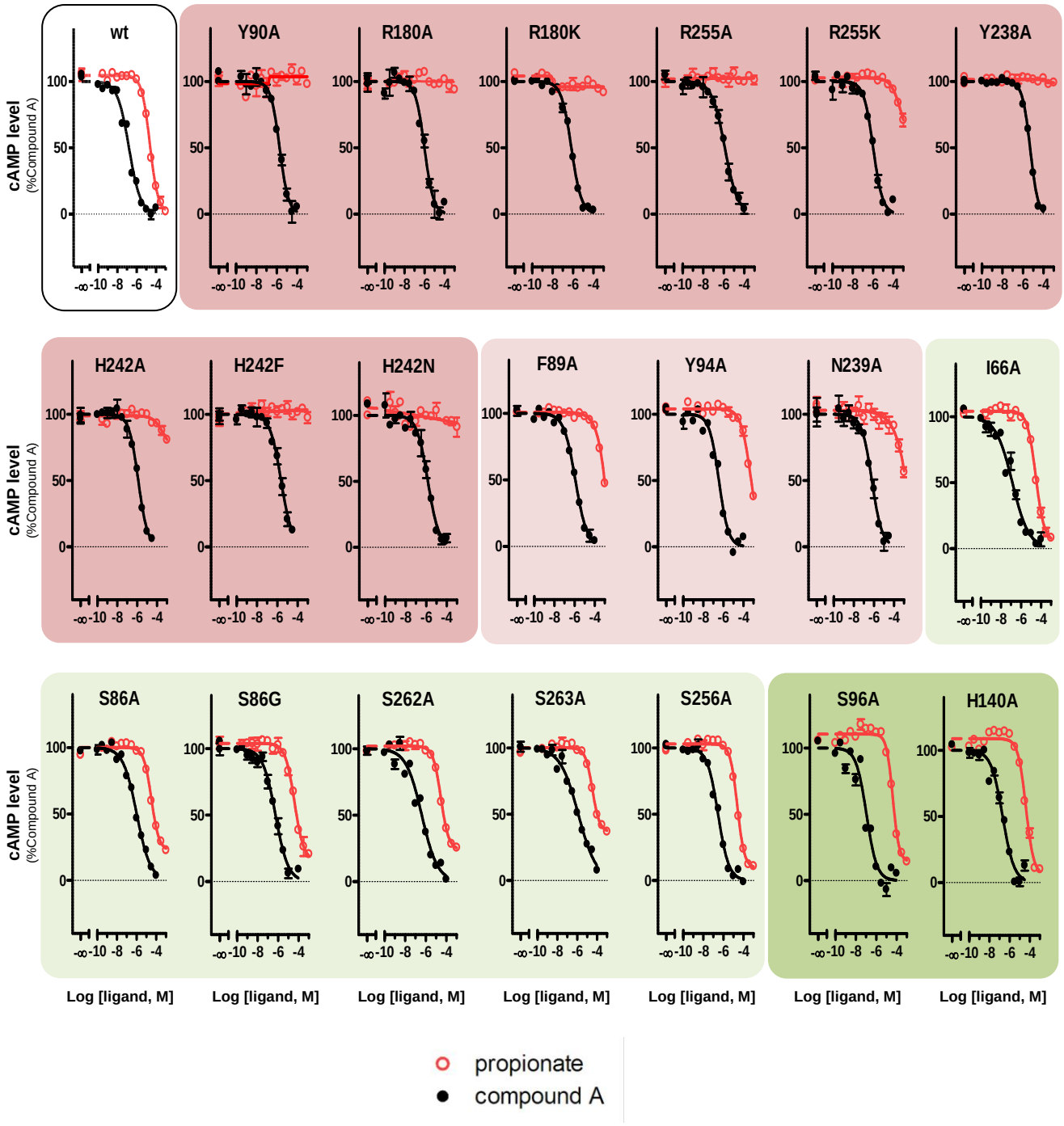

Fig. 26 : Effects of single point mutations of hFFA2 on the response to propionate or Compound A in cAMP assays.

ALPHAScreen cAMP assays were performed in the presence of 10µM forskolin with Hek293 Flpin cells expressing hFFA2 wild type (wt) or one of the mutated forms. Receptors for which the response of propionate was strongly affected by the mutation are shaded in dark red, slightly affected in light red, unaffected in light green, and enhanced in dark green. 100% represent the maximal effect of Compound A on each receptor in lowering cAMP concentration. For each graph, the x-axis represents the cAMP level and the Y-axis represents the ligand concentration on a logarithmic scale. Graphs are representative of 4-8 experiments. Error bars represent SEM, n=3.

Mutation position		Propionate			Compound A		
absolute	Ballesteros	pEC_{50}	% Effect	n	pEC_{50}	% Effect	n
wt		4.6±0.1	101±2	18	6.6±0.1	100±1	16
I66A	**I2.61A**	4.7±0.1	97±2	6	6.7±0.1	100±1	4
S86A	**S3.29A**	4.5±0.1	81±2	4	5.9±0.1	100±1	4
S86G	**S3.29G**	4.4±0.1	97±2	4	6.3±0.1	100±1	4
F89A	**F3.32A**	≤4	b	4	6.1±0.1	100±1	8
Y90A	**Y3.33A**	no response	-	5	5.8±0.1	100±1	4
Y94A	**Y3.37A**	≤4	c	4	6.5±0.1	100±1	4
S96A	**S3.39A**	4.5±0.1	93±2	8	7.1±0.1	100±1	8
H140A	**H4.44A**	4.5±0.1	100±1	8	7.0±0.1	100±1	8
R180A	**R5.39A**	no response	-	4	6.1±0.1	100±1	4
R180K	**R5.39K**	no response	-	8	6.1±0.1	100±1	8
Y238A	**Y6.51A**	no response	-	4	5.3±0.1	100±1	4
N239A	**N6.52A**	≤4	b	4	6.3±0.1	100±1	4
H242A	**H6.55A**	≤4	a	4	6.0±0.1	100±1	4
H242F	**H6.55F**	no response	-	5	5.9±0.1	100±1	4
H242N	**H6.55N**	no response	-	8	5.9±0.1	100±1	8
R255A	**R7.35A**	no response	-	5	5.9±0.1	100±1	4
R255K	**R7.35K**	≤4	a	8	6.1±0.1	100±1	8
S256A	**S7.36A**	4.6±0.1	99±2	4	6.5±0.1	100±1	4
S262A	**S7.42A**	4.7±0.1	82±4	8	6.6±0.2	100±1	8
S263A	**S7.43A**	4.7±0.1	75±2	8	6.6±0.3	100±1	8

Table 6 : Effect of mutations in hFFA2 on the potency and the efficiency of propionate and Compound A in cAMP assays.

Position of the mutation is given as absolute position in the protein sequence and according to the Ballesteros nomenclature (1995). Residual effect of 1mM propionate (in % effect of Compound A) is scaled from 20 to 40% (a), 40 to 60% (b), 60 to 80% (c). Receptors for which the response of propionate was strongly affected by the mutation are shaded in dark red, slightly affected in light red, unaffected in light green, and enhanced in dark green.

3.2.4. Comparative analysis of hFFA3 mutants in cAMP assays

We then analyzed the ability of propionate and Compound B to lower the forskolin-induced cAMP production in Hek293 Flpin cells expressing individually one hFFA3 mutated receptor, first for each ligand by itself and then both ligands in combination.

Strikingly, the F89A (3.33), R185A (5.39), H245A (6.55) and R258A (7.35) mutated receptors did not respond to propionate at all and showed only some residual response at high concentrations of Compound B (Table 7; Fig. 27). Moreover, mutation of the positively charged R185 and R258 to positively charged lysine (K) residues did not rescue this loss of function (Table 7; Fig. 27). Similarly, mutation of the aromatic H245 (6.55) residue was not rescued by the aromatic phenylalanine (F), or an asparagine (N) as present in hFFA1 in this position (Table 7; Fig. 27).
Interestingly, in hFFA2, the 5.39, 6.55 and 7.35 positions were shown to be crucial for binding of propionate, but affected only slightly the potency of Compound A (Fig. 26 and Table 6; Stoddart *et al.* 2008b; Sum *et al.* 2007). Taken together, these results support the idea that Compound B binds to a distinct pocket in hFFA3 than that of Compound A in hFFA2, although both compounds being allosteric activators of their cognate receptors.
In hFFA1, both R5.39 and R7.35 were shown to be essential for the binding of the synthetic carboxyl-containing GW9508 ligand (Sum *et al.*, 2007). However, GW9508 is supposed to partly overlap the binding site of the endogenous ligand linoleate (Sum *et al.*, 2007).
Regarding the 3.33 position, we are the first ones to show its importance in free fatty binding by FFA receptors.

In contrast, mutation of hFFA3 in positions M72 (2.61), Y100 (3.37) and N242 (6.52) revealed a less important role of these residues in ligand binding. Indeed, the M72A, Y100A and N242A mutated receptors were still able to lower the cAMP concentration when stimulated by propionate or Compound B (Table 7; Fig. 27). However, the N242A mutation was more severe than the M72A and Y100A mutations regarding their respective effects on the potency of propionate and Compound B.

These results are in line with our mutagenesis data on hFFA2, in which the mutation of the residues in positions 2.61, 3.37 and 6.52 modified only slightly the potency of propionate and Compound A, the 6.52 mutated receptor being the most affected by the mutation (Table 6; Fig. 26).

In order to refine the analysis of the effect of mutations in hFFA3 and the capacity of Compound B to act as an allosteric agonist, we conducted some combination experiments in which Compound B dose-response curves were performed in the presence of various concentrations of propionate, and conversely.

These experiments confirmed that the F89A, R185A, R185K, H245A, H245N, H245F, R258A and R258K mutations abolished the ability of propionate to activate the receptor and that Compound B was effective only at high doses, i.e. 100µM (Table 7; Fig. 27). However, for the M72A (2.61), Y100A (3.37) and N242A (6.52) mutated receptors, an interesting pattern appeared. Hence, we plotted the pEC50 of Compound B in function of the concentration of propionate and vice versa (Fig. 28A and B).

The EC_{50} of Compound B on the wt receptor diminished from 15µM to 0.4µM in presence of 1mM of propionate. Interestingly, the EC_{50} of Compound B for the M72A, Y100A and N242A mutants also reached the minimal value of 0.4µM in the presence of 1mM propionate, although being higher than the wild type receptor in the absence of propionate (Fig. 28A). Hence, the loss of potency of Compound B provoked by these mutations can be allosterically rescued by propionate.

In the converse experiment, the EC_{50} of propionate decreased from 53µM to 4µM in the presence of 0.1mM Compound B (Fig. 28B). On the M72A mutant, propionate also reached an EC_{50} value around 6µM in the presence of 0.1mM Compound B (Fig. 28B). In contrast, the Y100A and N242A mutations prevented propionate from reaching this maximal value, the EC_{50} of propionate remaining by 35µM in the presence of 0.1mM Compound B (Fig. 28B).

Concerning the N242A mutant receptor, we observe that the full ago-allosteric potency of Compound B is reached when propionate is present at high concentrations. However, high concentrations of Compound B can only slightly increase the potency of propionate.

This indicates that N242 is also somehow involved in the TM5-TM6-TM7 hydrogen-bonding network, which coordinates propionate.

The functionality of the Y100A mutant receptor is slightly altered in comparison to the wild-type FFA3 receptor, both ligands being less potent (Fig. 28A and B). This observation suggests that Y100 is involved in receptor activation, although the actual presence of Tyr is not crucial.

Finally, the M72A mutation, located on TM2, has very little effect on propionate potency. Thus, this position should not be directly involved in the activation network, probably because of its large distance to the propionate binding site and of the apolar nature of methionine. Therefore, the effect of M72A on the potency of Compound B could be attributed to direct interactions of Compound B with M72. We suggest that the Compound B binding site is located between TM2, TM3 and TM7 (Figure 29).

Moreover, it has been shown that Compound A was able to enhance allosterically the potency of the SCFA acetate not only on the wild-type FFA2 receptor, but also on the R5.39A and R7.35A mutated FFA2 receptors (Swaminath *et al.*, 2010). Indeed, Compound A was able to efficiently rescue the response of the R5.39A and R7.35A hFFA2 mutated receptors to the endogenous ligand acetate by allosteric activation (Swaminath *et al.*, 2010). For hFFA3, we did not observe such an allosteric rescuing of Compound B by propionate and vice versa, on the R5.39A and R7.35A mutated receptors (Fig. 27), indicating that allosterism in FFA2 and FFA3 may function differently.

Fig. 27: Effect of single point mutations on the response of hFFA3 to propionate or Compound B in cAMP assays.

ALPHAScreen cAMP assays were performed in the presence of 10μM forskolin with Hek293 Flpin cells expressing hFFA3 wild type (wt) or one of the mutated forms. [next page]. Dose-response curves of propionate (left side for each mutant) were tested in combination with various doses of Compound B (rainbow scale from 1mM to 3μM). Conversely, dose-response curves of Compound B (right side for each mutant) were tested in combination with various doses of propionate (rainbow scale from 0.1mM to 0.3μM). The x-axis represents the cAMP level normalized to the maximal effect of propionate on the wild type receptor and the y-axis represents the concentrations on a logarithmic scale of either propionate or Compound B. Graphs are representative of 4-8 experiments. Error bars represent SEM, n=3 for one experiment. [next page]

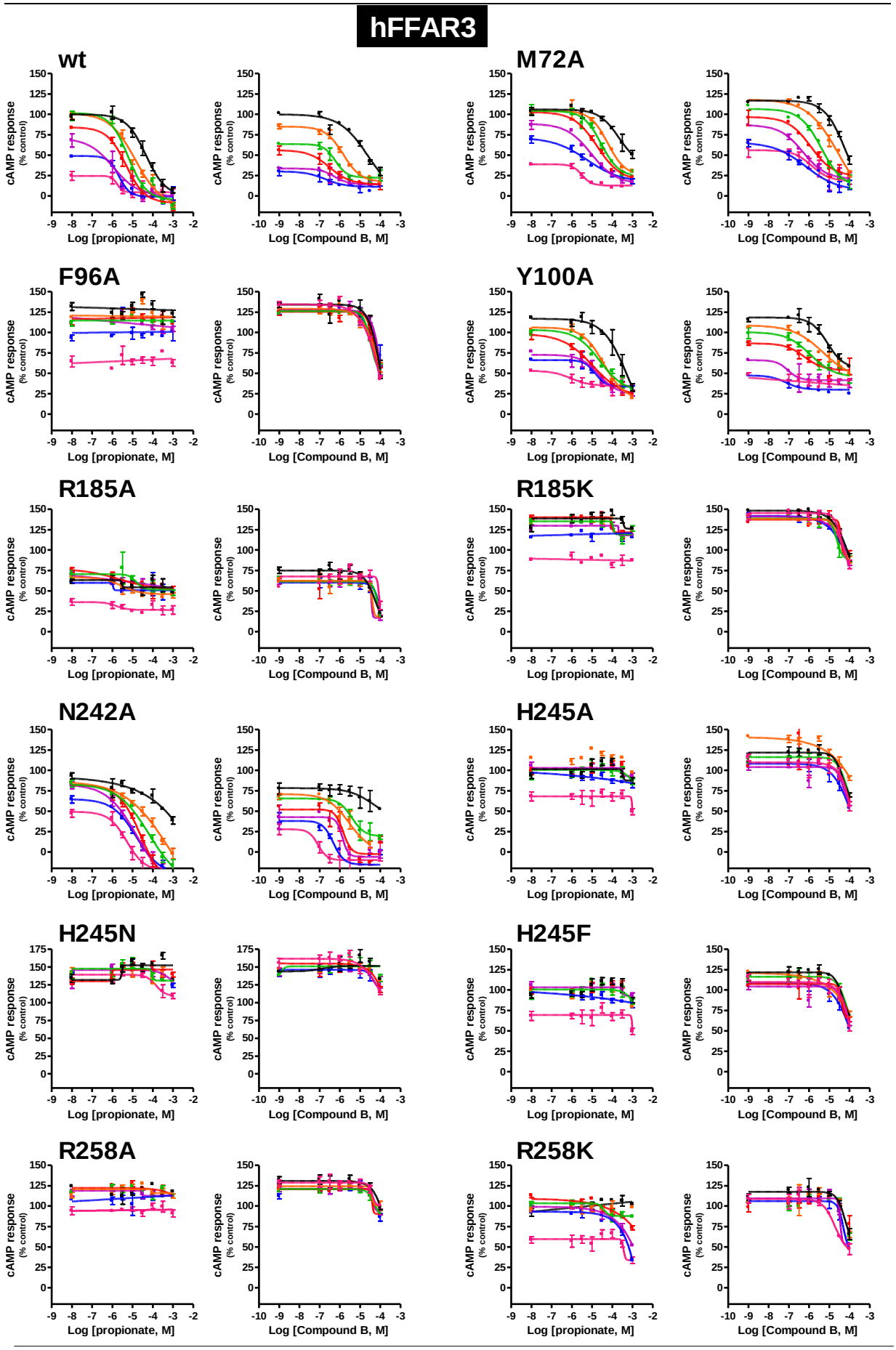
hFFAR3
wt
M72A
F96A
Y100A
R185A
R185K
N242A
H245A
H245N
H245F
R258A
R258K
cAMP response (% control)
Log [propionate, M]
Log [Compound B, M]
log[Compound B, M]
- -6.5 -6.0 -5.5 -5.0 -4.5 -4.0
log[propionate, M]
- -5.5 -5.0 -4.5 -4.5 -3.5 -3.0

Mutation position		Propionate			Compound B		
absolute	Ballesteros	pEC_{50}	% Effect	n	pEC_{50}	% Effect	n
wt		4.3±0.1	85±4	15	4.8±0.1	100±1	11
M72A	**M2.61A**	≤4	-	11	4.3±0.2	100±1	9
F96A	**F3.33A**	no response	-	18	≤4	-	18
Y100A	**Y3.37A**	≤4	-	24	4.5±0.2	100±1	11
R185A	**R5.39A**	no response	-	17	≤4	-	17
R185K	**R5.39K**	no response	-	17	≤4	-	17
N242A	**N6.52A**	≤4	-	25	4.1±0.2	100±1	25
H245A	**H6.55A**	no response	-	16	≤4	-	16
H245F	**H6.55F**	no response	-	16	≤4	-	16
H245N	**H6.55N**	no response	-	18	no response	-	18
R258A	**R7.35A**	no response	-	16	≤4	-	16
R258K	**R7.35K**	no response	-	17	≤4	-	17

Table 7 : Effect of mutations in hFFA3 on the potency and the efficiency of propionate and Compound B in cAMP assays.

The maximal response obtained with Compound B was set as 100% for each type of receptor in ALPHAScreen cAMP assays.

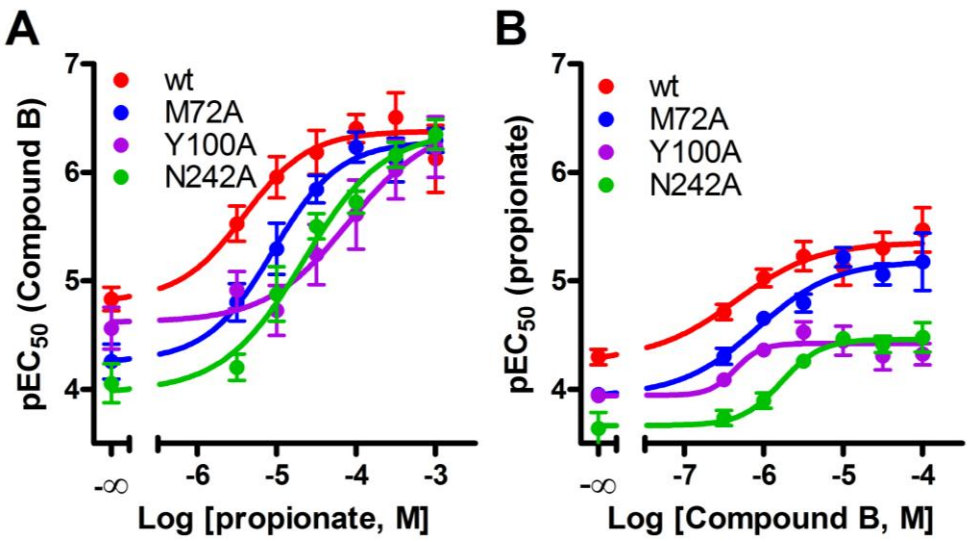

Fig. 28 : Allosteric effect of Compound B on hFFA3 wt or the FFA3 M72A, N242A and Y100A mutated receptors in cAMP assays.

A. Displacement of the potency of Compound B in function of the concentration of propionate. **B**. Displacement of the potency of propionate in function of the concentration of Compound B. The responses of hFFA3 wild type (wt) are represented in red, of the M72A mutant in blue, of the Y100A mutant in violet and of the N242A mutant in green. Shown are representative experiments. Errors bars represent SEM, n=3.

4. Designing structural models for hFFA2 and hFFA3 and ligand poses

By combining the information gained in our mutagenesis studies and the existing crystal structures of GPCRs, we were able to design new structural models for FFA2 and FFA3, and in particular of their ligand binding pockets, to improve the previous putative models proposed by Lee *et al.* (2008).

Fig. 29 : Homology receptor models for hFFA2 and hFFA3.

Three-dimensional structural models for hFFA2 (A to C) and hFFA3 (D to F). **A. and D.** Overall side-view of hFFA2 (A) or hFFA3 (D), showing the position of propionate (in green) and Compound A (**A**, in magenta) or Compound B (**D and I**, in magenta) bound to their respective receptors. **B. and E.** Top view of the binding pocket of hFFA2 (**B**) and hFFA3 (**E**), showing molecular interactions (dotted lines) between the ligands and the side-chains of the aminoacid residues. **C. and F.** Detailed side-view of the putative binding pocket. [next page]

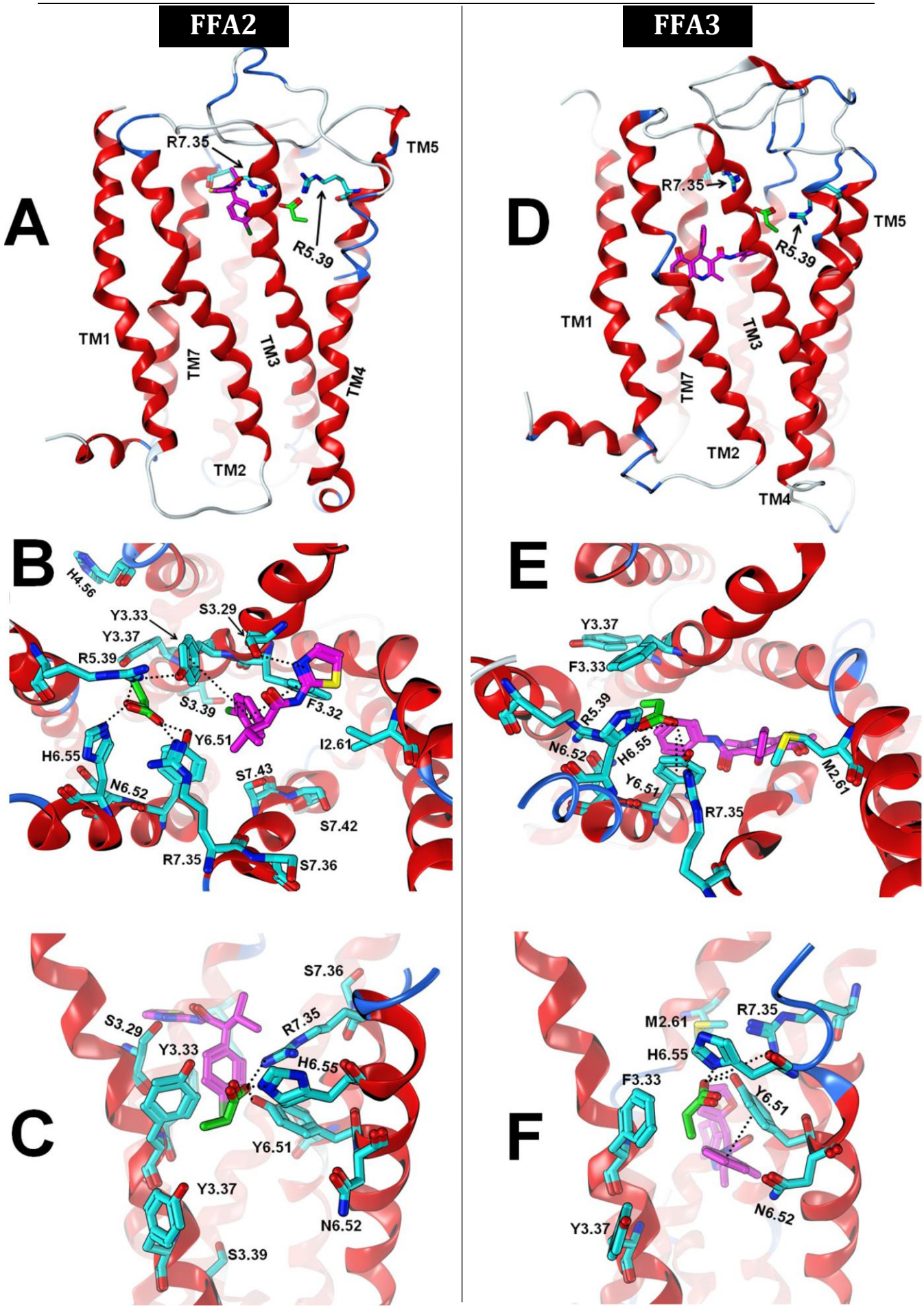
FFA2
FFA3
A
R7.35
TM5
R5.39
TM1
TM7
TM3
TM4
TM2
D
R7.35
TM5
R5.39
TM1
TM3
TM7
TM2
TM4
B
H4.56
Y3.33
S3.29
Y3.37
R5.39
S3.39
F3.32
Y6.51
I2.61
H6.55
S7.43
N6.52
S7.42
R7.35
S7.36
E
Y3.37
F3.33
R5.39
N6.52
H6.55
M2.61
Y6.51
R7.35
C
S7.36
S3.29
R7.35
Y3.33
H6.55
Y6.51
Y3.37
N6.52
S3.39
F
M2.61
R7.35
H6.55
F3.33
Y6.51
N6.52
Y3.37

As both FFA2 and FFA3 possess less than 20% sequence identity to any available GPCR template, we relied on multiple templates to create homology models for these receptors. To model FFA2 and FFA3, we used the crystal structures of the adenosine A_{2A} receptor (Jaakola *et al.*, 2008) and the β2-adrenergic receptor (Cherezov *et al.*, 2007) in inactive state. We subsequently introduced additional backbone modifications to construct a model of FFA2 and FFA3 receptors in an activated state. Indeed, TM6 was straightened by approximately 15° and moved towards the TM-cavity, according to a "toggle switch mechanism" (Schwartz *et al.*, 2006). The orientation of His6.55 supports this adjustment, because it brings this essential residue closer to the binding cavity in the models for both receptors.

Our models of FFA2 and FFA3 were checked for plausibility by comparing the putative binding site residues with published phylogenetic data (Surgand *et al.*, 2006). The second step of model validation was done by checking if the residues, which have been shown to influence ligand interactions in the mutagenesis experiments, are accessible from the ligand binding site. Once the models have been shown to be in accordance with the mutagenesis experiments and the literature, ligand docking was performed. For both receptors, propionate is interacting with the arginines on TM5 and TM7 (R5.39 and R7.35), forming ionic bonds with both of them (Fig. 29B and E). In both receptors, the rest of the propionate binding site involves amino acids which are close-by the guanidine groups of arginine residues.

For FFA2, the mutagenesis data maps the whole binding site of propionate and two types of interactions are found. On one hand, there are polar amino acid side chains, such as Y3.33, Y6.51, N6.52 and H6.55, which interact either directly with the carboxylic group of propionate or with the guanidine group of the two essential arginines to keep them in place. On the other hand, there is a small hydrophobic cavity found between TM3 and TM5, where Y3.33 forms the roof, Y3.37 the floor, and some aliphatic amino acids on TM5 form its back (L5.42 and L5.46 for FFA2 and M5.42 and L5.46 for FFA3). The size of the cavity is limited, thus explaining the preference of FFA2 for small carboxylic acids. Mutagenesis data confirmed the proposed propionate binding mode, where Y3.33, Y3.37, R5.39, Y6.51, N6.52, H6.55, and R7.35 were involved in propionate interaction. Mutation of these residues led to a complete loss in the ability of propionate

to activate the receptor. However, Compound A still activated all FFA2 mutants, thus ensuring that the signaling ability of the receptor was not impaired by these mutations. The fact that the substitution of R5.39 or R7.35 by lysine led to a receptor that did not respond to propionate is also a confirmation that the guanidine groups of the arginines are part of a hydrogen bond/ionic network, where several neighboring amino acids are involved. H6.55 has been mutated to A, F and N in order to see which features of this amino acid is important for interaction with propionate. Neither A nor F or N mutants could re-gain activity of the receptor, thus suggesting that a charged histidine is required for propionate binding. Any mutation in this proposed network affected only slightly the response of the receptor to Compound A. This observation suggests that an intact network may be preferable for receptor activation, even for allosteric agonists that do not necessarily bind to that network.

The binding site of Compound A has been recently suggested to be very close to EL2 (Lee *et al.*, 2008). However, our docking results and mutagenesis data indicate that this ligand binds to a close-by cavity between TM2, TM3 and TM7 (Fig. 29). Although most mutations had little effect on the potency of Compound A, our experimental data suggest that Y6.51 and S3.29 are involved in binding. Compound A and propionate occupy distinct regions in the putative binding site of FFA2 (Fig. 29). This binding mode is also in accordance with structure-activity relationship data for this structural class (Wang *et al.*, 2010). The region of the thiazole moiety has been extensively explored and a preferred position next to sulfur has been identified, where substituents can be attached without losing much in potency. This is in line with our model, where the thiazole ring points towards the membrane-solution interface and no steric hindrance for larger substituents is to be expected.

Regarding FFA3, we evaluated fewer mutations than for FFA2. However, due to the very high homology between the binding sites of the two receptors, propionate has been docked to FFA3 in the same way as FFA2 (Fig. 29). The location of the small hydrophobic pocket is nonetheless slightly different because, in position 3.33, the Tyr residue from FFA2 is replaced by a Phe in FFA3. Due to the lack of the hydrogen bond at this position, R5.39 may move slightly towards TM6, changing the shape of the hydrophobic pocket. F3.33 forms the roof of the hydrophobic pocket, being more flexible than its Tyr

counterpart in FFA2 due to the already mentioned lack of the hydrogen bond to R5.39. In consequence, that makes the unoccupied hydrophobic pocket a bit more floppy. It partially explains the lower potency of SCFAs for FFA3 than for FFA2 due to the larger loss in entropy upon ligand binding. These findings match with those by Schmidt *et al.* (2011). Our mutagenesis results for FFA3 are consistent with the proposed binding mode, because mutation of any amino acid predicted to be involved in binding makes the receptor irresponsive to propionate.

Compound B was docked into the putative allosteric binding site of FFA3, similarly to Compound A, in a cavity formed by TM2, TM3 and TM7, but slightly shifted to the intracellular side. Mutagenesis data make the validation of the binding mode quite difficult. Indeed, no large effect of the mutations could be monitored because of the low potency of the ligands. However, the ago-allosteric behavior of Compound B, illustrated by the Schild-like plots from Fig. 28, helped a lot to identify the region where the ligands bind. M2.61, Y3.37 and N6.52 still responded to propionate and Compound B showed a non-parallel behavior to the wild-type curves. These data suggest that all three mutants are involved in the binding of the agonists. It is obvious that Y3.37 and N6.52 are close to the propionate binding site, whereas M2.61 on TM2 seems to be involved in the binding of Compound B. This is in line with the proposed binding site of Compound B in the homology model. Further proposed interactions of Compound B to FFA3 are a hydrogen bond to S7.42 on TM7 and a π-stacking to Y6.51 on TM6. The furyl group of Compound B is proposed to weakly interact with M2.61. More experiments would be necessary to confirm the exact interaction partners on an atomistic level, but based on the present data, we are confident that the proposed binding modes are close to reality.

Conclusion and perspectives

Mounting evidence highlights the beneficial role of dietary fibers in metabolic diseases. For example, fiber supplementation improves glycemic control, decreases hyperinsulinemia, and lowers plasma lipid concentrations in patients with T2D (Chandalia *et al.*, 2000). Unfortunately, the present mean intake of dietary fibers in westernized diets is too low. For instance, the current average fiber intake of a North American is less than half of the US recommendations (Sleeth *et al.*, 2010). These observations stress the importance of the consumption of larger amounts of dietary fibers for weight controlling.

Additionally to the increased gastric distension caused by the ingestion of fiber-rich food, fermentable dietary fibers have an overall beneficial effect on the metabolic state of the organism via the SCFAs. SCFAs are products of the fermentation of dietary fibers by the intestinal microflora. Indeed, some dietary fibers, such as pectin, resistant starches, gums and polyfructans, are highly fermentable (Sleeth *et al.*, 2010). The resulting SCFAs are key regulators of essential metabolic functions in the body, like appetite, food intake and body weight (Sleeth *et al.*, 2010). An explanation for the beneficial effect of SCFAs is that they would promote the secretion of anorexigenic hormones like PYY, CCK, 5-HT or GLP-1 from enteroendocrine cells or leptin from adipocytes, as suggested by our findings and those of others (reviewed by Sleeth *et al.*, 2010).

The effects of SCFAs have been now identified as being mediated by the FFA2 and FFA3 receptors. In enteroendocrine cells, FFA2 and FFA3 receptors detect SCFAs that are present in the intestinal lumen and are in consequence the first line of nutrient sensors.

Additionally, a large part of the SCFAs produced in the gut enters the blood flow and can act on pancreatic β-cells and adipocytes, which also express FFA2 and/or FFA3.

In consequence, FFA2 and FFA3 receptors have become in the last years attractive potential therapeutic targets against a variety of metabolic diseases, mainly thanks to their potential beneficial effects on the metabolism.

During this PhD work, we succeeded in gaining additional knowledge about the human FFA2 and FFA3 receptors, regarding their respective localization, structure, functioning and pharmacology.

First, we confirmed the expression of FFA2 and/or FFA3 in enteroendocrine cells, adipocytes and pancreatic β-cells but also, at weaker levels, in some immune cells, supporting a role of SCFAs in all these cell types.

Then, using self-made cellular models, we dissected the pharmacology of the receptors and the signaling pathways generated in response to activation of the receptors by endogenous or synthetic agonists.
In the experiments that we conducted, we were able to show that endogenous ligands, such as propionate, but also synthetic agonists, such as Compound A or Compound B, were able to activate FFA2 and/or FFA3 and to induce various subsequent intracellular signaling events. Although both receptors respond to SCFAs and are partially expressed in the same tissues, FFA2 and FFA3 show specificity concerning their synthetic agonists Compound A and Compound B, respectively. Thus, a treatment with one of these synthetic agonists would target either FFA2 or FFA3, but not both receptors together.
Moreover, we demonstrated that activation of FFA2 or FFA3 provoked a decrease in cytosolic cAMP, phosphorylation of the ERK1/2 MAP kinase and cellular impedance changes. Additionally, we observed a transient increase of the cytosolic Ca^{2+} concentration, but uniquely in response to FFA2 activation. Furthermore, we showed that FFA2 coupled to $G\alpha_q$ and $G\alpha_i$ G proteins, whereas FFA3 appeared to couple solely to $G\alpha_i$ G proteins.

Besides, we demonstrated that Compound A and Compound B acted as allosteric agonists for FFA2 and FFA3, respectively. Moreover, we were able to identify cyclopropanecarboxylate as an agonist of both hFFA2 and hFFA3.

Interestingly, we observed that the affinity of FFA2 and FFA3 for SCFAs was quite low. Actually, in our cellular models, high concentrations of SCFAs - higher than normal physiological concentrations - were required to ensure a strong cellular response.
However, we also demonstrated that synthetic agonists, as allosteric agonists, could be used to potentiate the effects of SCFAs. Indeed, we observed in cAMP assays that the potency of propionate at FFA2 and FFA3 was increased in presence of synthetic compounds and vice versa. Moreover, in Ca^{2+} assays, as we stimulated FFA2 with a combination of propionate and Compound A, we obtained a stronger Ca^{2+} flux than when the ligands were tested separately.
Besides, in Ca^{2+} assays, we were able to show that the FFA2 receptor was reactivable 4 min after a first stimulation. This result indicates that a part of the receptors that are present on the cell is not desensitized or internalized, at least not in this time scale. Likewise, it would be interesting to assess a time course of the activability of the FFA3 receptor, for instance using the CellKey instrument, to know if the receptor is still activable after a first stimulation.

To complete the pharmacological profile of the receptors and to get a better computational view of the binding cavities of the synthetic and endogenous ligands, we performed site-directed mutagenesis and examined the role of a series of aminoacids that were suspected to be involved in ligand recognition and receptor function.
For instance, we identified some conserved positively charged aminoacid residues that anchor the carboxyl moiety of propionate in both FFA2 and FFA3. Additionally, other residues located deeper in the TM bundle were shown to form binding sites for the synthetic agonists Compound A and Compound B on FFA2 and FFA3, respectively. However, we demonstrated that Compounds A and B do not share exactly the same binding sites on their respective receptors, Compound B being more oriented towards the SCFA binding site than Compound A.

The structural models and the binding poses that we propose here allow a better visualization of the structure of the ligand binding sites of both receptors. In consequence, our structural models are precious tools in view of finding new synthetic agonists for FFA2 and FFA3. For instance, it would be possible to design an array of new compounds deriving from Compound A or Compound B, but with selected chemical modifications.

In addition to our *in silico* structural models, we also developed an efficient, simple and standardized assay - namely the cAMP assay – that could be easily used for high-throughput screening. Indeed, given its sensitivity, its relative simplicity to perform and the fact that it suits both FFA2 and FFA3, our cAMP assay using the cell lines that we established and that express the wild-type forms of FFA2 and FFA3 would be appropriate for this purpose.

After screening with the cAMP assays, a next step in this strategy would be to test the hits in secondary cAMP assays, but this time with the cell lines that we established and that express the mutated forms of FFA2 and FFA3. This step should bring valuable information about the mechanisms of interaction of the new substances with FFA2 and FFA3. Additionally, it would be necessary to test the selectivity of the best new FFA2 and FFA3 agonists on receptors that are structurally similar to human FFA2 and FFA3, like FFA1, the receptors for dicarboxylic acids GPR80 and GPR91, or also homologues for FFA2 and FFA3 from other species, like hamster, mouse or rat, in view of animal *in vivo* experiments.

Finally, it would be also interesting to investigate the effect of such synthetic compounds on the closely related GPR42 receptor, whose function is still unknown. Indeed, new synthetic agonists of FFA3 could theoretically also activate GPR42 (at least the functional isoform that is presumably borne in a large part of the population). Regarding the lack of knowledge concerning the function of GPR42, unexpected adverse effects due to its non-wanted activation could be possible and should therefore be carefully controlled.

Hopefully, this strategy will end up in finding new synthetic agonists of FFA2 or FFA3, with higher potencies than Compound A or Compound B, that will be one day used as therapeutic drugs.

Although it is possible to find new synthetic agonists for FFA2 and FFA3 with high potencies, satisfying bio-availability, low toxicity and without deleterious side effects, it is still unsure if these substances could really be used as therapeutic drugs to remedy metabolic diseases. Indeed, before using FFA2 and FFA3 agonists as drug, fundamental questions and major issues have to be solved.

One major issue is that the physiological functions of FFA2 and FFA3 are still poorly understood. In consequence, the *in vivo* effects of FFA2 or FFA3 pharmacological modulation are not certain.

However, given the multiple range of action of the SCFAs, it is possible to predict possible effects of drugs targeting FFA2 or FFA3. Theoretically, agonists for FFA2 or FFA3 would have multifaceted actions on the patient and would strengthen the beneficial effects of SCFAs on glucose and fat metabolism (Fig. 30).

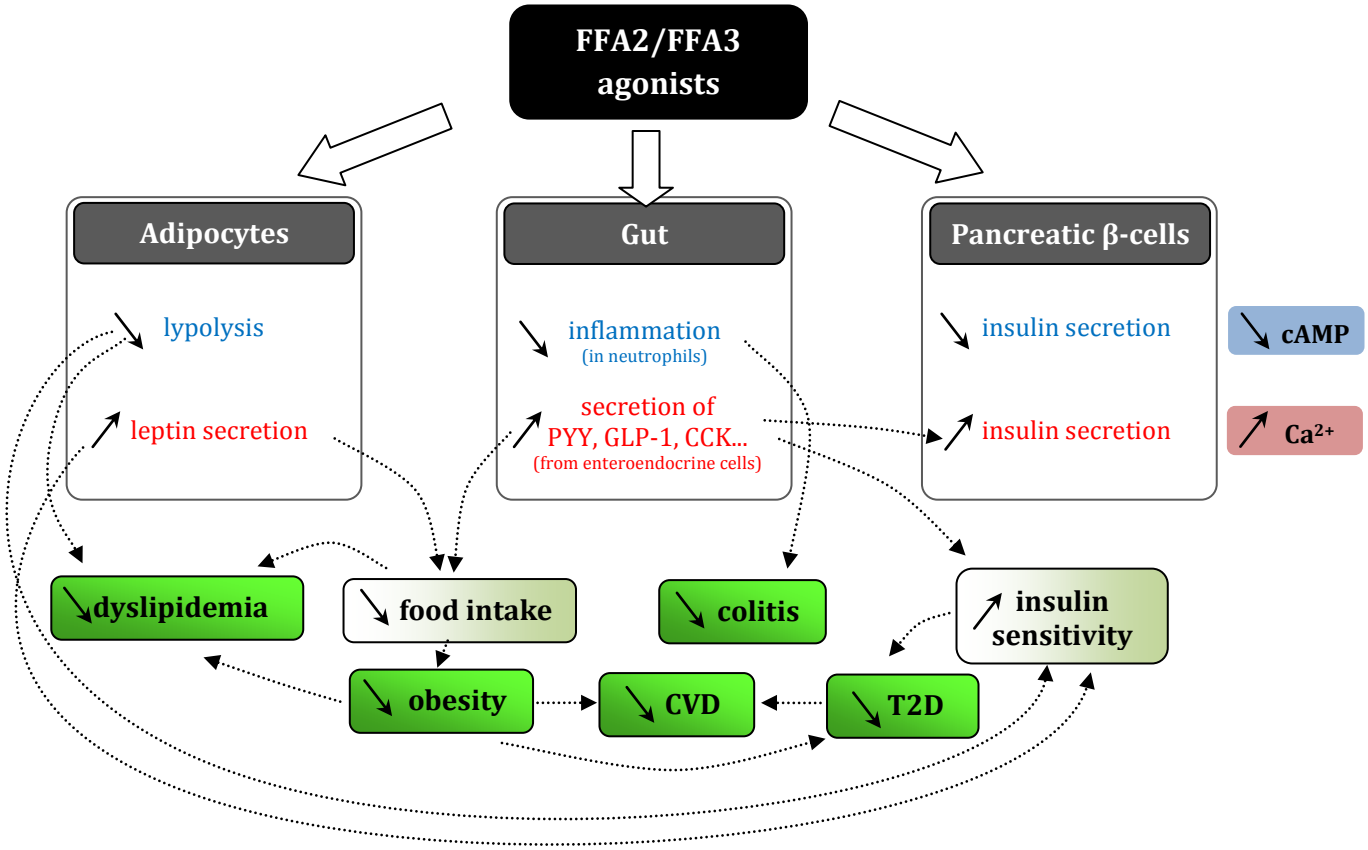

Fig. 30 : Putative systemic effects of agonists for FFA2 or FFA3.

Pharmacological treatment with agonists for FFA2 or FFA3 would have different effects depending on the cell types where the receptors are expressed and on the signaling pathways engendered by the activation of the receptors (in blue, a decrease in cytosolic cAMP content; in red, a transient increase of the cytosolic Ca^{2+} concentration). These cellular events would have for final effect the improvement of a variety of diseases including colitis, dyslipidemia, obesity, type 2 diabetes (T2D) and cardiovascular diseases (CVD).

From a physiological point of view, we showed that FFA2 and/or FFA3 were expressed in insulinoma cells, enteroendocrine cells and adipocytes, confirming a probable involvement of these receptors in metabolic regulation.
However, in the present work, we only used for functional assays Hek293 Flpin cells, which derive from kidneys, and no enteroendocrine cells, adipocytes or β-cells, that would be physiologically more relevant. In consequence, we do not have data on the physiological effect of FFA2 or FFA3 modulation in their endogenous biological systems. Based on the literature, it is possible to extrapolate our results coming from the Hek293 cells and speculate on what would happen in enteroendocrine cells, adipocytes or pancreatic β-cells and subsequently in the whole organism after FFA2 or FFA3 activation (Fig. 30).

In enteroendocrine cells, the secretion of incretin hormones is triggered by transient elevations in cytosolic Ca^{2+} concentration. We showed that FFA2 activation provokes an increase in Ca^{2+} via activation of the $G\alpha_q$ pathway. Consequently, in enteroendocrine cells, FFA2 activation would finally lead to the secretion of some hormones, like PYY, CCK, 5-HT or GLP-1. Then, for example, it is possible to speculate that GLP-1 would enhance insulin secretion from pancreatic β-cells, increase insulin sensitivity, inhibit gastric emptying, reduce appetite in the brain and enhance insulin sensitivity in skeletal muscles, as reviewed by Drucker (2005).

In adipocytes, the release of free fatty acids resulting from the breakdown of triglycerides is regulated by the hormone-sensitive lipase, according to the cytosolic concentration in cAMP (Duncan *et al.*, 2007). We demonstrated that activation of FFA2 or FFA3 provoked a decrease in cytosolic cAMP concentration. In adipocytes, this cellular event has been shown to inhibit lipolysis. Indeed, nicotinic acid also causes a reduction of cAMP contents via a $G\alpha_i$-coupled receptor (Tunaru *et al.*, 2003). Clinically, nicotinic acid has been proven a potent anti-dyslipidemic drug, although provoking a disturbing skin flushing effect (Chapman *et al.*, 2010). An addition, nicotinic acid is able to improve insulin-sensitivity and glucose tolerance in obese diabetic and non-diabetic patients (Santomauro *et al.*, 1999). FFA2 or FFA3 agonists may likewise inhibit lipolysis in adipocytes via their $G\alpha_i$-coupling, thus improving dyslipidemia, insulin sensitivity and

glucose tolerance, but without causing the flushing adverse effect of nicotinic acid. To support this idea, SCFAs have been shown to inhibit lipolysis in mice, without causing flushing (Ge *et al.*, 2008), and to promote adipogenesis, i.e. the storage of triacylglycerides, preventing ectopic fat deposits (Hong *et al.*, 2005). Finally, injection of acetate has been shown to reduce the level of FFA in the blood (Ge *et al.*, 2008). Interestingly, Robertson *et al.* (2005) suggested that a dietary supplementation with resistant starch, that is supposed to be fermented into SCFAs, ameliorates *in vivo* insulin sensitivity in human.

In pancreas, the role of FFA receptors is less clear and actually depends on their coupling with signaling pathways. For instance, if a transient elevation in cytosolic Ca^{2+} concentration is induced in response to activation FFA2, it would probably enhance the secretion of insulin.
Conversely, if the activation of FFA2 or FFA3 induces a decrease in cAMP via the $G\alpha_i$-pathway, it may prevent the secretion of insulin. Evidence for this is illustrated by the fact that, in isolated rat pancreatic β-cells and in Min6 cells, SCFAs inhibit glucose-induced insulin secretion (Leonard *et al.*, 2006; Ximenes *et al.*, 2007).
Consequently, the exact effect of FFA2 and FFA3 agonists on the insulin secretion seems to be dual and need further investigations to be clearly determined.

Of course, one can also think of the negative effects of such drugs. For instance, if agonists for FFA2 inhibit lipolysis in adipocytes, they prevent the release of FFA in the blood flow, but also promote fat storing in the adipocytes. However, since such treatment will comes in complement to a controlled and reduced food intake, patients that receive such treatments should not gain weight.
Other possible negative or unwanted effects of FFA2 and FFA3 pharmacological modulation could be due to their possible involvement in the immune system. Indeed, we and others also found expression of these receptors at a low but not negligible level in immune cells (LePoul *et al.*, 2003; Cox *et al.*, 2009). Therefore, the effects of FFA modulation on the immune system should be taken into consideration for the development of FFA agonists. It is necessary to perform further in depth investigation to

determine the real impact of FFA2 or FFA3 modulation on the immune system before any commercialization of such a drug. On the other hand, if agonists for FFA2 and/or FFA3 exhibit inhibitory effects on the immune system, they would be also of interest in view of developing new anti-inflammatory drugs. For instance, the anti-inflammatory properties of SCFAs have been proposed to show beneficial effects against colitis (Cox *et al.*, 2009). Moreover, since inflammation is a key component of the insulin resistance process (Schenk *et al.*, 2008), treatment with FFA2 or FFA3 agonists may help restoring insulin sensitivity.

From a pharmacological point of view, one can speculate that agonists for FFA2 or FFA3 would be of first interest in the treatment of metabolic diseases. As we showed in our cAMP and Ca^{2+} assays, they effectively potentiate the effects of the SCFAs and that even at low concentrations.
In contrast to the existing pharmacological strategies that target the feeding behavior, a FFA2 or FFA3 pharmacological modulation would show probably less problematic side effects. Indeed, the use of molecules that control the feeding behavior in the CNS is controversial due to possible psychiatric side effects. For instance, the antagonist of the cannabinoid CB1 receptor (Acomplia™) was withdrawn from the market in 2006 because of risks of depression. FFA2 and FFA3 agonists have the advantage not to bind directly to the receptors that control satiety in the CNS : they would only enhance the secretion of beneficial hormones involved in weight control, like leptin, GLP-1 or CCK by acting on the metabolic organs.

However, further in depth investigation is still required before therapeutic use of FFA2 or FFA3 agonists. Next steps to this work will necessarily concern their physiological relevance in the whole body, i.e. a better understanding of the biological functions of the FFA receptors, including GPR42, first in animal models and then in the human organism. However, suitable tools for such investigation are still lacking.

Appendices

1. Aminoacid properties

Aminoacid	3-letter code	1-letter code	Side-group	Charge properties/ Hydrophobicity
Alanine	Ala	A	Aliphatic	NH
Arginine	Arg	R	Basic	+
Asparagine	Asn	N	Amide	PU
Aspartic acid	Asp	D	Acidic	-
Cysteine	Cys	C	Sulfhydryl	PU
Glutamic acid	Glu	E	Acidic	-
Glutamine	Gln	Q	Amide	PU
Glycine	Gly	G	Aliphatic	PU
Histidine	His	H	Basic	+
Isoleucine	Ile	I	Aliphatic	NH
Leucine	Leu	L	Aliphatic	NH
Lysine	Lys	K	Basic	+
Methionine	Met	M	Aliphatic	NH
Phenylalanine	Phe	F	Aromatic	NH
Proline	Pro	P	Imino	NH
Serine	Ser	S	Hydroxyl	PU
Threonine	Thr	T	Hydroxyl	PU
Tryptophan	Trp	W	Aromatic	NH
Tyrosine	Tyr	Y	Aromatic	PU
Valine	Val	V	Aliphatic	NH

NH : non-polar, hydrophobic; PU : polar, uncharged; + : positively charged; - : negatively charged

2. Publication

Allosteric activation of free fatty acid receptors 2 and 3

Elisabeth Lamodière, Christofer S. Tautermann and Remko A. Bakker

Boehringer Ingelheim Pharma GmbH & Co. KG, Departments of CardioMetabolic Diseases Research and Lead Identification and Optimization Support, 88397 Biberach an der Riß, Germany (EL, CT, RAB), and INSERM U866, Lipides Nutrition Cancer, UFR Sciences de la Vie, 6 boulevard Gabriel, 21000 Dijon, France (EL).

Abstract

FFA2 and FFA3, also known as GPR43 and GPR41, respectively, are two recently identified receptors for short-chain fatty acids such as acetate, propionate and butyrate. In the current study, we investigate the molecular pharmacology of FFA2 and FFA3 using a variety of methods. First, we characterized the endogenous mRNA expression of these receptors and the signal transduction initiated upon activation of heterologously expressed receptors by either endogenous or synthetic agonists. Moreover, we investigated by site-directed mutagenesis the molecular determinants contributing to the role of certain amino acid residues within the transmembrane regions of these receptors in agonist binding/receptor activation upon stimulation with either the endogenous agonist propionate or a synthetic FFA2 or FFA3 agonist. Based on these results we designed structural models showing the agonists bound to their respective FFA receptor. This is the first study describing the interaction of both an endogenous and a synthetic small molecule agonist with FFA3, and our data show that the synthetic FFA3 agonist acts as an ago-allosteric FFA3 agonist. Our findings provide additional insight into the functioning of FFA2 and FFA3 and may aid future efforts of designing agonists for these receptors.

In the quest for novel drug targets a variety of orphan ligand-receptor pairs have been identified over recent years, including G-protein coupled receptors (GPCRs) for free fatty acids (FFA). Given the important physiological functions of FFAs, these FFA receptors have become of considerable interest for their potential roles in various metabolic functions (reviewed in Stoddart *et al.*, 2008b), illustrated by the progress into clinical development of agonists for FFA receptor 1 (FFA1, formerly known as GPR40) as well as for the fatty acid amide receptor GPR119, both for the treatment of diabetes. The FFA receptors, that besides FFA1 include FFA2 and FFA3, as well as GPR84 and GPR120, are attributed specificity for certain FFAs and are classified accordingly (Stoddart *et al.*, 2008b). In the current study, we focus on FFA2 and FFA3 (formerly known as GPR43 and GPR41, respectively). These receptors exhibit only subtle differences in their endogenous agonists as both are preferentially activated by short-chain fatty acids (SCFAs), such as propionate or butyrate (see Figure 1A), which are products of carbohydrate fermentation by the intestinal flora (Le Poul *et al.*, 2003). However, the SCFA acetate has an appreciable potency for FFA2, while being only a very weak FFA3 agonist (Brown *et al.*, 2003). Activation of FFA2 results in the Gq- and Gi-mediated elevation of intracellular calcium levels and lowering of intracellular cAMP levels, respectively, whereas FFA3 exclusively couples to Gi (Brown *et al.*, 2003).
The functions of FFA2 and FFA3 are not fully understood, but are suggested to include the modulation of adipocyte lipolysis (Hong *et al.*, 2005;Ge *et al.*, 2008) and the mediation of leptin secretion (Zaibi *et al.*, 2010;Al-Lahham *et al.*, 2010), an hormone that regulates appetite and energy metabolism, from adipose tissue (Xiong *et al.*, 2004), as well as the regulation of intestinal flow and absorption through its presence on enteroendocrine cells (Samuel *et al.*, 2008), and a possible modulation of the immune system (Maslowski *et al.*, 2009;Samuel *et al.*, 2008;Sina *et al.*, 2009;Cox *et al.*, 2009;Al-Lahham *et al.*, 2010). The reported mRNA expression profiles for FFA2 and FFA3 are not very consistent and include adipocytes (Xiong *et al.*, 2004), pancreas and insulinoma cells

Abbreviations: 1, 4-furan-2-yl-2-methyl-5-oxo-1,4,5,6,7,8-hexahydro-quinoline-3-carboxylic acid-o-3 tolylamide; 2, 2-(4-chloro-phenyl)-3-methyl-N-thiazol-2-yl-butyramide; BSA, bovine serum 4 albumin; DMEM, Dulbecco's modified Eagle's medium; EL, extracellular loop; ERK, 5 extracellular signal-regulated kinase; FBS, fetal bovine serum; FFA, free fatty acid; GPCR, G 6 protein-coupled receptor; HBSS, Hank's balanced salt solution; HRP, horseradish peroxidase; 7 MOE, molecular operating environment; PBS, phosphate buffer saline; PTX, pertussis toxin; 8 SCFA, short-chain fatty acid; TM, transmembrane domain; Tween 20, 9 polyoxyethylenesorbitan monolaurate.

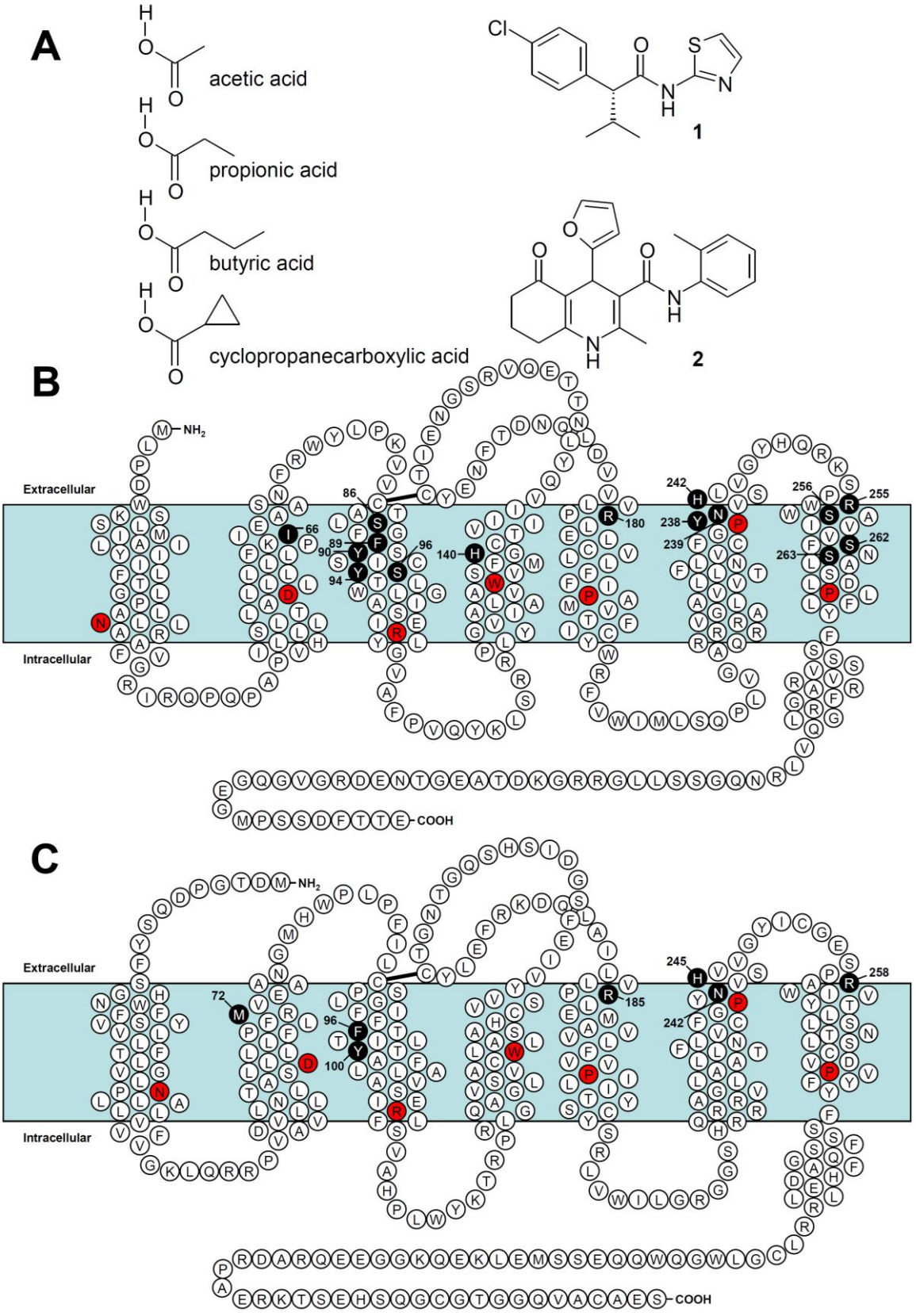

Fig.1. Structure of several FFA2 and FFA3 receptor agonists used in this study and schematic figure of both receptors. *A*, the structure of the known endogenous FFA2 and FFA3 agonists acetate, propionate and butyrate as well as the cyclized cyclopropanecarboxylic acid, and the small-molecule synthetic FFA2 (***1***) and FFA3 (***2***) receptor agonists that were investigated in the present study (Lee et al., 2008; Leonard et al., 2009; Wang et al., 2010). Serpentine diagram of the FFA2 (***B***) and FFA3 (***C***) receptors. The residues mutated in the present study are highlighted in black, for FFA2: $I^{2.61}$, $S^{3.29}$, $F^{3.32}$, $Y^{3.33}$, $Y^{3.37}$, $S^{3.39}$, $H^{4.44}$, $R^{5.39}$, $Y^{6.51}$, $N^{6.52}$, $H^{6.55}$, $R^{7.35}$, $S^{7.36}$, $S^{7.42}$, and $S^{7.43}$, and for FFA3: $M^{2.61}$, $F^{3.33}$, $Y^{3.37}$, $R^{5.39}$, $N^{6.52}$, $H^{6.55}$, and $R^{7.35}$. The numbering in *B* and *C* corresponds to the actual amino-acid number of the given residue. For reference, the highly conserved residue in each helix is highlighted in red ($N^{1.50}$, $D^{2.50}$, $R^{3.50}$, $W^{4.50}$, $P^{5.50}$, $P^{6.50}$, and $P^{7.50}$) in accordance to the standardized nomenclature (Ballesteros and Weinstein, 1995).

(Leonard *et al.*, 2006), spleen, colon and enteroendocrine cells (Karaki *et al.*, 2006;Karaki *et al.*, 2007;Dass *et al.*, 2007;Samuel *et al.*, 2008;Tazoe *et al.*, 2008;Tazoe *et al.*, 2009), placenta, liver (Wilkes *et al.*, 2009), lung, bone marrow and peripheral blood monocytes (Le Poul *et al.*, 2003;Brown *et al.*,2003;Cox *et al.*, 2009;Maslowski *et al.*, 2009;Nilsson *et al.*, 2003).

To date there are only very few pharmacological tools available to investigate FFA2 and FFA3. Given the suggested physiological relevance of these receptors in various metabolic diseases, we set out to characterize the mRNA expression and pharmacological properties of these receptors further utilizing the recently reported ago-allosteric agonist for FFA2 (Lee *et al.*, 2008) and a selected FFA3 agonist reported in the patent literature (Leonard *et al.*, 2006) (1 and 2, respectively; see also Figure 1A), alongside propionate as an endogenous orthosteric agonist for both receptors. Guided by molecular modeling site-directed mutagenesis studies of numerous amino acids in FFA2 and FFA3 (see Figure 1B and 1C), we investigated the molecular determinants contributing to the roles of certain amino acid residues in the transmembrane regions in agonist binding/receptor activation of FFA2 and FFA3 upon stimulation by either the endogenous agonist propionate or a synthetic agonist. Given their diverse structural features compared to the endogenous agonists for these receptors, we suspected both these synthetic ligands to possess allosteric binding sites, which we confirmed in our pharmacological characterization using site-directed mutagenesis. Our results have been incorporated in structural models of the receptors which may aid future drug design efforts allowing for the discovery of FFA2 and FFA3 agonists suitable for elucidating further their potential (patho-) physiological roles.

Materials and Methods

Materials - Hank's balanced salt solution (HBSS), Hek293 Flpin cells, HEPES, Hygromycin B, pEF5/FRT/V5DEST, sodium pyruvate, and Zeocin were purchased from Invitrogen (Hamburg, Germany). Cell culture media were obtained from Lonza (Basel, Switzerland), cell culture consumables as well as Vacutainer cell preparation tubes from Becton Dickinson GmbH (Heidelberg, Germany), and Fetal Bovine Serum (FBS) from Biological Industries (Beit Haemek, Israel). β-mercaptoethanol, chloroform-isoamylalcohol, collagenase II, corticosterone, forskolin, 3-isobutyl-1-methylxanthine (IBMX), insulin from bovine pancreas, phenol-chloroform-isoamylalcohol, phorbol myristate acetate, skim milk powder, sodium propionate, sodium butyrate, Tris hydrochloride, and Tween 20 were obtained from Sigma-Aldrich (Seelze, Germany). Fatty-acid free albumin bovine fraction V (BSA), sodium acetate, and NC2 nitrocellulose membrane and sodium dodecyl sulphate were purchased from Serva (Heidelberg, Germany) and cyclopropanecarboxylic acid from Acros Organics (Geel, Belgium). Oligonucleotides were synthesized by either Biomers (Ulm, Germany) or Eurofins MWG Operon (Ebersberg, Germany). Rosiglitazone, 2-(4-chloro-phenyl)-3-methyl-N-thiazol-2-yl-butyramide (***1***; (Lee *et al.*, 2008)), and 4-furan-2-yl-2-methyl-5-oxo-1,4,5,6,7,8-hexahydro-quinoline-3-carboxlic acid o-tolylamide (***2***; (Leonard *et al.*, 2006)) were synthesized in-house. MIN6-c4 cells were licensed from Prof. Dr. J.-I-Miyazaki (Osaka University, Japan). 3T3-L1 cells were obtained from the ATCC (CL-173). Amplified Luminescent Proximity Homogeneous Assay (ALPHAScreen) cAMP kits were obtained from Perkin Elmer (Waltham, MA), BCA protein assay kit from ThermoScientific (Bonn, Germany), Criterion polyacrylamide gels from Biorad (Munich, Germany), anti-ERK1/2 MAPK, anti-ERK1/2 phosphoThr202/Tyr204 MAPK antibodies, and 1X Cell lysis buffer from Cell Signaling Technology (Danvers, MA). Anti-rabbit horseradish peroxidase (HRP) - conjugated antibodies were obtained from Promega (Mannheim, Germany), LumiLightplus Western Blot substrate from Roche (Mannheim, Germany), and the QuikChange Mutagenesis kit from Stratagene (La Jolla, CA). The endotoxin-free plasmid purification kit, Polyfect, QiaShredder columns, RNAse-free DNAse set, RNeasy Mini kit, and the RLT-buffer were obtained from Qiagen (Hilden, Germany), the High Capacity cDNA Reversion Transcription kit and TaqMan Universal PCR Master mix from Applied Biosystems (Darmstadt, Germany), and the Lymphoprep tubes from Axis Shield (Oslo, Norway).

Cloning and site-directed mutagenesis - The coding sequence of human FFA2 (NM_005306) and FFA3 (NM_005304) was amplified by PCR from a commercial DNA template (Multispan, Hayward, CA) using the forward primer 5'- AAAAAGCAGGCTTCGAAGGAGATAGAACCATG CTGCCGGACTGG-3' and the reverse primer 5'-GAAAGCTGGGT CCTACTCTGTAGTGAAGTC-3' for FFA2 and the sense primer 5'-ACTATGCTCGAGGGATCTGGAGATACAGGCCC-3' and the antisense primer 5'-CTGCGCGGATCTAAGCTTCTAGCTTTCAGCACAGGCC-3' for FFA3. For FFA2 a second PCR was performed using the forward primer 5'-GGGGACAAGTTTGTACAAAAAAGCAGGCT-3' and the reverse primer 5'-GGGGACCACTTTGTACAAGAAAGCTGGGT-3' to add appropriate Gateway adapters. The products obtained for both FFA2 and FFA3 were subsequently cloned using the Gateway technology into pEF5/FRT/V5DEST. Single-point mutations were generated using the QuikChange Mutagenesis kit following the manufacturer's instructions. Endotoxin-free plasmid was obtained for transfection purposes using an endotoxin-free plasmid purification kit after verification of their sequences.

Cell isolation, culture & transfection - All cell types were cultured at 37°C, 5% CO2, 95% humidity in medium containing 4.5g/l glucose and 2mM L-glutamine. INS-1E cells were cultured in collagen I-coated plates, in Roswell Park Memorial Institute (RPMI) 1640 medium supplemented with 10% FBS, 50μM β-mercaptoethanol, 10mM HEPES, and 1mM sodium pyruvate. MIN6-c4 cells were cultured in Dulbecco's modified Eagle's medium (DMEM) supplemented with 15% FBS and 50μM -mercaptoethanol. STC-1 and Hek293 Flpin cells were cultured in DMEM supplemented with 10% FBS. NCI-H716 and THP-1 cells were cultured in RPMI 1640 supplemented with 10% FBS.

Human peripheral blood mononuclear cells (PBMC) were isolated by density gradient centrifugation using Lymphoprep cell preparation tubes as per the manufacturer's instructions.

Untransfected Hek293 Flpin cells were maintained in culture medium containing 100μg/ml Zeocin. Recombinant cells were selected with 100μg/ml Hygromycin B 48h after the cells were co-transfected using Polyfect with cDNAs encoding the FFA2 or the FFA3 receptor, respectively, and the recombinase-coding pOG44 vector (Invitrogen) at a molecular ratio of 1:9, respectively.

cAMP assays - Intracellular cyclic adenosine monophosphate (cAMP) levels were determined using an ALPHAScreen cAMP kit as per the manufacturer's instructions. Cells were seeded in 384-well Optiplates at a density of 14,000 cells/well and stimulated for 1h with ligands in the presence of 10μM forskolin in HBSS (pH 7.4) containing 5mM HEPES, 0.1% (*w:v*) free-fatty acid BSA, and 1U Acceptor beads/well. Stimulation was stopped by addition of lysis buffer (5mM HEPES, 0.3% (*v:v*) Tween 20, 0.1% (*w:v*) BSA, 1U/well Donor beads, 1U/well biotinylated cAMP, pH 7.4). Plates were read using an EnVision multiplate reader (Perkin Elmer) 2h after lysing the cells with lysis buffer and storing the plates in the dark at room temperature.

Western Blot – Cells were cultured in 6-well collagenI plates to confluency and serum-starved for 16h prior to stimulation. Cells were lysed on ice with 1X Cell lysis buffer, freshly supplemented with 1mM phenylmethanesulfonyl fluoride (PMSF), after the cells were treated with ligands in serum-free medium for 10min at 37°C. Samples were subsequently denatured at 95°C for 5min in loading buffer (62.5mM Tris.HCl (pH 6.8) containing 1.5% (*v:v*) β-mercaptoethanol, and 1.5% (*w:v*) sodium dodecyl sulphate). Proteins were loaded (80μg protein/lane) on a 10% Tris-HCl Criterion polyacrylamide gel and transferred to a NC2 nitrocellulose membrane. The membrane was blocked with 5% skim milk powder and incubated o/n at 4°C with rabbit primary antibodies, either anti-ERK1/2 antibodies or anti-ERK1/2 phosphoThr202/Tyr204 antibodies. Secondary anti-rabbit HRP conjugated antibodies were incubated for 1h at room temperature. HRP was detected using LumiLightplus Western Blot substrate.

Protein determinations - Protein concentrations of cell lysates were quantified by using the BCA protein assay kit, as per manufacturer's instructions.

Cell differentiation - Before performing experiments, NCI-H716 cells were differentiated for 9 days on Matrigel plates, while THP-1 cells were differentiated for 2 days in medium containing 20ng/ml phorbol myristate acetate. 3T3-L1 cells were differentiated upon confluency as previously described (Hong *et al.*, 2005), and harvested 10 days after initiation of differentiation for gene expression analysis.

Rat preadipocytes were isolated from male Wistar rats, essentially as previously described (Rodbell, 1964). In brief, epidydimal and perirenal fat tissues were minced, digested with 1mg/ml collagenase II and filtered through a gauze. Preadipocytes were separated from adipocytes by centrifugation at 400*g* for 10min and washed before being seeded in 6-well plates. Once confluent, preadipocytes were treated for 2 days with 0.5mM 3-isobutyl-1-methyl-xanthine, 100nM corticosterone and 1nM insulin in DMEM supplemented with 5% FBS and finally maintained in DMEM supplemented with 5% FBS, 100nM corticosterone and 1nM insulin until the end of the experiment. Nine days after the initiation of differentiation, rat adipocytes were harvested for gene expression analysis.

RNA extraction and TaqMan gene expression analysis - For the isolation of total RNA, cells were lysed using RLT-buffer supplemented with 0.1% (*v:v*) β-mercaptoethanol, and samples were sheared by centrifugation at 10,000*g* for 2min through QiaShredder columns. For adipocytes and fat tissues, a 1:1 (*v:v*) mix of RLT buffer and phenol-chloroform-isoamylalcohol (25:24:1; *v:v*) was used to lyse the cells instead, lysates were subsequently centrifuged at 10,000*g* for 5min, and 1 volume of chloroform-isoamyl alcohol (24:1; *v:v*) was added to the upper aqueous phase and re-centrifuged at 10,000*g* for 5min. RNA was precipitated by addition of 1 volume of 70% ethanol and purified using an RNeasy Mini kit, following the manufacturer's instructions. Genomic DNA was eliminated by digestion with the RNAse-free DNAse set. Reverse-transcription was achieved using the High Capacity cDNA Reversion Transcription kit, with random hexamer primers. Real-time polymerase chain reaction was performed in a 7000 Sequence Detection System device (Applied Biosystems) with TaqMan Universal PCR Master mix and analyzed with the ABI Prism SDS 1.2.3. software (Applied Biosystems). The PCR program was 50°C for 2 min, 95°C for 10 min and 40 cycles at 95°C for 15 sec and 60°C for 1 min. We used the primers and 5'-6FAM/3'-TAMRA labelled probes that are presented in the table below. To detect the expression of human FFA3, we used two different sets of primers; we used primer set #2 for the detection of FFA3 mRNA in Hek293 Flpin cells heterologously expressing FFA3.

Extracellular impedance assay - The day before the assay, cells were plated in collagen I-coated 384-well CellKey plates at a density of 20,000 cells/well in growth medium and centrifuged at 200*g* for 3min to remove air bubbles. On the assay day, adherent cells were washed twice with 50µl assay buffer (HBSS containing 5mM HEPES, 1% (*v:v*) dimethyl sulfoxide (DMSO), 0.1% (*w:v*) fatty-acid free BSA, pH 7.4) directly using the CellKey instrument (MDS Analytical technologies, Ismaning, Germany), equilibrated in assay buffer for 90min and subsequently stimulated with compounds. Changes in extracellular impedance were monitored for 20min after addition of compounds. Equilibration and stimulation steps were performed at 28°C or 37°C for cells expressing either human FFA3 or FFA2, respectively. Untransfected cells were tested at both 28°C and 37°C.

Cytosolic calcium measurement using the FLIPR system - Cells were seeded 24h before the assay in black clear-bottom collagenI-coated 384-well plates, at a density of 25,000 cells/well, in growth medium. For pertussis toxin (PTX) treatments, cells were incubated for 16-18h with 100ng/ml PTX (final concentration) in growth medium. On the assay day, medium was replaced by assay buffer (HBSS containing 20mM HEPES). Before stimulation, cells were loaded with the Ca^{2+}-sensitive fluorescent dye from the Calcium4 Assay kit (MDS Analytical technologies, Ismaning, Germany) for 90min at room temperature, in the presence of 2mM probenicid. Changes in cytosolic Ca^{2+} concentration upon compound addition were monitored using a FLIPR Tetra device (Fluorescence Imaging Plate Reader; MDS Analytical technologies).

Data analysis - All linear and non-linear regression fittings, calculations of pEC50 and extrapolations from standard curves were performed using GraphPad Prism 5.02 software (San Diego, CA). Values are given as mean S.E.M., unless otherwise stated. Quantification of the Western Blot analysis was performed by densitometric analysis using Advanced Image Data Analyzer (AIDA, version 4.15.205, Raytest, Straubenhardt, Germany).

Numbering scheme of GPCRs –Residues are identified by the general numbering scheme of Ballesteros and Weinstein (1995) that allows easy comparison among residues in the 7TM segments of different receptors.

Homology modeling - A homology modeling procedure employing Modeller (Martí-Renom *et al.*, 2000;Sali and Blundell, 1993) was applied for obtaining models for the human FFA2 and FFA3 receptors using the recently resolved inactive structures of β2 adrenergic receptor (pdb code: 2RH1) (Cherezov *et al.*, 2007) and A2A adenosine receptor (pdb code: 3EML) (Jaakola *et al.*, 2008) as templates. The sequence alignment was performed using Molecular Operating Environment (MOE; Chemical Computing Group, version 2008, Montreal, Canada) with the BLOSUM30 substitution matrix and a gap penalty of 20. First, an alignment of the FFA receptor family was created, and the β2 and A2A receptor sequences were subsequently aligned to the FFA receptor family alignment, ensuring the correct positioning of the highly conserved sequence motifs known in class A GPCRs. Based on this alignment, and with the additional constraint of maintaining the conserved disulfide bridge between TM3 and EL2, 100 homology models were constructed for FFA2 and FFA3. The most appropriate models, based on the presence of a suitable ligand-binding pocket as well as having side-chain orientations in agreement with our experimental findings from single point mutagenesis experiments, were further refined by backbone modifications. In line with the proposed 'toggle switch mechanism' of GPCR activation (Schwartz *et al.*, 2006), TM6 was straightened by approximately 15°, to better represent the activated state of the ligand-binding region within the FFA2 and FFA3 receptors. This adjustment brings the essential residue H6.55 closer to the binding cavity. The resulting receptor models get protonated and gradually relaxed with the Amber99 forcefield as implemented in MOE, always keeping spatial restraints on the backbone in the TM region in order to avoid degradation of the receptors. The EL2 region is modeled such that the conserved cysteins are aligned with their cystein counterparts in the templates. By that, the conserved disulfide bond between EL2 and the top of TM3 is enforced. Bearing in mind that the EL2 regions of most structurally resolved GPCRs differ strongly, the EL2 of the final model is subjected to a short molecular dynamics simulation (1,000ps, 300K, NVT, Δt=0.002ps, water box) in MOE, where the positions of the TM-backbones are fixed and only the extracellular loops are allowed to move.

		ID	Forward primer 5'-3'	Reverse primer 5'-3'	TaqMan probe 5'FAM-3'TAMRA
FFA2	**Human**	NM_005306	GCTTTCCCCGTGCAGTACAA	CCAGAGCTGCAATCACTCCAT	CTCTCCCGCCGGCCTCTG
	Mouse	NM_146187	CATCAGCATGGAACGCTACCT	TGGCCGGCGGGATAA	AGTGGCCTTCCCGGTGCAGTACAA
	Rat	NM_001005877	CCGCCGGCCACTGTAC	TGCAATGGCCAAAGGACAT	AGTGATCGCTGCTCTGGTGGCCTG
FFA3	**Human #1**	NM_005304	GCTTTGGGCCCTACAACGT	CACGCCGGGCTTTCAC	TCCCATGTCGTGGGCTATATCTG
	Human #2	NM_005304	GAGATGGCTGTGGTCCTCTTT	CCAGGCGGCTGTAGCAGTA	TGGTCCCGCTGATCATCACCAG
	Mouse	NM_001033316	GCTTTGGGCCCTACAACGT	CACGCCGGGCTTTCAC	TCCCATGTCGTGGGCTATATCTG
	Rat	NM_001108912	TGGTGTTCCTCGTGGGACTAC	GCGGCGACGCAGCTT	CAACGTGATGGCCCTGGTGGTCTT
RNA pol II	**Human**	NM_000937	GCAAGCGGATTCCATTTGG	TCTCAGGCCCGTAGTCATCCT	AAGCACCGGACTCTGCCTCACTTCATC
	Mouse	NM_009089	GCCAAAGACTCCTTCACTCACTGT	TTCCAAGCGGCAAAGAATGT	TGGCTCTTTCAGCATCTCGTGCAGATT
	Rat	XM_001079162	GCAGGCGAGAGCGTTGAG	CATTGGTATAATCAAAACGGAACTTC	CTGGCTACACTTAAGCCTTCTAATAAAGC

Ligand docking – The agonists propionate and ***1*** for FFA2 and propionate and ***2*** for FFA3, were flexibly docked into the obtained model of FFA2 and FFA3, respectively, employing GOLD (Verdonk *et al.*, 2003) with flexible side-chains in the proposed ligand-binding regions. Specifically, residues 3.32, 3.33, 6.51, 6.55, 7.35, 7.39 and 7.42 were allowed to move and the best 10 top scoring poses were kept and visually inspected. In a last step, the receptor and the ligand-poses were manually readjusted to be in accordance with mutagenesis data, and the resulting complex subsequently underwent gradual minimization with the MMFF94x force field as implemented in MOE with a tethered protein backbone. The plausibility of the poses were checked using a short molecular dynamics simulation (1,000ps, 300K, NVT, Δt=0.002ps) in MOE with constrained backbone positions. However, no significant ligand shifts have been observed, suggesting stability of the ligand-receptor complexes.

Results

Expression pattern of FFA2 and FFA3.

FFA2 and FFA3 receptor mRNA expression, as reported in several studies that are not fully consistent (Brown *et al.*, 2003;Le Poul *et al.*, 2003;Samuel *et al.*, 2008;Xiong *et al.*, 2004), is expected in numerous tissues and cell types, including monocytes (Le Poul *et al.*, 2003), enteroendocrine cells (Samuel *et al.*, 2008), the pancreas (Brown *et al.*, 2003), adipose tissue (Brown *et al.*, 2003;Xiong *et al.*, 2004) and 3T3-L1 cells (Brown *et al.*, 2003). Therefore we first set out using quantitative real-time PCR to verify the expression of FFA2 and FFA3 receptor mRNA in a number of cell lines and tissues of particular interest in regard to the presumed implication of these receptors in metabolic diseases.

As shown in Figure 2, we find a high mRNA copy number for FFA2 and FFA3 in the mouse -cell line MIN6c4 (2528±390 and 1870±290 copies, respectively, n=6) and in the rat -cell line Ins-1E (512±126 and 1010±68 copies, respectively, n=6). We find a moderate to low expression of FFA2 and FFA3 mRNA in rat adipocytes, THP-1 cells, human peripheral blood mononuclear cells (PBMCs) and human NCI-H716 enteroendocrine L-cells. While we find a high mRNA copy number for FFA2 in differentiated 3T3-L1 cells (4227±1183 copies, n=6), we did not detect FFA3 mRNA expression in these cells. In contrast, we detected a moderate FFA3 mRNA expression in mouse L-enteroendocrine STC-1 cells (88±6 copies, n=6) in which we did not detect FFA2 mRNA expression.

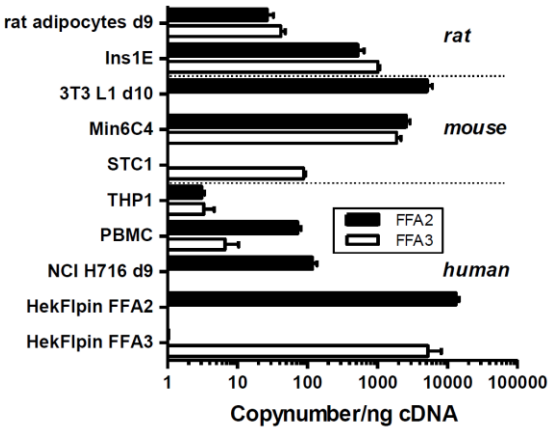

Fig.2. mRNA expression profile of FFA2 and FFA3 as obtained by Taqman analysis using rat, mouse, and human cells and tissues. Data are presented as copynumber per ng of cDNA encoding the respective rat, mouse or human FFA2 or FFA3. Also shown are the mRNA levels achieved upon expression of the human FFA2 and FFA3 in Hek293 Flpin cells.

Generation and characterization of HEK cells expressing FFA2 or FFA3.

We generated Hek293 Flpin cell lines expressing either human FFA2 or FFA3, allowing us to further characterize their pharmacological and signaling properties. As there is no suitable radioligand available for these receptors, we relied on the confirmation of mRNA expression by quantitative real-time PCR for monitoring receptor expression. Our results indicated that a substantial mRNA expression was achieved using the Flpin system for both human FFA2 (13042±1466 copies, n=6) and human FFA3 (6959±3181 copies, n=7). We failed to detect FFA2 mRNA in our Hek293 Flpin FFA3 cell line and FFA3 mRNA in our Hek293 Flpin FFA3 cell line, nor could we detect any FFA2 or FFA3 mRNA expression in untransfected Hek293 Flpin cells (Figure 2).

CellKey impedance-based measurements

We subsequently performed a variety of signaling assays to verify functional FFA2 and FFA3 expression in the generated Hek293 Flpin cell lines. CellKey experiments indicated the presence of concentration-dependent functional responses to propionate and to the synthetic FFA2 agonist ***1*** in the FFA2 expressing cells (Figure 3A) and to propionate and the synthetic FFA3 agonist ***2*** in FFA3 expressing cells (Figure 3B), with the FFA2 expressing cells giving a somewhat larger response. In line with the known G-protein coupling specificity of FFA2 and FFA3 (Brown *et al.*, 2003;Le Poul *et al.*, 2003), PTX pretreatment of the cells resulted in either a partial or a complete prevention of the FFA2- (Figure 3A) or FFA3- (Figure 3B) mediated responses, respectively. Interestingly, the tracings obtained in the first minutes after stimulation with ***2*** appear to be somewhat different from those obtained for the higher concentrations of propionate (Figure 3B), suggesting both agonists may induce slightly different signal-transduction pathways downstream of FFA3. This led us to investigate the potential effects of the FFA2 and FFA3 agonists in a variety of other signaling assays: ERK1/2 phosphorylation, calcium mobilization and the inhibition of cellular cAMP levels.

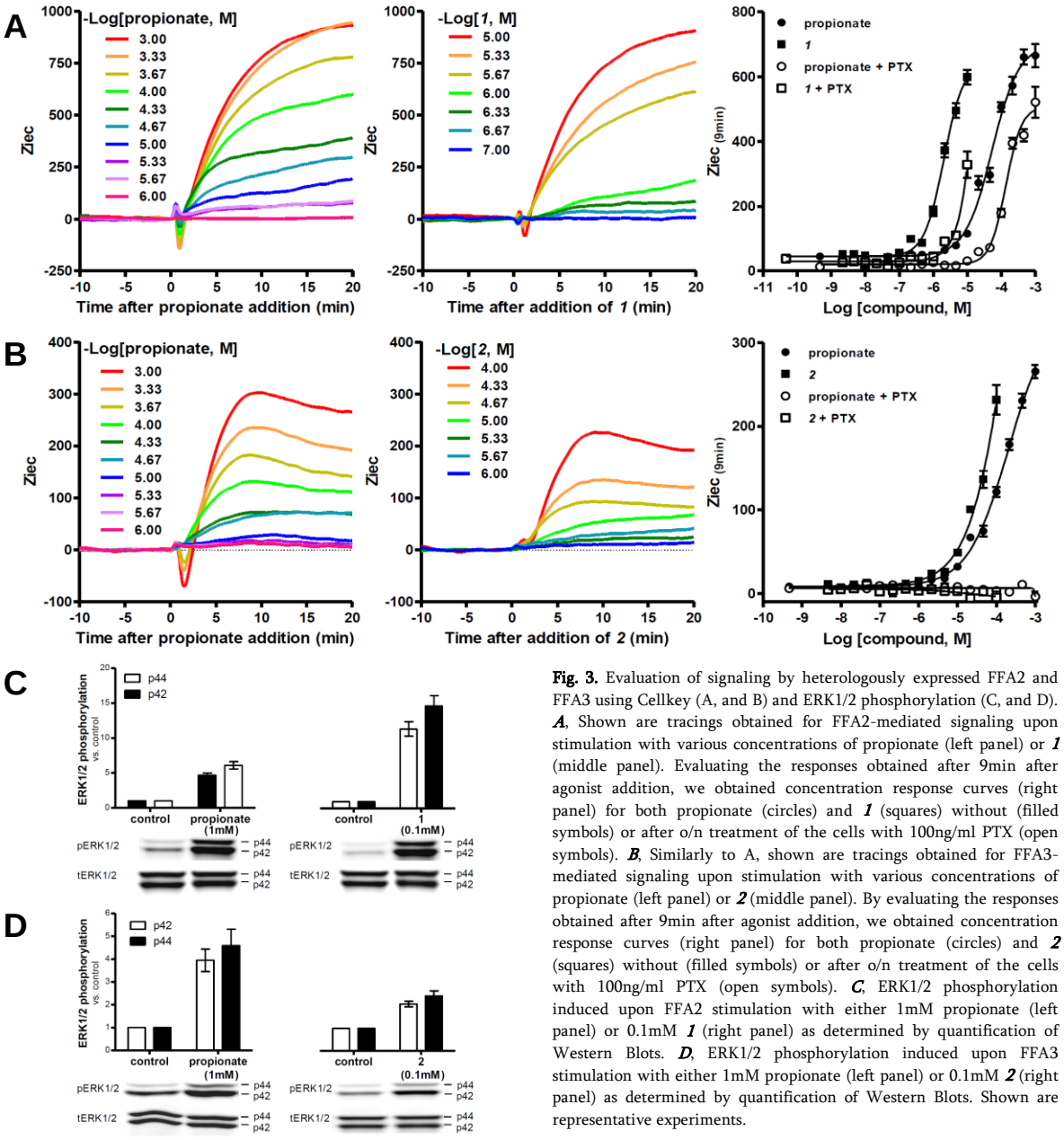

Fig. 3. Evaluation of signaling by heterologously expressed FFA2 and FFA3 using Cellkey (A, and B) and ERK1/2 phosphorylation (C, and D). ***A***, Shown are tracings obtained for FFA2-mediated signaling upon stimulation with various concentrations of propionate (left panel) or ***1*** (middle panel). Evaluating the responses obtained after 9min after agonist addition, we obtained concentration response curves (right panel) for both propionate (circles) and ***1*** (squares) without (filled symbols) or after o/n treatment of the cells with 100ng/ml PTX (open symbols). ***B***, Similarly to A, shown are tracings obtained for FFA3-mediated signaling upon stimulation with various concentrations of propionate (left panel) or ***2*** (middle panel). By evaluating the responses obtained after 9min after agonist addition, we obtained concentration response curves (right panel) for both propionate (circles) and ***2*** (squares) without (filled symbols) or after o/n treatment of the cells with 100ng/ml PTX (open symbols). ***C***, ERK1/2 phosphorylation induced upon FFA2 stimulation with either 1mM propionate (left panel) or 0.1mM ***1*** (right panel) as determined by quantification of Western Blots. ***D***, ERK1/2 phosphorylation induced upon FFA3 stimulation with either 1mM propionate (left panel) or 0.1mM ***2*** (right panel) as determined by quantification of Western Blots. Shown are representative experiments.

ERK1/2 phosphorylation

Agonist activation of FFA2 or FFA3 resulted in the stimulation of ERK1/2 phosphorylation, with propionate yielding a 4- and 6-fold stimulation for FFA2 and FFA3, respectively (Figures 3C and 3D). Also the stimulation of FFA2 with ***1*** (Figure 3C) and FFA3 with ***2*** (Figure 3D) resulted in ERK1/2 phosphorylation, however, at the tested concentrations, ***1*** appears to induce a greater response and ***2*** a reduced response compared to respective propionate responses. The levels of ERK1/2 phosphorylation in untransfected Flpin cells are unaffected upon stimulation with these compounds (data not shown).

Calcium mobilization

Propionate induced a robust calcium mobilization in cells expressing FFA2 that was PTX sensitive (top-left panel in Figure 4A), whereas 10µM ***1*** induced only a small PTX-sensitive response (top-right panel in Figure 4A). In contrast to the effects obtained with cells expressing FFA2, neither propionate nor ***2*** elicited a calcium mobilization response in cells expressing FFA3 (bottom panels of Figure 4A). Evaluating the concentration-dependent responses of propionate and ***1*** revealed that both compounds are able to induce a robust FFA2-mediated calcium mobilization response (see Figure 4B) that is only partially PTX sensitive. Interestingly, in this calcium assay, these two compounds appear to yield a different kinetic tracing of the fluorescence changes, whereas this effect is not so much apparent upon PTX-1 treatment of the cells.

Modulation of cAMP levels

As both FFA2 and FFA3 appeared to couple to Gi/o proteins, we resorted to cAMP assays to evaluate their pharmacological profiles in more detail. We find that the naturally occurring

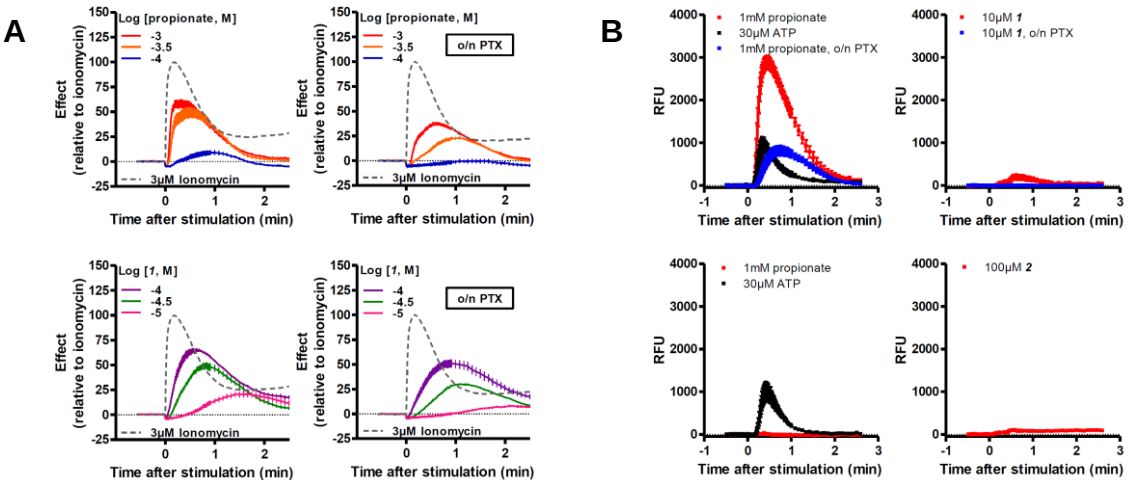

Fig. 4. Evaluation of signaling by heterologously expressed FFA2 and FFA3 using the monitoring of intracellular calcium mobilization. ***A***, Representative tracings for the effects of 30μM ATP, and 1mM propionate (upper left panel) or 10μM ***1*** (upper right panel) without (in red) or after o/n treatment of FFA2 expressing cells with 100ng/ml PTX (in blue); similarly, for the effects of 30μM ATP, and 1mM propionate (bottom left panel) or 100μM ***2*** (bottom right panel) on calcium mobilization using FFA3 expressing cells (in blue). ***B***, Tracings of the effects of the stimulation of FFA2 expressing cells with varying concentrations of propionate (top panels) or ***1*** (bottom panels) without (left panels) or after o/n treatment of the cells with 100ng/ml PTX (right panels). Data are represented relative to the calcium mobilizing effect induced by 3μM ionomycin.

SCFAs acetate, propionate, and butyrate, as well as the synthetic SCFA cyclopropanecarboxylic acid (Figures 5A and 5B) are able to inhibit the forskolin-induced elevation of cAMP levels in FFA2 and in FFA3 expressing Flpin cells with the following rank order of potencies for FFA2: propionate > acetate ≥ cyclopropanecarboxylic acid > butyrate, and for FFA3: propionate > cyclopropanecarboxylic acid ≥ butyrate. As can be seen in Table 1, and in agreement with the published literature (Brown *et al.*, 2003;Le Poul *et al.*, 2003), the potency of acetate is very weak in inhibiting the forskolin-induced response via FFA3 while exhibiting a reasonable potency for FFA2.

In agreement with the published literature (Lee *et al.*, 2008;Wang *et al.*, 2010), we find that phenylacetamide ***1*** is a full FFA2 agonist and inhibits the forskolin-induced levels of cAMP in FFA2 receptor expressing cells to the same extent as propionate with a pEC50 value of 6.5±0.1 (Figure 5A). We find that the synthetic agonist ***2*** is able to inhibit the forskolin-induced levels of cAMP in FFA3 receptor expressing cells to the same extent as propionate, indicative of compound ***2*** being a full FFA3 agonist, with a pEC50 value of 4.8±0.1 (Figure 5B). We were unable to modulate the forskolin-induced cAMP levels in untransfected Flpin cells with neither these SCFAs nor these synthetic agonists (data not shown).

Table 1. Potency of ligands for hFFA2 and hFFA3 in cAMP assay.
[a], percentage effect of propionate was set to 100%.

	FFA2			FFA3		
	pEC50	% effect[a]	n	pEC50	% effect[a]	n
acetate	5.1±0.1	94±4	14	3.9±0.1	27±3	8
propionate	4.5±0.1	100±1	18	4.3±0.1	100±1	8
butyrate	4.8±0.1	70±3	10	4.3±0.1	74±5	8
cycloprop. acid	4.9±0.1	95±2	8	4.7±0.1	116±4	8
1	6.5±0.2	110±10	16	<4	-	4
2	<4	-	6	4.8±0.1	103±5	10

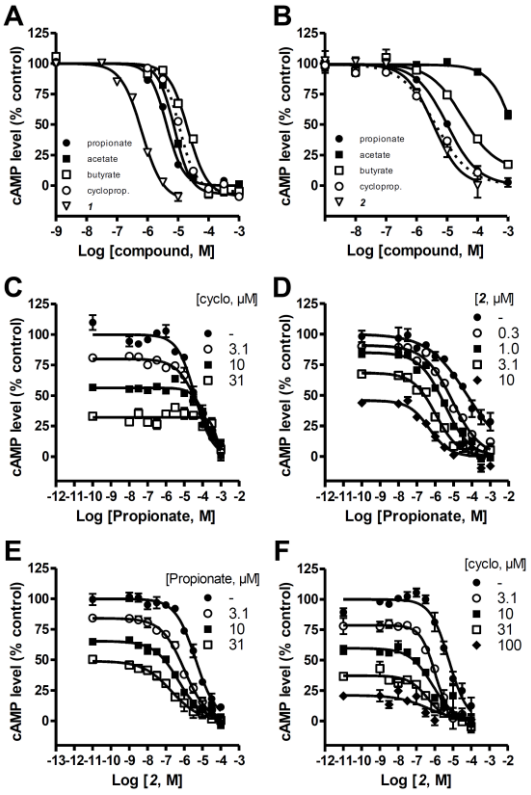

Fig.5. Evaluation of the ability of heterologously expressed FFA2 and FFA3 to inhibit forskolin-induced cAMP elevation. ***A***, The coupling of FFA2 to Gi was evaluated upon stimulation with acetate, propionate, butyrate, cyclopropanecarboxylic acid (cycloprop., dashed line), and ***1***. ***B***, The coupling of FFA3 to Gi was evaluated upon stimulation with acetate, propionate, butyrate, cyclopropanecarboxylic acid (cycloprop., dashed line), and ***2***. ***C-F***, Investigating potential allosteric interactions between propionate, cyclopropanecarboxylic acid, and ***2*** for FFA3. Shown are concentration response curves for propionate (***C*** and ***D***) and ***2*** (***E*** and ***F***) in the absence or presence of varying concentrations of cyclopropanecarboxylic acid (cyclo; ***C*** and ***F***), ***2*** (***D***), or propionate (***E***) as indicated in the graphs. Data shown are representative experiments, each performed in triplicate, and expressed as a percentage of the 10μM forskolin-induced response.

Table 2. Relative expression level and potency of propionate and *1* on wild-type and mutated FFA2 receptors in cAMP assays. [a], mRNA expression relative to WT; [b], percentage effect of ***1*** was set to 100%; - : could not be determined; WT, wild-type

	relative mRNA		propionate			***1***		
	expression[a]	n	pEC_{50}	% Effect[b]	n	pEC_{50}	% Effect[b]	n
WT	100±1	9	4.6±0.1	101±2	18	6.6±0.1	100±1	16
$I^{2.61}A$	68±1	9	4.7±0.1	97±2	6	6.7±0.1	100±1	4
$S^{3.29}A$	75±1	9	4.5±0.1	81±2	4	5.9±0.1	100±1	4
$S^{3.29}G$	58±1	9	4.4±0.1	97±2	4	6.3±0.1	100±1	4
$F^{3.32}A$	106±1	9	<4	-	4	6.1±0.1	100±1	8
$Y^{3.33}A$	111±1	9	<4	-	5	5.8±0.1	100±1	4
$Y^{3.37}A$	104±1	9	<4	-	4	6.5±0.1	100±1	4
$S^{3.39}A$	98±1	9	4.5±0.1	93±2	8	7.1±0.1	100±1	8
$H^{4.44}A$	124±1	9	4.5±0.1	100±1	8	7.0±0.1	100±1	8
$R^{5.39}A$	63±1	9	<4	-	4	6.1±0.1	100±1	4
$R^{5.39}K$	67±1	9	<4	-	8	6.1±0.1	100±1	8
$Y^{6.51}A$	89±1	9	<4	-	4	5.3±0.1	100±1	4
$N^{6.52}A$	97±1	9	<4	-	4	6.3±0.1	100±1	4
$H^{6.55}A$	218±1	9	<4	-	4	6.0±0.1	100±1	4
$H^{6.55}F$	70±1	9	<4	-	5	5.9±0.1	100±1	4
$H^{6.55}N$	57±1	9	<4	-	8	5.9±0.1	100±1	8
$R^{7.35}A$	47±1	8	<4	-	5	5.9±0.1	100±1	4
$R^{7.35}K$	98±1	9	<4	-	8	6.1±0.1	100±1	8
$S^{7.36}A$	49±1	9	4.6±0.1	99±2	4	6.5±0.1	100±1	4
$S^{7.42}A$	109±1	9	4.7±0.1	82±4	8	6.6±0.2	100±1	8
$S^{7.43}A$	160±1	9	4.7±0.1	75±2	8	6.6±0.3	100±1	8

Allosteric agonism for FFA2 and FFA3?

While our functional studies indicate that ***1*** and ***2*** are FFA2 and FFA3 agonists, respectively, their dissimilarity in molecular structure compared to the proposed endogenous SCFA agonists led us to assume that they might have distinct binding sites in the receptor. We therefore explored the presence of an allosteric agonist binding-site in FFA2 and FFA3.

In line with published results (Lee *et al.*, 2008), we could confirm that ***1*** is able to allosterically potentiate the agonistic effects of SCFAs like propionate on FFA2-mediated inhibition of forskolin-induced elevation of cAMP levels, and therefore that ***1*** acts as an ago-allosteric FFA2 agonist (data not shown). We subsequently investigated the potential allosteric activation of FFA3. The presence of the structurally highly similar cyclopropanecarboxylic acid did not affect propionate's potency to inhibit the forskolin-induced cAMP responses via FFA3 (Figure 5C). The pEC50 values for propionate assessed through concentrations response curves in the presence of varying concentrations of cyclopropanecarboxylic acid do not increase in comparison to those obtained in the absence of this co-agonist (4.3±0.1, n=15), suggesting both propionate and cyclopropanecarboxylic acid share an overlapping binding-site on the human FFA3 receptor. In contrast, a gradual, concentration-dependent, leftward shift in the concentrations response curves for propionate is observed in the presence of increasing concentrations of compound ***2*** (Figure 5D). In the presence of 10μM compound ***2*** propionate's potency is increased about 20-fold (pEC50 = 5.6±0.4, see Figure 5D). In the converse experiment, a gradual, concentration-dependent, leftward shift in the concentrations response curves for compound ***2*** is observed in the presence of increasing concentrations of either propionate or cyclopropanecarboxylic acid (Figure 5E and 5F, respectively). In the presence of either 31μM propionate or cyclopropanecarboxylic acid, the potency of compound ***2*** is increased nearly 20-fold (pEC50 = 6.1±0.2, and pEC50 = 6.0±0.4, respectively). These data demonstrate that, 5 while the natural FFA3 receptor agonist propionate and cyclopropanecarboxylic acid have an overlapping binding site, the FFA3 binding site for the synthetic agonist ***2*** is non-overlapping with these two agonists, hence constitutes an allosteric site of interaction. As compound ***2*** is an agonist by itself, collectively these data indicate compound ***2*** is an ago-allosteric agonist for FFA3.

Identification of the orthosteric and allosteric binding sites in the FFA2 and FFA3 receptors

To date, only few mutagenesis studies have been reported for FFA2 and FFA3 (Brown *et al.*, 2003;Stoddart *et al.*, 2008a;Swaminath *et al.*, 2010;Schmidt *et al.*, 2011;Swaminath *et al.*, 2011). To gain a better understanding of the biomolecular interface between the ligands and FFA2 and/or FFA3, we examined the functional effects of the introduction of mutations at specific locations within the TM domains of the receptors. A number of amino acids were selected (see Figure 1B and 1C for FFA2 and FFA3, respectively) for this site-directed mutagenesis approach as they likely point toward the inside of a potential agonist-binding cavity and could therefore constitute key agonist-interacting residues. These identified residues in FFA2: I2.61, 22 S3.29, F3.32, Y3.33, Y3.37, S3.39, H4.56, R5.39, Y6.51, N6.52, H6.55, R7.35, S7.36, S7.42, and S7.43, were each mutated individually to an alanine, whereas S3.29 was also mutated to a glycine, and R5.39 and R7.35 were also individually mutated to lysine, and H6.55 also to a phenylalanine and to an asparagine.

For FFA3, these identified residues, M2.61, F3.33, Y3.37, R5.39, N6.52, H6.55, and R7.35, were each mutated individually to an alanine, whereas R5.39 and R7.35 were also individually mutated to lysine, and H6.55 also to a phenylalanine and to an asparagine.

We established stable cell lines by transfecting Hek293 Flpin cells with the individual mutant FFA2 or FFA3 receptor coding

vectors and, in the absence of a suitable radioligand for determining the expression of either FFA2 or FFA3, we assessed their mRNA expression levels using quantitative real-time PCR (see Table 2 and 3). While most mutant FFA2 and FFA3 receptor mRNA levels are comparable to the expression level of their respective wild-type FFA2 or FFA3 receptor, we find an approximate 1.5- to more than 2-fold higher mRNA expression level compared to wild-type for FFA2 H6.55A, FFA2 S7.43A, and FFA3 M2.61A. In contrast, the expression of the wild-type receptor mRNA is about 2- to 3-fold higher than that of either FFA2 R7.35A, FFA2 S7.36A, FFA3 Y3.37A, FFA3 H6.55N, or FFA3 R7.35A receptor mutants. We subsequently examined the ability, in cAMP assays, of propionate and compound ***1*** to activate mutant FFA2, and of propionate and compound ***2*** to activate mutant FFA3.

Direct activation of mutant FFA2 receptors – To determine the role of the aforementioned amino acid residues in FFA2 activation, we assayed the ability of propionate and compound **1** for each mutant FFA2 receptor to modulate forskolin-induced cAMP levels. We found that, in comparison to the wild-type FFA2 receptor, the mutation in FFA2 of either I2.61, S3.29, S7.36, S7.42 or S7.43 to an alanine residue, or S3.29 to a glycine residue, had little effect on the intrinsic activity and potency of either propionate or ***1*** (Table 2). Intriguingly, the potency of compound ***1***, but not that of propionate, for the mutant FFA2 S3.39A and FFA2 H4.56A receptors is increased 3-fold compared to the wild-type receptor. In contrast, all other FFA2 mutant receptors we evaluated lost their ability to respond to propionate whereas compound ***1*** retained its agonistic properties with potencies of around 0.3-5 μM (Table 2).

Direct activation of mutant FFA3 receptors – Similarly, we assayed the ability of propionate and compound ***2*** for each mutant FFA3 receptor to modulate forskolin-induced cAMP levels. The assessment of the ability of propionate to activate the various mutant FFA3 receptors (see Figure S1) yielded that mutation in FFA3 of either F3.33, R5.39, H6.55, or R7.35 to an alanine residue, R5.39 to a lysine, H6.55 to either a phenylalanine or an asparagine, or R7.35 to lysine residue, greatly affects receptor function as we could not detect any effects of stimulation of these mutant receptors with propionate in this assay. In contrast, these mutant receptors appear to retain some ability to interact with and be activated by compound ***2*** as high concentrations of this compound (≈100μM) lower the forskolin-induced elevation of cAMP. An exception is the FFA3 R7.35A mutant receptor, which does not seem to be activated by either propionate or compound ***2*** (see Figure S1K).

On the other hand, mutation in FFA3 of either M2.61, Y3.37, or N6.52 to an alanine residue yielded mutant FFA3 receptors

Fig. 6. Graphical representation of the influence of propionate on the potency of ***2*** (***A***) and of ***2*** on the potency of propionate (***B***) in the cAMP assay for the wild-type FFA3 receptor (red), and the mutant receptors FFA3 M2.61A (blue), FFA3 Y3.37A (violet), and FFA3 N6.52A (green).

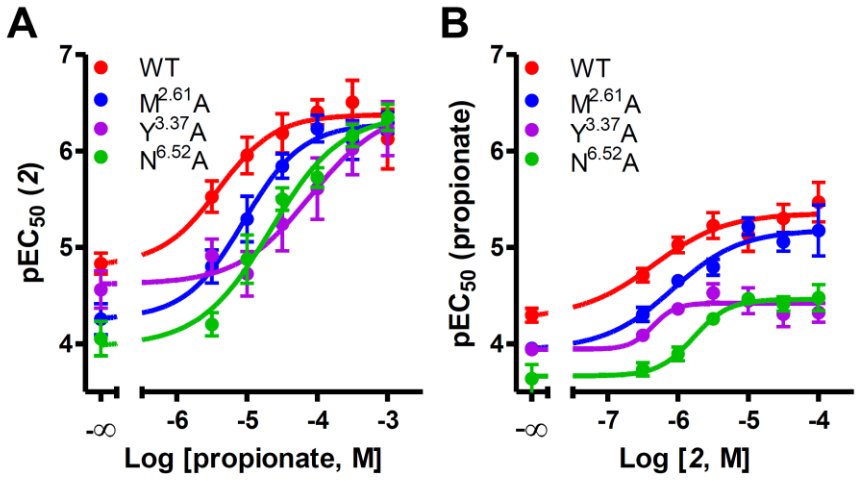

Table 3. Relative expression level and potency of propionate and *1* on wild-type and mutated FFA3 receptors in cAMP assays.[a], mRNA expression relative to WT; [b], percentage effect of ***1*** was set to 100%; - : could not be determined; WT, wild-type

	relative mRNA expression[a]	n	propionate pEC50	propionate % Effect[b]	n	*2* pEC50	*2* % Effect[b]	n
WT	100±1	9	4.3±0.1	85±4	15	4.8±0.1	100±1	11
$M^{2.61}A$	155±1	9	<4	59±6	11	4.3±0.2	100±1	9
$F^{3.33}A$	67±1	9	<4	-	18	<4	-	18
$Y^{3.37}A$	53±1	9	<4	78±6	24	4.5±0.2	100±1	11
$R^{5.39}A$	79±1	9	<4	-	17	<4	-	17
$R^{5.39}K$	81±1	9	<4	-	17	<4	-	17
$N^{6.48}A$	108±1	9	<4	34±2	25	4.1±0.2	100±1	25
$H^{6.45}A$	67±1	9	<4	-	16	<4	-	16
$H^{6.45}F$	80±1	9	<4	-	16	<4	-	16
$H^{6.45}N$	51±1	9	<4	-	18	<4	-	18
$R^{7.35}A$	29±1	9	<4	-	16	<4	-	16
$R^{7.35}K$	87±1	9	<4	-	17	<4	-	17

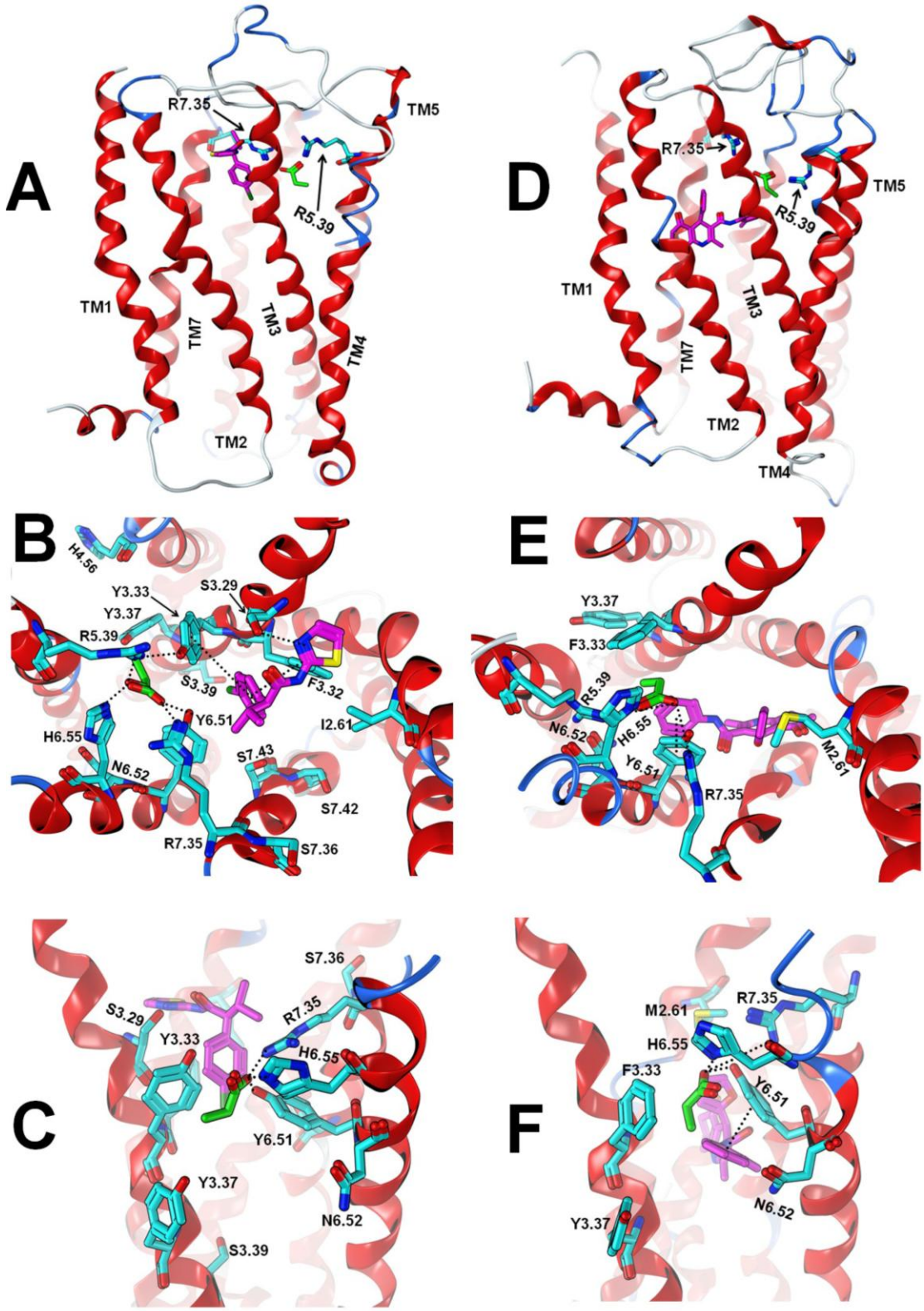

Fig.7. Proposed ligand binding modes and interaction partners for propionate as well as the ago-allosteric agonists ***1*** (***A***,***B***,***C***) and ***2*** (***D***,***E***,***F***) in homology models for the FFA2 and FFA3 receptors. The top panels show a side view of full membrane spanning domains for FFA2 (***A***) and FFA3 (***D***), the center panels shown the top view of FFA2 (***B***) and FFA3 (***E***) from the extracellular side with EL2 removed for clarity, and the bottom panels show the side view of FFA2 (***C***) and FFA3 (***F***) in which TM5 has been removed for clarity. Propionate is shown in green in both FFA2 and FFA3while the synthetic ago-allosteric agonists ***1*** and ***2*** are shown in magenta in FFA2 and FFA3, respectively.

exhibiting more subtle changes in their pharmacological profile. The potencies of propionate and compound **2** are reduced up to ~5-fold for the FFA3 M2.61A and FFA3 Y3.37A mutant receptors compared to the wild-type receptor in inhibiting the forskolin-induced cAMP accumulation. In contrast, both propionate and compound **2** exhibit only residual agonist activity for the mutant FFA3 N6.52A receptor (see Figure S1G) having EC50 values ≥ 100μM.

Allosteric effects on mutant FFA*3 receptors* – We then set out to explore the effects of the introduced mutations on the ability of compound **2** to act as an allosteric agonist. We stimulated the cells expressing either the wild-type or a mutant FFA3 receptor with propionate in the absence or the presence of a varying concentration of compound **2** as a co-agonist (left panels in Figure S1). Conversely, we also evaluated the effects of stimulation of these cells with compound **2** in the absence or the presence of a varying concentration of propionate as a co-agonist (right panels in Figure S1). In agreement with the data presented in Figure 3, we find both agonists to allosterically interact on the wild-type FFA3 receptor (Figure S1A). Similarly, we find both agonists to act allosterically on the mutant M2.61A, Y3.37A, and N6.52A FFA3 receptors (Figures S1B, D, and G, respectively), while there are clearly no functional responses for the cells expressing the mutant FFA3 R7.35A receptor even upon co-incubation with both agonists (Figure S1K). For the F3.33A, R5.39A, R5.39K, H6.55A, H6.55N, H6.55F, and R7.35K mutant FFA3 receptors the co-incubation with both agonists confirms the residual responses of the mutant receptors towards compound **2**, as well as the lack of effects of propionate at concentrations up to 1mM on the response of compound **2** (Figure S1C, E-F, H-J, and L, respectively). Plotting the dependency of the observed sinistral shifts in the concentration response curves for the primary agonist on the concentration of the co-agonist for the wild-type and the mutant M2.61A, Y3.37A, and N6.52A FFA3 receptors (Figure 6) indicates a sigmoidal interaction. The graphs recapitulate the findings obtained for the direct activation of the receptor using only one agonist in that propionate's ability to allosterically affect the potency of compound **2** is only marginally altered for the M2.61A FFA3 mutant, but more so for both the Y3.37A and N6.52A FFA3 mutants, compared to the wild-type FFA3 receptor (Figure 6A). Interestingly, irrespective of the changed potency of compound **2** for the mutant M2.61A, Y3.37A, and N6.52A FFA3 receptors in the absence of co-agonist, compound **2**'s potency for the wild-type and these three mutant receptors is enhanced to the same level in the presence of a full efficacious concentration of propionate (1mM). A similar picture is emerging only in part for the converse experiment. Compound **2** does not seem to be able to enhance the potency of propionate for the mutant Y3.37A and N6.52A mutant receptors to the same level that is achieved for both the wild-type and the M2.61A mutant FFA3 receptors (Figure 6B).

Homology modeling of FFA2 and FFA3

As both FFA2 and FFA3 possess less than 20% sequence identity to any available GPCR template, we relied on multiple templates to create homology models for these receptors. This approach has proven to be beneficial to homology modeling (Larsson *et al.*, 2009), especially for GPCRs (Kneissl *et al.*, 2009). The available crystal structures of the inactive state of the adenosine A2A receptor (Jaakola *et al.*, 2008) and the 2-adrenergic receptor (Cherezov *et al.*, 2007) were employed for our homology modeling efforts. However, we introduced additional backbone modifications to construct a model of an activated FFA2 and FFA3 receptor state. A common theory for the initial steps in receptor activation of class A GPCRs proposes a toggle switch mechanism, where TM6 straightens and moves inwards towards the TM-cavity (Schwartz *et al.*, 2006), followed by additional movements within the TM regions. In line with the proposed 'toggle switch mechanism' of GPCR activation (Schwartz *et al.*, 2006), TM6 was straightened by approximately 15° to better represent an activated receptor. The orientation of His6.55 supports this adjustment, because it brings this essential residue closer to the binding cavity in the models for both receptors.

Our models of FFA2 and FFA3 are checked for plausibility by comparing the putative binding site residues with published phylogenetic data (Surgand *et al.*, 2006). The second step of model validation is done by checking if the residues, which have been shown to influence ligand interactions in the mutagenesis experiments, are accessible from the ligand binding site. Once the models have been shown to be in accordance with the mutagenesis experiments and the literature, ligand docking was performed. For both receptors, propionate is interacting with the arginines on TM5 and TM7 (R5.39 and R7.35), forming ionic bonds to both of them, as shown in Figures 7B and 7E for FFA2 and FFA3, respectively. The rest of the propionate binding site in both receptors involves amino acids which are close-by the guanidine groups of the arginines. For FFA2 the mutagenesis data maps the whole binding site of propionate and two types of interactions are found. On one hand, there are polar amino acid side chains, such as Y3.33, Y6.51, N6.52 and H6.55, which interact either directly with the carboxylic group of propionate or with the guanidine group of the two essential arginines to keep them in place. On the other hand, there is a small hydrophobic cavity found between TM3 and TM5, where Y3.33 forms the roof, Y3.37 the floor, and some aliphatic amino acids on TM5 form its back (L5.42 and L5.46 for FFA2 and M5.42 and L5.46 for FFA3). The size of the cavity is limited, thus explaining the preference of FFA2 for small carboxylic acids. Mutagenesis data confirms the proposed propionate binding mode, showing that Y3.33, Y3.37, R5.39, Y6.51, N6.52, H6.55, and R7.35 are involved in propionate interaction. Mutation of these residues leads to a complete loss in the ability of propionate to activate the receptor. However, **1** can still activate FFA2 for all the mutants, thus ensuring that the signaling ability of the receptor is not impaired by these mutants. The fact that the substitution of R5.39 or R7.35 by lysine leads to a FFA2 which is not responding to propionate is also a confirmation that the guanidine groups of the arginines are part of a hydrogen bond/ionic network, where several neighboring amino acids are involved. H6.55 has been mutated to A, F and N in order to see which features of this amino acid is important for propionate interactions. Neither A nor F or N mutants could re-gain activity for the receptor, thus suggesting that a charged histidine is important for propionate binding. The observation that any mutation in this suggested network may still be activated by **1**, but with a slightly worse pEC50 value, suggests that an intact network is preferable for receptor activation also for allosteric agonists.

The binding site of **1** has recently been suggested to be very close to EL2 (Lee *et al.*, 2008), however our docking results and mutagenesis data indicate that this ligand binds to a close-by

cavity between TM2, TM3 and TM7. The effects on the pEC50 of ***1*** was very small for most of the mutants, but experimental data suggests that Y6.51 and S3.29 are involved in binding. Figure 7 shows the proposed binding modes of ***1*** and propionate, which occupy different regions of the putative binding site of FFA2. This binding mode is also in accordance with extensive SAR data for this structural class (Wang *et al.*, 2010). The region of the thiazole moiety has extensively been explored and a preferred position next to sulfur has been identified, where substituents can be attached without losing much in potency. This is in line with our model, where the thiazole ring points towards the membrane-solution interface and no steric hindrance for larger substituents is to be expected. For FFA3 fewer mutations have been evaluated. However, due to the very high homology of the binding site of the two receptors, propionate is docked to FFA3 similarly to FFA2 (Figure 7). The location of the small hydrophobic pocket is slightly different, because Y3.33 from FFA2 corresponds to F3.33 in FFA3. Due to the lack of the hydrogen bond from position 3.33, R5.39 may move slightly towards TM6, changing the shape of the hydrophobic pocket. F3.33 forms the roof of the hydrophobic pocket, being more flexible than its Y counterpart in FFA2 due to the already mentioned lack of the hydrogen bond to R5.39. That makes the unoccupied hydrophobic pocket a bit more floppy and therefore the lower pEC50 values of SCFAs or FFA3 than for FFA2 may be explained due to the larger loss in entropy upon ligand binding. These findings are corroborated by recent findings (Schmidt *et al.*, 2011). Mutagenesis results for FFA3 are in line with the proposed binding mode, because mutation of any amino acid predicted to be involved in binding makes the receptor irresponsive to propionate.

Compound ***2*** was docked into the putative binding site allosteric to propionate and it is found, similarly to ***1***, in a cavity formed by TM2, TM3 and TM7, but slightly shifted to the intracellular side. Mutagenesis results make the validation of the binding mode quite difficult. Indeed, because of the low potency of the ligand, no large effects can be monitored. However, due to the ago-allosteric behavior of ***2***, the Schild-like plots from Figure 6 help a lot to identify the region where the ligands bind. All three mutants still respond to propionate and ***2*** show non-parallel behavior to the wild type curves. These data suggests all three mutants are involved in binding of one of the two allosteric agonists. Whereas it is obvious that Y3.37 and N6.52 are close to the propionate binding site, M2.61 on TM2 seems to be involved in the binding of ***2***. This s in line with the proposed binding site of ***2*** in the homology model. Further proposed interactions of ***2*** to FFA3 are a hydrogen bond to S7.42 on TM7 and a π-stacking to Y6.51 on TM6. The furyl-residue is proposed to weakly interact with M2.61. However, further experiments would be needed to confirm the interaction partners on an atomistic level.

Discussion

The FFA receptors have attracted substantial attention as potential therapeutic targets due to their suggested implication in various immunological and metabolic conditions The FFA receptors have attracted substantial attention as potential therapeutic targets due to their suggested implication in various immunological and metabolic conditions, including diabetes, colitis and arthritis. These implications have initially largely been based on their expression patterns as well as the known physiological effects of their endogenous ligands (Stoddart *et al.*, 2008b). Our knowledge on FFA2 and FFA3 is quite rudimentary, and pharmacological investigations for FFA2 and FFA3 are greatly hampered by the lack of suitable selective pharmacological tools for these recently deorphanized receptors. Apart from the ubiquitous endogenous short chain FFA (SCFA) agonists, only few ligands are known. Most notably, phenylacetamides have been identified as ago-allosteric FFA2 agonists (Lee *et al.*, 2008), while a recent patent application (Leonard *et al.*, 2006) identifies 5-quinolines as FFA3 agonists. We resynthesized the FFA2 agonist ***1*** from Lee *et al.,* (2008), and the FFA3 agonist ***2*** from Leonard *et al.,* (2006) in order to allow a better characterization of FFA2 and FFA3 (structures shown in Fig 1A). Guided by the recent publications by Gershengorn's group on FFA1, we thus embarked on the exploration of the molecular pharmacological characteristics of FFA2 and FFA3. In the absence of appropriate radioligands or antibodies for these receptors, we first relied on real-time RT-PCR to assess the mRNA expression profile of these receptors. We subsequently searched for and used robust functional assays in which we relied the receptors to couple to endogenous G proteins, to evaluate the endogenous SCFA agonist propionate, and the reported synthetic small molecule agonists ***1*** (Lee *et al.*, 2008) and ***2*** (Leonard *et al.*, 2006), as FFA2 and FFA3 agonists, respectively.

FFA2 and FFA3 exhibit overlapping expression profiles, with the exceptions that we were unable to detect FFA2 mRNA in STC-1 cells and FFA3 mRNA expression in differentiated 3T3-L1 and NCI-H716 cells. Our data are consistent with recent findings (Brown *et al.*, 2003;Hong *et al.*, 2005), in that FFA3 mRNA is either very scarce or absent in adipose tissue, and that both FFA2 and FFA3 are expressed in immune cells (Le Poul *et al.*, 2003).

We used label-free impedance-based measurements to evaluate the integral response upon activation of FFA2 and FFA3 and find both receptors to differ in their capacity to transduce signaling events. Our results are compliant with the known coupling specificities of these receptors in that we observe a Gi-mediated response for both FFA2 and FFA3, while FFA2 is also able to yield responses that are resistant to PTX that most likely represents a coupling to Gq proteins. These findings are consistent for both the endogenous as well as the synthetic agonists we tested. Nonetheless, for FFA3 we observe a slightly different response for ***2*** immediately after compound addition in comparison to propionate (Fig 3B), which might reflect a difference in the signaling pathways induced by stimulation of FFA3 with either propionate of ***2***. In addition, by using ERK1/2 phosphorylation as an integral signaling readout for FFA2 and FFA3 activation, we find clear induction of ERK1/2 phosphorylation by propionate as well as the synthetic agonists we tested. For further detailed characterizations of FFA2 and FFA3, we evaluated calcium mobilization (Figure 4) and cAMP (Figure 5) responses to the stimulation with agonists.

In contrast to the effects obtained with the stimulation of FFA2 expressing cells with FFA2 agonists, neither propionate nor ***2*** elicited a calcium mobilization response in cells expressing FFA3. In combination with the robust cAMP lowering of forskolin-induced elevation of cAMP levels upon FFA3 activation observed in the same cells, these data suggest that FFA3 does not couple to members of the Gq-family of G proteins, and that FFA3 couples to members of the Gi/o-family of G proteins that are not able to induce calcium mobilization. Strikingly, stimulation of FFA2 induces a reduced calcium mobilization after PTX-treatment of the cells to inactivate Gi-

proteins, indicating that FFA2 couples to and activates both Gq- and Gi-proteins, and that activation of heterotrimetic Gi-protein complexes contributes to the FFA2-mediated induction of calcium mobilization. Interestingly, propionate and the synthetic FFA2 agonist ***1*** appear to yield a different kinetic tracing of the calcium mobilization response, whereas this difference is not so much apparent upon PTX-pretreatment of the cells (Figure 4B). The PTX-insensitive contribution to the calcium response therefore appears to occur secondary to the PTX-sensitive contribution. These results suggest that ***1*** may have a somewhat slower onset of action on FFA2, or, alternatively, the differences in efficacy between endogenous and synthetic ligands in different assays could be the result of differences in coupling efficiencies of Gαi *versus* Gαq subunits to FFA2 for the two distinct classes of ligands.

Nonetheless, these findings, although they may well be specific for the cell line we used, clearly compromise a facile interpretation of pharmacological data we intended to generate on these ligands for both the wild-type and mutant FFA2 and FFA3 receptors. Hence, we evaluated the ability of FFA2 and FFA3 to modulate the forskolin-induced elevation of levels of intracellular cAMP. Among the different assay formats we evaluated for FFA2 and FFA3, we find these cAMP assays to be the most robust and straightforward in their interpretation. cAMP assays also provide the advantage that we can use one assay system to compare the two receptors in one assay format that relies on the natural coupling of the receptors.

In such cAMP assays, we could reproduce the different sensitivities that both receptors exhibit towards different SCFAs (Table 1 and Figure 6), as well as the ago-4 allosteric nature of FFA2 agonist ***1*** (data not shown). Likewise to the findings of Lee *et al.* (2008) for FFA2, both the SCFAs and ***2*** are agonists for the FFA3 receptor although these two classes of ligands have structurally little in common, suggesting ***2*** may well act allosterically at FFA3. We find that ***2*** potentiates the effects of SCFAs while producing direct agonism simultaneously, indicating compound ***2*** is an 'ago-allosteric' ligand for FFA3 (Figures 6D-F). Having identified ***2*** as an ago-allosteric FFA3 agonist, we setout to evaluate whether ***1*** and ***2*** have similar modes of interaction with FFA2 and FFA3, respectively, by using a multidisciplinary approach combining molecular modeling and site-directed mutagenesis directed by functional data from cellular cAMP assays.

Employing a substantial number of mutant receptors, we explored the binding sites of propionate and the synthetic ago-allosteric agonists ***1*** and ***2***. The selection of mutations was guided by existing data from literature and homology models for FFA2 and FFA3. The binding site of propionate could be determined quite accurately, whereas for the binding sites of ***1*** and ***2*** the location, but not the interactions at atomistic resolution could be reliably elucidated. For FFA2 we show that, apart from the known R5.39, H6.55, and R7.35 (Stoddart *et al.*, 2008a;Schmidt *et al.*, 2011), also amino acids F3.32, Y3.33, Y3.37, Y6.51, and N6.52 are involved in propionate binding. While R5.39 and R7.35 bind to the carboxylic group of propionate, we postulate that Y3.33, Y5.61, N6.52, and H6.55 are involved in a hydrogen bond network, which either directly interacts with the carboxylate or contributes to keep the guanidine groups of R5.39 and R7.35 in position. This proposed hydrogen-bond network is thought to be important for receptor activation, because mutation of any of the amino acids involved reduces the potency of ***1***. This is also true for mutations retaining the physicochemical behavior (e.g., R5.39K, R7.35K, H6.55N, and H6.55F), emphasizing the accurately adjusted hydrogen bond pattern within the proposed network. Importantly, the mutant FFA2 receptors studied herein are activated by ***1***, thus verifying their functionality and confirming the involvement of the aforementioned residues in propionate binding and not receptor activation per se.

In contrast to FFA2 where Y3.33 is hydrogen bonded to R5.39, the FFA3 propionate binding-site is more flexible as the corresponding F3.33 residue is unable to form the hydrogen bonding with R5.39. This explains the preference of FFA2 for short chain carboxylic acids with sp^2- or sp-hybridized α-carbons (Schmidt *et al.*, 2011).

The binding site of the synthetic agoallosteric agonist ***1*** is proposed to be located between TM2, TM3 and TM7. Mutation of S3.29 in FFA2 to alanine reduces its potency whereas this mutation does not affect propionate ability to activate the receptor. Thus, homology modeling and additional mutagenesis data from FFA2 suggests that ***1*** resides in a small hydrophobic pocket and interacts with S3.29, Y3.33, 18 and Y6.51.

Our data suggest that ***2*** binds to FFA3 in a pocket between TM2, TM3 and TM7. Due to the relatively poor agonists potencies for FFA3, large potency changes as result of the introduced mutations could not be monitored. Therefore, we investigated the ago-allosteric effects of ***2*** and propionate in detail. These experiments on FFA3 M2.61A, Y3.37A, and N6.52A mutant receptors implicate M2.61 in the binding of ***2***, while Y3.37 and N6.52 are involved in the binding of propionate. With this information ***2*** is modeled into a FFA3 pocket that is positioned slightly below the corresponding binding site of ***1*** in FFA2. The derived model suggests S7.42 and Y6.51 as additional binding partners of ***2***, however, further studies will be needed in order to confirm this hypothesis.

In conclusion, our investigations have gained more insight into how endogenous and synthetic ligands activate FFA2 and FFA3. To our knowledge, this is the first study describing a synthetic small molecule FFA3 (ago-allosteric) agonist. There is a need 8 for potent and selective FFA2 and FFA3 modulators to probe the physiological functions of these receptors. Currently, such tool compounds are lacking and the identification of allosteric sites on FFA2 and FFA3 may aid the design of FFA2 and FFA3 modulators suitable for *in vivo* characterization of these receptors.

Acknowledgments

The authors thank Julia Dennemoser, Sebastian Eder, Sybille Fässler, Eva Hammer, Dr. Silke Hobbie, Andrea Lorenz, Oscar McCook, Werner Moreth, Susanne Müller, Silke Rist, Yvonne Roth, Karoline Schwarz and Irina Stengele for excellent technical assistance, providing material, help and advice.

Note

Send reprint requests to:
Dr. Remko A. Bakker
Boehringer Ingelheim Pharma GmbH & Co. KG
Department of CardioMetabolic Diseases Research
Birkendorferstraße 65
88397 Biberach an der Riß
Germany
Tel.: +49 (7351) 54-92298
Fax: +49 (7351) 54-2187
E-mail: Remko.Bakker@boehringer-ingelheim.com

References

Al-Lahham SH, Roelofsen H, Priebe M, Weening D, Dijkstra M, Hoek A, Rezaee F, Venema K and Vonk R J (2010) Regulation of Adipokine Production in Human Adipose Tissue by Propionic Acid. *Eur J Clin Invest* **40**:401-407.

Ballesteros JA and Weinstein H (1995) Integrated Methods for the Construction of Three Dimensional Models and Computational Probing of Structure Function Relations in G Protein-Coupled Receptors. *Methods Neurosciences* **25**:366-428.

Brown AJ, Goldsworthy S M, Barnes A A, Eilert M M, Tcheang L, Daniels D, Muir A I, Wigglesworth M J, Kinghorn I, Fraser N J, Pike N B, Strum J C, Steplewski K M, Murdock P R, Holder J C, Marshall F H, Szekeres P G, Wilson S, Ignar D M, Foord S M, Wise A and Dowell S J (2003) The Orphan G Protein-Coupled Receptors GPR41 and GPR43 Are Activated by Propionate and Other Short Chain Carboxylic Acids. *J Biol Chem* **278**:11312-11319.

Cherezov V, Rosenbaum D M, Hanson M A, Rasmussen S G F, Thian F S, Kobilka T S, Choi H J, Kuhn P, Weis W I, Kobilka B K and Stevens R C (2007) High-Resolution Crystal Structure of an Engineered Human 2-Adrenergic G Protein Coupled Receptor. *Science* **318**:1258-1265.

Cox MA, Jackson J, Stanton M, Rojas-Triana A, Bober L, Laverty M, Yang X, Zhu F, Liu J, Wang S, Monsma F, Vassileva G, Maguire M, Gustafson E, Bayne M, Chou C C, Lundell D and Jenh C H (2009) Short-Chain Fatty Acids Act As Antiinflammatory Mediators by Regulating Prostaglandin E(2) and Cytokines. *World J Gastroenterol* **15**:5549-5557.

Dass NB, John A K, Bassil A K, Crumbley C W, Shehee W R, Maurio F P, Moore G B, Taylor C M and Sanger G J (2007) The Relationship Between the Effects of Short-Chain Fatty Acids on Intestinal Motility in Vitro and GPR43 Receptor Activation. *Neurogastroenterol Motil* **19**:66-74.

Ge H, Li X, Weiszmann J, Wang P, Baribault H, Chen J L, Tian H and Li Y (2008) Activation of G Protein-Coupled Receptor 43 in Adipocytes Leads to Inhibition of Lipolysis and Suppression of Plasma Free Fatty Acids. *Endocrinology* **149**:4519-4526.

Hong YH, Nishimura Y, Hishikawa D, Tsuzuki H, Miyahara H, Gotoh C, Choi K C, Feng D D, Chen C, Lee H G, Katoh K, Roh S G and Sasaki S (2005) Acetate and Propionate Short Chain Fatty Acids Stimulate Adipogenesis Via GPCR43. *Endocrinology* **146**:5092-5099.

Jaakola VP, Griffith M T, Hanson M A, Cherezov V, Chien E Y T, Lane J R, IJzerman A P and Stevens R C (2008) The 2.6 Angstrom Crystal Structure of a Human A2A Adenosine Receptor Bound to an Antagonist. *Science* **322**:1211-1217.

Karaki S, Mitsui R, Hayashi H, Kato I, Sugiya H, Iwanaga T, Furness J B and Kuwahara A (2006) Short-Chain Fatty Acid Receptor, GPR43, Is Expressed by Enteroendocrine Cells and Mucosal Mast Cells in Rat Intestine. *Cell Tissue Res* **324**:353-360.

Karaki SI, Tazoe H, Hayashi H, Kashiwabara H, Tooyama K, Suzuki Y and Kuwahara A (2007) Expression of the Short-Chain Fatty Acid Receptor, GPR43, in the Human Colon. *J Mol Histol* **39**:135-142.

Kneissl B, Leonhardt B, Hildebrandt A and Tautermann C S (2009) Revisiting Automated G-Protein Coupled Receptor Modeling: The Benefit of Additional Template Structures for a Neurokinin-1 Receptor Model 11. *J Med Chem*.

Larsson P, Wallner B, Lindahl E and Elofsson A. (2009) Using Multiple Templates to Improve Quality of Homology Models in Automated Homology Modeling 7. *Protein Science* **17**:990-1002.

Le Poul E, Loison C, Struyf S, Springael J Y, Lannoy V, Decobecq M E, Brezillon S, Dupriez V, Vassart G, Van D J, Parmentier M and Detheux M (2003) Functional Characterization of Human Receptors for Short Chain Fatty Acids and Their Role in Polymorphonuclear Cell Activation. *J Biol Chem* **278**:25481-25489.

Lee T, Schwandner R, Swaminath G, Weiszmann J, Cardozo M, Greenberg J, Jaeckel P, Ge H, Wang Y, Jiao X, Liu J, Kayser F, Tian H and Li Y (2008) Identification and Functional Characterization of Allosteric Agonists for the G Protein-Coupled Receptor FFA2. *Mol Pharmacol* **74**:1599-1609.

Leonard JN, Chu Z L, Bruce M A and Boatman P D (2006) GPR41 and Modulators Thereof for the Treatment of Insulin-Related Disorders PCT/US2005/039551 (WO 2006/052566 A2).

Martí-Renom MA, Stuart A C, Fiser A, Sánchez R, Melo F and Šali A (2000) Comparative Protein Structure Modeling Of Genes And Genomes. *Annual Review of Biophysics and Biomolecular Structure* **29**:291-325.

Maslowski KM, Vieira A T, Ng A, Kranich J, Sierro F, Yu D, Schilter H C, Rolph M S, Mackay F, Artis D, Xavier R J, Teixeira M M and Mackay C R (2009) Regulation of Inflammatory Responses by Gut Microbiota and Chemoattractant Receptor GPR43. *Nature* **461**:1282-1286.

Nilsson NE, Kotarsky K, Owman C and Olde B (2003) Identification of a Free Fatty Acid Receptor, FFA2R, Expressed on Leukocytes and Activated by Short-Chain Fatty Acids. *Biochem Biophys Res Commun* **303**:1047-1052.

Rodbell M (1964) Metabolism of Isolated Fat Cells. I. Effects of Hormones on Glucose Metabolism and Lipolysis. *J Biol Chem* **239**:375-380.

Sali A and Blundell T L (1993) Comparative Protein Modelling by Satisfaction of Spatial Restraints. *Journal of Molecular Biology* **234**:779-815.

Samuel BS, Shaito A, Motoike T, Rey F E, Backhed F, Manchester J K, Hammer R E, Williams S C, Crowley J, Yanagisawa M and Gordon J I (2008) Effects of the Gut Microbiota on Host Adiposity Are Modulated by the Short-Chain Fatty-Acid Binding G Protein-Coupled Receptor, Gpr41. *Proc Natl Acad Sci U S A* **105**:16767-16772.

Schmidt J, Smith N J, Christiansen E, Tikhonova I G, Grundmann M, Hudson B D, Ward R J, Drewke C, Milligan G, Kostenis E and Ulven T (2011) Selective Orthosteric Free Fatty Acid Receptor 2 (FFA2) Agonists. *Journal of Biological Chemistry* **286**:10628-10640.

Schwartz TW, Frimurer T M, Holst B, Rosenkilde M M and Elling C E (2006) Molecular Mechanism of 7TM Receptor Activation--a Global Toggle Switch Model. *Annu Rev Pharmacol Toxicol* **46**:481-519.

Sina C, Gavrilova O, Forster M, Till A, Derer S, Hildebrand F, Raabe B, Chalaris A, Scheller J, Rehmann A, Franke A, Ott S, Hasler R, Nikolaus S, Folsch U R, Rose-John S, Jiang H P, Li J, Schreiber S and Rosenstiel P (2009) G Protein-Coupled Receptor 43 Is Essential for Neutrophil Recruitment During Intestinal Inflammation. *J Immunol* **183**:7514-7522.

Stoddart LA, Smith N J and Milligan G (2008) International Union of Pharmacology. LXXI. Free Fatty Acid Receptors FFA1, -2, and -3: Pharmacology and Pathophysiological Functions. *Pharmacol Rev* **60**:405-417.

Stoddart LA, Smith N J, Jenkins L, Brown A J and Milligan G (2008) Conserved Polar Residues in Transmembrane Domains V, VI, and VII of Free Fatty Acid Receptor 2 and Free Fatty Acid Receptor 3 Are Required for the Binding and Function of Short Chain Fatty Acids 32. *J Biol Chem* **283**:32913-32924.

Surgand JS, Rodrigo J, Kellenberger E and Rognan D (2006) A Chemogenomic Analysis of the Transmembrane Binding Cavity of Human G Protein-Coupled Receptors. *Proteins* **62**:509-538.

Swaminath G (2008) Fatty Acid Binding Receptors and Their Physiological Role in Type 2 Diabetes *Arch Pharm (Weinheim)* **341**:753-761.

Swaminath G, Jaeckel P, Guo Q, Cardozo M, Weiszmann J, Lindberg R, Wang Y, Schwandner R and Li Y (2011) Mutational Analysis of G-Protein Coupled Receptor - FFA2.

Biochemical and Biophysical Research Communications **405**:122-127.

Tazoe H, Otomo Y, Kaji I, Tanaka R, Karaki S I and Kuwahara A (2008) Roles of Short-Chain Fatty Acids Receptors, GPR41 and GPR43 on Colonic Functions. *J Physiol Pharmacol* **59 Suppl 2**:251-262.

Tazoe H, Otomo Y, Karaki S, Kato I, Fukami Y, Terasaki M and Kuwahara A (2009) Expression of Short-Chain Fatty Acid Receptor GPR41 in the Human Colon. *Biomed Res* **30**:149-156.

Verdonk ML, Cole J C, Hartshorn M J, Murray C W and Taylor R D (2003) Improved Protein-Ligand Docking Using GOLD. *Proteins: Structure, Function, and Genetics* **52**:609-623.

Wang Y, Jiao X, Kayser F, Liu J, Wang Z, Wanska M, Greenberg J, Weiszmann J, Ge H, Tian H, Wong S, Schwandner R, Lee T and Li Y (2010) The First Synthetic Agonists of FFA2: Discovery and SAR of Phenylacetamides As Allosteric Modulators. *Bioorg Med Chem Lett* **20**:493-498.

Wilkes JJ, Lloyd D J and Gekakis N (2009) Loss-of-Function Mutation in Myostatin Reduces Tumor Necrosis Factor Alpha Production and Protects Liver Against Obesity-Induced Insulin Resistance. *Diabetes* **58**:1133-1143.

Xiong Y, Miyamoto N, Shibata K, Valasek M A, Motoike T, Kedzierski R M and Yanagisawa M (2004) Short-Chain Fatty Acids Stimulate Leptin Production in Adipocytes Through the G Protein-Coupled Receptor GPR41. *Proc Natl Acad Sci U S A* **101**:1045-1050.

Zaibi MS, Stocker C J, O'Dowd J, Davies A, Bellahcene M, Cawthorne M A, Brown A J, Smith D M and Arch J R (2010) Roles of GPR41 and GPR43 in Leptin Secretory Responses of Murine Adipocytes to Short Chain Fatty Acids. *FEBS Lett* **584**:2381-2386.

Supplementary material

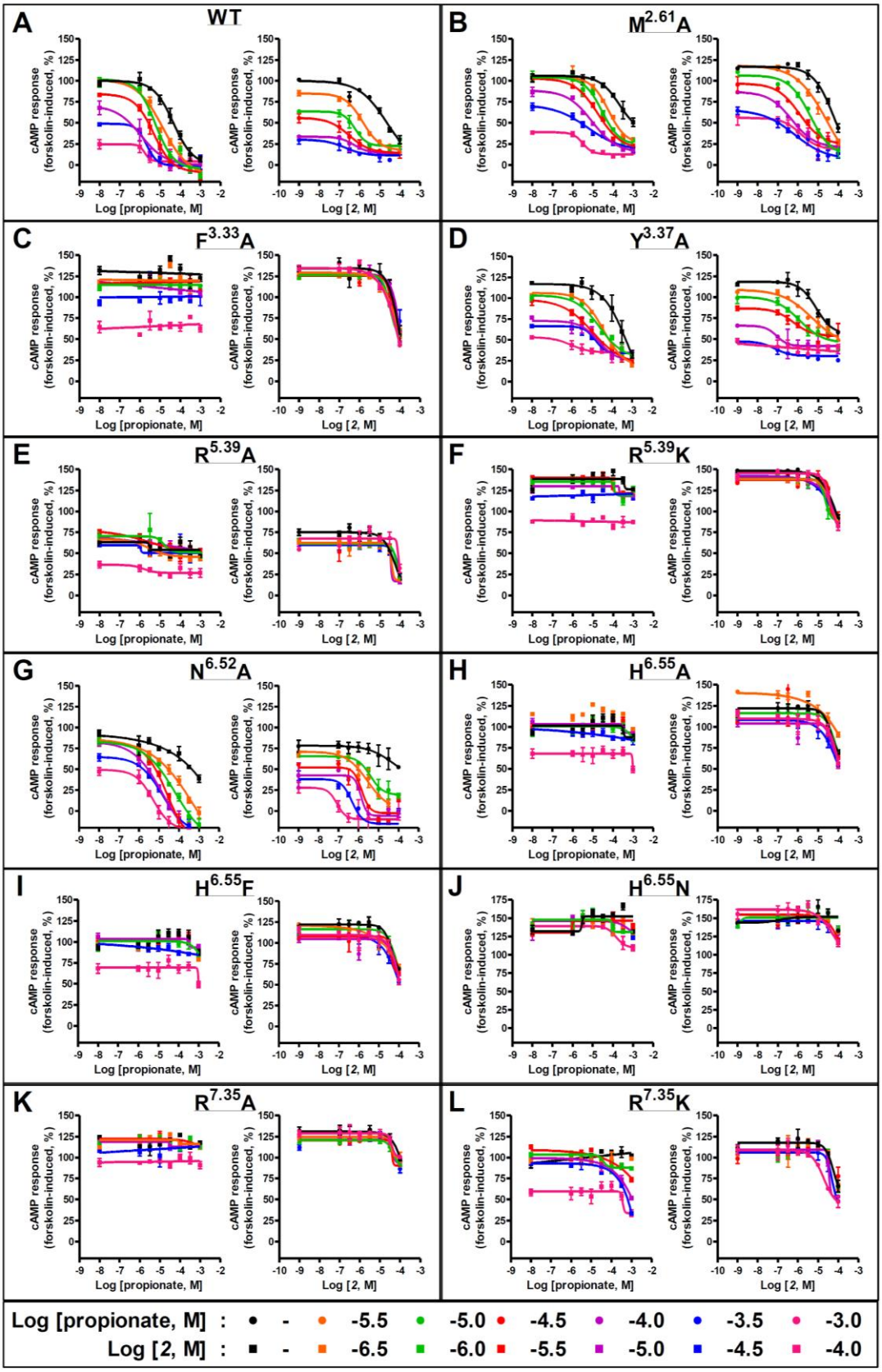

Fig. S1. Pharmacological characterization of the mutant human FFA3 receptors using a cAMP assay. Characterization of wild-type (WT) FFA3 (***A***), FFA3 M2.61A (***B***), FFA3 F3.33A (***C***), FFA3 Y3.37A (***D***), FFA3 R5.39A (***E***), FFA3 R5.39K (***F***), FFA3 N6.52A (***G***), FFA3 H6.55A (***H***), FFA3 H6.55F (***I***), FFA3 H6.55N (***J***), FFA3 R7.35A (***K***), and FFA3 R7.35K (***L***) upon stimulation with propionate in the presence or absence of varying concentrations of ***2*** (left panels) and with ***2*** in the presence or absence of varying concentrations of propionate (right panels), in comparison to the WT FFA3 receptor (***A***). The concentrations of ***2*** and propionate used in the left and right panels, respectively, are shown in the legend at the bottom of the graphs.

References

Ahren,B. (2009) Islet G protein-coupled receptors as potential targets for treatment of type 2 diabetes. *Nat. Rev. Drug Discov.* **8,** 369-385.

Bagchi,D. and Preuss,H. (2007) Obesity - Epidemiology, pathophysiology and prevention [Book]. *CRC Press* 3-20.

Ballesteros,J.A. and Weinstein,H. (1995) Integrated methods for the construction of three-dimensional models and computational probing of structure-function relations in G protein-coupled receptors. *Methods Neuroscience* **25,** 366-428.

Beckman,J.A., Creager,M.A., and Libby,P. (2002) Diabetes and atherosclerosis: epidemiology, pathophysiology, and management. *JAMA* **287,** 2570-2581.

Bokoch,M.P., Zou,Y., Rasmussen,S.G.F., Liu,C.W., Nygaard,R., Rosenbaum,D.M., Fung,J.J., Choi,H.J., Thian,F.S., Kobilka,T.S. *et al.* (2010). Ligand-specific regulation of the extracellular surface of a G protein-coupled receptor. *Nature* **463,** 108-112.

Bougnères,P. (2002) Genetics of obesity and type 2 diabetes. *Diabetes* **51,** S295-S303.

Briaud,I., Lingohr,M.K., Dickson,L.M., Wrede,C.E., and Rhodes,C.J. (2003) Differential activation mechanisms of ERK1/2 and p70S6K by glucose in pancreatic beta-cells. *Diabetes* **52,** 974-983.

Briscoe,C.P., Tadayyon,M., Andrews,J.L., Benson,W.G., Chambers,J.K., Eilert,M.M., Ellis,C., Elshourbagy,N.A., Goetz,A.S., Minnick,D.T. *et al.* (2003) The orphan G protein-coupled receptor GPR40 is activated by medium- and long-chain fatty acids. *J. Biol. Chem.* **278,** 11303-11311.

Brown,A.J., Goldsworthy,S.M., Barnes,A.A., Eilert,M.M., Tcheang,L., Daniels,D., Muir,A.I., Wigglesworth,M.J., Kinghorn,I., Fraser,N.J. *et al.* (2003) The orphan G protein-coupled receptors GPR41 and GPR43 are activated by propionate and other short-chain carboxylic acids. *J. Biol. Chem.* **278,** 11312-11319.

Chandalia,M., Garg,A., Lutjohann,D., von Bergmann,K., Grundy,S.M., and Brinkley,L.J. (2000) Beneficial effects of high dietary fiber intake in patients with type 2 diabetes mellitus. *N. Engl. J. Med.* **342,** 1392-1398.

Chapman,M.J., Redfern,J.S., McGovern,M.E., and Giral,P. (2010) Niacin and fibrates in atherogenic dyslipidemia: pharmacotherapy to reduce cardiovascular risk. *Pharmacol. Ther.* **126,** 314-345.

Cherezov,V., Rosenbaum,D.M., Hanson,M.A., Rasmussen,S.G.F., Thian,F.S., Kobilka,T.S., Choi,H.J., Kuhn,P., Weis,W.I., Kobilka,B.K. *et al.* (2007) High-resolution crystal structure of an engineered human β2-adrenergic G protein-coupled receptor. *Science* **318,** 1258-1265.

Chien,E.Y.T., Liu,W., Zhao,Q., Katritch,V., Won Han,G., Hanson,M.A., Shi,L., Newman,A.H., Javitch,J.A., Cherezov,V. et al. (2010) Structure of the human dopamine D3 receptor in complex with a D2/D3 selective antagonist. *Science* **330,** 1091-1095.

Costes,S., Broca,C., Bertrand,G., Lajoix,A.D., Bataille,D., Bockaert,J., and Dalle,S. (2006) ERK1/2 control phosphorylation and protein level of cAMP-Responsive Element Binding Protein : a key role in glucose-mediated pancreatic beta-cell survival. *Diabetes* **55,** 2220-2230.

Cox,M.A., Jackson,J., Stanton,M., Rojas-Triana,A., Bober,L., Laverty,M., Yang,X., Zhu,F., Liu,J., Wang,S. *et al.* (2009) Short-chain fatty acids act as antiinflammatory mediators by regulating prostaglandin E2 and cytokines. *World J. Gastroenterol.* **15,** 5549-5557.

Cummings,J.H., Pomare,E.W., Branch,W.J., Naylor,C.P., and Macfarlane,G.T. (1987) Short-chain fatty acids in human large intestine, portal, hepatic and venous blood. *Gut* **28,** 1221-1227.

Dass,N.B., John,A.K., Bassil,A.K., Crumbley,C.W., Shehee,W.R., Maurio,F.P., Moore,G.B., Taylor,C.M., and Sanger,G.J. (2007) The relationship between the effects of short-chain fatty acids on intestinal motility in vitro and GPR43 receptor activation. *Neurogastroenterol. Motil.* **19,** 66-74.

Duncan,R.E., Ahmadian,M., Jaworski,K., Sarkadi-Nagy,E., and Sul,H.S. (2007) Regulation of lipolysis in adipocytes. *Annu. Rev. Nutr.* **27,** 79-101.

Drucker,D.J. (2005) Biologic actions and therapeutic potential of the proglucagon-derived peptides. *Nat. Clin. Pract. Endocrinol. Metab* **1,** 22-31.

Fang,Y., Frutos,A.G., and Verklereen,R. (2008) Label-free cell-based assays for GPCR screening. *Comb. Chem. High Throughput Screen.* **11,** 357-369.

Flier,J.S. (2004) Obesity wars: molecular progress confronts an expanding epidemic. *Cell* **116,** 337-350.

Fredriksson,R., Lagerström,M.C., Lundin,L.G., and Schiöth,H.B. (2003) The G protein-coupled receptors in the human genome form five main families. Phylogenetic analysis, paralogon groups, and fingerprints. *Mol. Pharmacol.* **63,** 1256-1272.

Ge,H., Li,X., Weiszmann,J., Wang,P., Baribault,H., Chen,J.L., Tian,H., and Li,Y. (2008) Activation of G protein-coupled receptor 43 in adipocytes leads to inhibition of lipolysis and suppression of plasma free fatty acids. *Endocrinology* **149,** 4519-4526.

Gordon,J.I., Samuel,B.S., Yanagisawa,M., Shaito,A., and Motoike,T. (2010) Regulating intestinal microbiota dependent signaling as a means to modulate body fat and/or weight loss. *Patent WO 2010/030997*.

Guerciolini,R. (1997) Mode of action of orlistat. *Int. J. Obes. Relat. Metab. Disord.* **21 Suppl 3,** S12-S23.

Harmar,A.J., Hills,R.A., Rosser,E.M., Jones,M., Buneman,O.P., Dunbar,D.R., Greenhill,S.D., Hale,V.A., Sharman,J.L., Bonner,T.I. *et al.* (2009) IUPHAR-DB: the IUPHAR database of G protein-coupled receptors and ion channels. *Nucleic Acids Res.* **37,** D680-D685.

He,W., Miao,F.J.P., Lin,D.C.H., Schwandner,R.T., Wang,Z., Gao,J., Chen,J.L., Tian,H., and Ling,L. (2004) Citric acid cycle intermediates as ligands for orphan Gprotein-coupled receptors. *Nature* **429,** 188-193.

Hirasawa,A., Tsumaya,K., Awaji,T., Katsuma,S., Adachi,T., Yamada,M., Sugimoto,Y., Miyazaki,S., and Tsujimoto,G. (2005) Free fatty acids regulate gut incretin glucagon-like peptide-1 secretion through GPR120. *Nat. Med.* **11,** 90-94.

Hong,Y.H., Nishimura,Y., Hishikawa,D., Tsuzuki,H., Miyahara,H., Gotoh,C., Choi,K.C., Feng,D.D., Chen,C., Lee,H.G. *et al.* (2005) Acetate and propionate short-chain fatty acids stimulate adipogenesis via GPCR43. *Endocrinology* **146,** 5092-5099.

Huang,C., Jacobson,K., and Schaller,M.D. (2004) MAP kinases and cell migration. *J. Cell Sci.* **117,** 4619-4628.

Hur,E.M. and Kim,K.T. (2002) G protein-coupled receptor signaling and cross-talk: Achieving rapidity and specificity. *Cell. Signal.* **14,** 397-405.

Jaakola,V.P., Griffith,M.T., Hanson,M.A., Cherezov,V., Chien,E.Y.T., Lane,J.R., IJzerman,A.P., and Stevens,R.C. (2008) The 2.6 Å crystal structure of a human A2A adenosine receptor bound to an antagonist. *Science* **322,** 1211-1217.

Jacoby,E., Bouhelal,R., Gerspacher,M., and Seuwen,K. (2006) The seven transmembrane domains G-protein-coupled receptor target family. *Chem. Med. Chem.* **1,** 761-782.

Kaji,I., Karaki,S.I., Tanaka,R., and Kuwahara,A. (2011) Density distribution of free fatty acid receptor 2 (FFA2)-expressing and GLP-1-producing enteroendocrine L cells in human and rat lower intestine, and increased cell numbers after ingestion of fructo-oligosaccharide. *J. Mol .Histol.* **42,** 27-38.

Karaki,S., Mitsui,R., Hayashi,H., Kato,I., Sugiya,H., Iwanaga,T., Furness,J.B., and Kuwahara,A. (2006) Short-chain fatty acid receptor, GPR43, is expressed by enteroendocrine cells and mucosal mast cells in rat intestine. *Cell Tissue Res.* **324,** 353-360.

Karaki,S., Tazoe,H., Hayashi,H., Kashiwabara,H., Tooyama,K., Suzuki,Y., and Kuwahara,A. (2008) Expression of the short-chain fatty acid receptor, GPR43, in the human colon. *J. Mol. Histol.* **39,** 135-142.

Karra,E., Chandarana,K., and Batterham,R.L. (2009) The role of peptide YY in appetite regulation and obesity. *J. Physiol.* **587,** 19-25.

Kebede,M.A., Alquier,T., Latour,M.G., and Poitout,V. (2009) Lipid receptors and islet function: therapeutic implications? *Diabetes Obes. Metab.* **11 Suppl 4,** 10-20.

Kelesidis,T., Kelesidis,I., Chou,S., and Mantzoros,C.S. (2010) The role of leptin in human physiology: emerging clinical applications. *Ann. Intern. Med.* **152,** 93-100.

Kristiansen,K. (2004) Molecular mechanisms of ligand binding, signaling, and regulation within the superfamily of G-protein-coupled receptors: molecular modeling and mutagenesis approaches to receptor structure and function. *Pharmacol. Ther.* **103,** 21-80.

Lagerström,M.C. and Schiöth,H.B. (2008) Structural diversity of G protein-coupled receptors and significance for drug discovery. *Nat. Rev. Drug. Discov.* **7,** 339-357.

Lee,T., Schwandner,R., Swaminath,G., Weiszmann,J., Cardozo,M., Greenberg,J., Jaeckel,P., Ge,H., Wang,Y., Jiao,X. *et al.* (2008) Identification and functional characterization of allosteric agonists for the G protein-coupled receptor FFA2. *Mol. Pharmacol.* **74,** 1599-1609.

Leonard,J., Chu,Z.L., Bruce,M.A., and Boatman,D.P. (2007) GPR41 and modulators thereof for the treatment of insulin-related disorders. *Patent WO 2006/052566 A2*.

LePoul,E., Loison,C., Struyf,S., Springael,J.Y., Lannoy,V., Decobecq,M.E., Brezillon,S., Dupriez,V., Vassart,G., Van Damme,J. *et al.* (2003) Functional characterization of human receptors for short-chain fatty acids and their role in polymorphonuclear cell activation. *J. Biol. Chem.* **278,** 25481-25489.

Liaw,C.W. and Connolly,D.T. (2009) Sequence polymorphisms provide a common consensus sequence for GPR41 and GPR42. *DNA Cell Biol.* **28,** 555-560.

Lim,G.E., Huang,G.J., Flora,N., LeRoith,D., Rhodes,C.J., and Brubaker,P.L. (2009) Insulin regulates glucagon-like peptide-1 secretion from the enteroendocrine L cell. *Endocrinology.* **150,** 580-591.

Luttrell,D.K. and Luttrell,L.M. (2003) Signaling in time and space: G protein-coupled receptors and mitogen-activated protein kinases. *ASSAY Drug Dev. Technol.* **1,** 327-338.

Marinissen,M.J. and Gutkind,J.S. (2001) G protein-coupled receptors and signaling networks: emerging paradigms. *Trends Pharmacol. Sci.* **22,** 368-376.

Martí-Renom,M.A., Stuart,A.C., Fiser,A., Sánchez,R., Melo,F., and Sali,A. (2000) Comparative protein structure modeling of genes and genomes. *Annu. Rev. Biophys. Biomol. Struct.* **29,** 291-325.

Maslowski,K.M., Vieira,A.T., Ng,A., Kranich,J., Sierro,F., Di,Y., Schilter,H.C., Rolph,M.S., Mackay,F., Artis,D. *et al.* (2009) Regulation of inflammatory responses by gut microbiota and chemoattractant receptor GPR43. *Nature* **461,** 1282-1286.

McCudden,C.R., Hains,M.D., Kimple,R.J., Siderovski,D.P., and Willard,F.S. (2005) G-protein signaling: back to the future. *Cell. Mol. Life Sci.* **62,** 551-577.

McGuinness,R. (2007) Impedance-based cellular assay technologies: recent advances, future promise. *Curr. Opin.Pharmacol.* **7,** 535-540.

McGuinness,R.P., Proctor,J.M., Gallant,D.L., van Staden,C.J., Ly,J.T., Tang,F.L., and Lee,P.H. (2009) Enhanced selectivity screening of GPCR ligands using a label-free cell based assay technology. *Comb. Chem. High Throughput Screen.* **12,** 812-823.

Mielenz,M., Seybold,C., and Sauerwein,H. (2008) Effects of short-term infusion with propionate on the mRNA expression of a putative G-protein coupled receptor 41 (GPR41) in adipose tissue of goats. *Livestock Science* **116,** 328-331.

Milligan,G. and Kostenis,E. (2006) Heterotrimeric G-proteins: a short history. *Br. J. Pharmacol.* **147,** 46-55.

Mooradian,A.D. (2009) Dyslipidemia in type 2 diabetes mellitus. *Nat. Clin. Pract. End. Met.* **5,** 150-159.

Narayan,K.M.V., Boyle,J.P., Thompson,T.J., Gregg,E.W., and Williamson,D.F. (2007) Effect of BMI on lifetime risk for diabetes in the U.S. *Diabetes Care* **30,** 1562-1566.

Nathan,D.M., Buse,J.B., Davidson,M.B., Ferrannini,E., Holman,R.R., Sherwin,R., and Zinman,B. (2009) Medical management of hyperglycemia in type 2 diabetes: a consensus algorithm for the initiation and adjustment of therapy. *Diabetes Care* **32,** 193-203.

Nilsson,N.E., Kotarsky,K., Owman,C., and Olde,B. (2003) Identification of a free fatty acid receptor, FFA2R, expressed on leukocytes and activated by short-chain fatty acids. *Biochem. Biophys. Res. Commun.* **303,** 1047-1052.

Ono,T., Guthold,R., and Strong,K. (2005) Global comparable estimates. https://apps.who.int/infobase. *World Health Organization website*.

Osmond,R.I.W., Sheehan,A., Borowicz,R., Barnett,E., Harvey,G., Turner,C., Brown,A., Crouch,M.F., and Dyer,A.R. (2005) GPCR screening via ERK1/2: a novel platform for screening G protein-coupled receptors. *J. Biomol. Screen* **10,** 730-737.

Palczewski,K., Kumasaka,T., Hori,T., Behnke,C.A., Motoshima,H., Fox,B.A., Le,T., I, Teller,D.C., Okada,T., Stenkamp,R.E. *et al.* (2000) Crystal structure of rhodopsin: a G protein-coupled receptor. *Science* **289,** 739-745.

Patel,T.B. (2004) Single transmembrane spanning heterotrimeric G protein-coupled receptors and their signaling cascades. *Pharmacol. Rev.* **56,** 371-385.

Petersen,R.K., Madsen,L., Pedersen,L.M., Hallenborg,P., Hagland,H., Viste,K., Doskeland,S.O., and Kristiansen,K. (2008) Cyclic AMP (cAMP)-mediated stimulation of adipocyte differentiation requires the synergistic action of Epac- and cAMP-dependent protein kinase-dependent processes. *Mol. Cell Biol.* **28,** 3804-3816.

Plaisancié,P., Dumoulin,V., Chayvialle,J.A., and Cuber,J.C. (1996) Luminal peptide YY-releasing factors in the isolated vascularly perfused rat colon. *J. Endocrinol.* **151,** 421-429.

Powell,T. and Khera,A. (2010) Therapeutic approaches to obesity. *Curr. Treat. Options Cardiovasc. Med.* **12,** 381-395.

Quitterer,U. and Lohse,M.J. (1999) Crosstalk between $G\alpha_i$- and $G\alpha_q$-coupled receptors is mediated by $G\beta\gamma$ exchange. *Proc. Natl. Acad. Sci.* **96,** 10626-10631.

Rasmussen,S.G.F., Choi,H.J., Rosenbaum,D.M., Kobilka,T.S., Thian,F.S., Edwards,P.C., Burghammer,M., Ratnala,V.R.P., Sanishvili,R., Fischetti,R.F. *et al.* (2007) Crystal structure of the human β2 adrenergic G protein-coupled receptor. *Nature* **450,** 383-387.

Robertson,M.D., Bickerton,A.S., Dennis,A.L., Vidal,H., and Frayn,K.N. (2005) Insulin-sensitizing effects of dietary resistant starch and effects on skeletal muscle and adipose tissue metabolism. *Am. J. Clin. Nutr.* **82,** 559-567.

Rodbell,M. (1964) Metabolism of isolated fat cells. I. Effects of hormones on glucose metabolism and lipolysis. *J. Biol. Chem.* **239,** 375-380.

Rosenbaum,D.M., Rasmussen,S.G.F., and Kobilka,B.K. (2009) The structure and function of G protein-coupled receptors. *Nature* **459,** 356-363.

Roux,P.P. and Blenis,J. (2004) ERK and p38 MAPK-activated protein kinases: a family of protein kinases with diverse biological functions. *Microbiol. Mol. Biol. Rev.* **68,** 320-344.

Rovati,G.E., Capra,V., and Neubig,R.R. (2007) The highly conserved DRY motif of class A G protein-coupled receptors: beyond the ground state. *Mol. Pharmacol.* **71,** 959-964.

Samuel,B.S., Shaito,A., Motoike,T., Rey,F.E., Backhed,F., Manchester,J.K., Hammer,R.E., Williams,S.C., Crowley,J., Yanagisawa,M. *et al.* (2008) Effects of the gut microbiota on host adiposity are modulated by the short-chain fatty acid binding G protein-coupled receptor, GPR41. *Proc. Natl. Acad. Sci.* **105,** 16767-16772.

Santomauro,A.T., Boden,G., Silva,M.E., Rocha,D.M., Santos,R.F., Ursich,M.J., Strassmann,P.G., and Wajchenberg,B.L. (1999) Overnight lowering of free fatty acids with Acipimox improves insulin resistance and glucose tolerance in obese diabetic and nondiabetic subjects. *Diabetes* **48,** 1836-1841.

Sawzdargo,M., George,S.R., Nguyen,T., Xu,S., Kolakowski,L.F., and O'dowd,B.F. (1997) A cluster of four novel human G protein-coupled receptor genes occurring in close proximity to CD22 gene on chromosome 19q13.1. *Biochem. Biophys. Res. Commun.* **239,** 543-547.

Schenk,S., Saberi,M., and Olefsky,J.M. (2008) Insulin sensitivity: modulation by nutrients and inflammation. *J. Clin. Invest.* **118,** 2992-3002.

Schwartz,T.W., Frimurer,T.M., Holst,B., Rosenkilde,M.M., and Elling,C.E. (2006) Molecular mechanism of 7TM receptor activation - A global toggle switch model. *Annu. Rev. Pharmacol. Toxicol.* **46,** 481-519.

Schmidt,J., Smith,N.J., Christiansen,E., Tikhonova,I.G., Grundmann,M., Hudson,B.D., Ward,R.J., Drewke,C., Milligan,G., Kostenis,E. *et al.* (2011) Selective Orthosteric Free Fatty Acid Receptor 2 (FFA2) Agonists. *J. Biol. Chem.* **286,** 10628-10640.

Seamon,K.B., Padgett,W., and Daly,J.W. (1981) Forskolin: unique diterpene activator of adenylate cyclase in membranes and in intact cells. *Proc. Natl. Acad. Sci.* **78,** 3363-3367.

Senga,T., Iwamoto,S., Yoshida,T., Yokota,T., Adachi,K., Azuma,E., Hamaguchi,M., and Iwamoto,T. (2003) LSSIG is a novel murine leukocyte-specific GPCR that is induced by the activation of STAT3. *Blood* **101,** 1185-1187.

Sicree,R., Shaw,J., and Zimmet,P. (2010) Diabetes and IGT - The global burden; diabetes and impaired glucose tolerance. http://www.diabetesatlas.org/content/diabetes-and-impaired-glucose-tolerance. *IDF Diabetes Atlas, 4th edition*.

Sleeth,M.L., Thompson,E.L., Ford,H.E., Zac-Varghese,S.E., and Frost,G. (2010) Free fatty acid receptor 2 and nutrient sensing: a proposed role for fibre, fermentable carbohydrates and short-chain fatty acids in appetite regulation. *Nutr. Res. Rev.* **23,** 135-145.

Smrcka,A. (2008) G protein βγ subunits: central mediators of G protein-coupled receptor signaling. *Cell. Mol. Life Sci.* **65,** 2191-2214.

Soliman,M., Kimura,K., Ahmed,M., Yamaji,D., Matsushita,Y., Okamatsu-Ogura,Y., Makondo,K., and Saito,M. (2007) Inverse regulation of leptin mRNA expression by short- and long-chain fatty acids in cultured bovine adipocytes. *Domest. Anim. Endocrinol.* **33,** 400-409.

Stoddart,L.A., Smith,N.J., and Milligan,G. (2008a) Free fatty acid receptors FFA1, -2, and -3: Pharmacology and pathophysiological functions. *Pharmacol. Rev.* **60,** 405-417.

Stoddart,L.A., Smith,N.J., Jenkins,L., Brown,A.J., and Milligan,G. (2008b) Conserved polar residues in transmembrane domains V, VI, and VII of free fatty acid receptor 2 and free fatty acid receptor 3 are required for the binding and function of short-chain fatty acids. *J. Biol. Chem.* **283,** 32913-32924.

Sum,C.S., Tikhonova,I.G., Neumann,S., Engel,S., Raaka,B.M., Costanzi,S., and Gershengorn,M.C. (2007) Identification of residues important for agonist recognition and activation in GPR40. *J. Biol. Chem.* **282,** 29248-29255.

Surgand,J.S., Rodrigo,J., Kellenberger,E., and Rognan,D. (2006) A chemogenomic analysis of the transmembrane binding cavity of human G protein-coupled receptors. *Proteins* **62,** 509-538.

Swaminath,G., Jaeckel,P., Guo,Q., Cardozo,M., Weiszmann,J., Lindberg,R., Wang,Y., Schwandner,R., and Li,Y. (2010) Allosteric rescuing of loss-of-function FFA2 mutations. *FEBS Lett.* **584,** 4208-4214.

Tanaka,T., Katsuma,S., Adachi,T., Koshimizu,T.A., Hirasawa,A., and Tsujimoto,G. (2008) Free fatty acids induce cholecystokinin secretion through GPR120. *Naunyn-Schmiedeberg's Arch. Pharmacol.* **377,** 523-527.

Tazoe,H., Otomo,Y., Kaji,I., Tanaka,R., Karaki,S.I., and Kuwahara,A. (2008) Roles of short-chain fatty acids receptors GPR41 and GPR43 on colonic functions. *J. Physiol. Pharmacol.* **59 [Suppl 2],** 251-262.

Tazoe,H., Otomo,Y., Karaki,S., Kato,I., Fukami,Y., Terasaki,M., and Kuwahara,A. (2009) Expression of short-chain fatty acid receptor GPR41 in the human colon. *Biomed. Res.* **30,** 149-156.

Tedelind,S., Westberg,F., Kjerrulf,M., and Vidal,A. (2007) Anti-inflammatory properties of the short-chain fatty acids acetate and propionate: a study with relevance to inflammatory bowel disease. *World J. Gastroenterol.* **13,** 2826-2832.

Tintinger,G.R., Steel,H.C., Theron,A.J., and Anderson,R. (2008) Pharmacological control of neutrophil-mediated inflammation: strategies targeting calcium handling by activated polymorphonuclear leukocytes. *Drug. Des. Devel. Ther.* **2,** 95-104.

Topping,D.L. and Clifton,P.M. (2001) Short-chain fatty acids and human colonic function: roles of resistant starch and nonstarch polysaccharides. *Physiol. Rev.* **81,** 1031-1064.

Tschöp,M. and Heiman,M.L. (2001) Rodent obesity models: an overview. *Exp. Clin Endocrinol. Diabetes.* **109,** 307-319.

Tunaru,S., Kero,J., Schaub,A., Wufka,C., Blaukat,A., Pfeffer,K., and Offermanns,S. (2003) PUMA-G and HM74 are receptors for nicotinic acid and mediate its anti-lipolytic effect. *Nat. Med.* **9,** 352-355.

Verdonk,E., Johnson,K., McGuinness,R., Leung,G., Chen,Y.W., Tang,H.R., Michelotti,J.M., and Liu,V.F. (2006) Cellular dielectric spectroscopy: a label-free comprehensive platform for functional evaluation of endogenous receptors. *ASSAY Drug Dev. Technol.* **4,** 609-619.

Verdonk,M.L., Cole,J.C., Hartshorn,M.J., Murray,C.W., and Taylor,R.D. (2003) Improved protein-ligand docking using GOLD. *Proteins* **52,** 609-623.

Vinolo,M.A., Rodrigues,H.G., Hatanaka,E., Hebeda,C.B., Farsky,S.H., and Curi,R. (2009) Short-chain fatty acids stimulate the migration of neutrophils to inflammatory sites. *Clin Sci. (Lond)* **117,** 331-338.

Wang,L., Martin,B., Brenneman,R., Luttrell,L.M., and Maudsley,S. (2009a). Allosteric modulators of G protein-coupled receptors: future therapeutics for complex physiological disorders. *J. Pharmacol. Exp. Ther.* **331,** 340-348.

Wang,A., Gu,Z., Heid,B., Akers,R.M., and Jiang,H. (2009b). Identification and characterization of the bovine G protein-coupled receptor *GPR41* and *GPR43* genes. *J. Dairy Sci.* **92,** 2696-2705.

Wang,Y., Jiao,X., Kayser,F., Liu,J., Wang,Z., Wanska,M., Greenberg,J., Weiszmann,J., Ge,H., Tian,H. *et al.* (2010) The first synthetic agonists of FFA2: discovery and SAR of phenylacetamides as allosteric modulators. *Bioorg. Med. Chem. Lett.* **20,** 493-498.

Warne,T., Serrano-Vega,M.J., Baker,J.G., Moukhametzianov,R., Edwards,P.C., Henderson,R., Leslie,A.G.W., Tate,C.G., and Schertler,G.F.X. (2008) Structure of a β1-adrenergic G protein-coupled receptor. *Nature* **454,** 486-491.

Warne,T., Moukhametzianov,R., Baker,J.G., Nehme,R., Edwards,P.C., Leslie,A.G.W., Schertler,G.F.X., and Tate,C.G. (2011). The structural basis for agonist and partial agonist action on a β1-adrenergic receptor. *Nature* **469,** 241-244.

Wettschureck,N. and Offermanns,S. (2005) Mammalian G proteins and their cell type specific functions. *Physiol. Rev.* **85,** 1159-1204.

Wolever,T.M., Josse,R.G., Leiter,L.A., and Chiasson,J.L. (1997) Time of day and glucose tolerance status affect serum short-chain fatty acid concentrations in humans. *Metabolism* **46,** 805-811.

Wu,B., Chien,E.Y.T., Mol,C.D., Fenalti,G., Liu,W., Katritch,V., Abagyan,R., Brooun,A., Wells,P., Bi,F.C. et al. (2010) Structures of the CXCR4 chemokine GPCR with small-molecule and cyclic peptide antagonists. *Science* **330,** 1066-1071.

Ximenes,H.M., Hirata,A.E., Rocha,M.S., Curi,R., and Carpinelli,A.R. (2007) Propionate inhibits glucose-induced insulin secretion in isolated rat pancreatic islets. *Cell Biochem. Funct.* **25,** 173-178.

Xiong,Y., Miyamoto,N., Shibata,K., Valasek,M.A., Motoike,T., Kedzierski,R.M., and Yanagisawa,M. (2004) Short-chain fatty acids stimulate leptin production in adipocytes through the G protein-coupled receptor GPR41. *Proc. Natl. Acad. Sci.* **101,** 1045-1050.

Xue,B., Greenberg,A.G., Kraemer,F.B., and Zemel,M.B. (2001) Mechanism of intracellular calcium ($[Ca^{2+}]_i$) inhibition of lipolysis in human adipocytes. *FASEB J.* **15,** 2527-2529.

Zaibi,M.S., Stocker,C.J., O'Dowd,J., Davies,A., Bellahcene,M., Cawthorne,M.A., Brown,A.J., Smith,D.M., and Arch,J.R. (2010) Roles of GPR41 and GPR43 in leptin secretory responses of murine adipocytes to short chain fatty acids. *FEBS Lett.* **584,** 2381-2386.